University of Berne
Department of Biology
Institute of Biochemistry
and Molecular Medicine

Establishment and comparison of static and fluidic microvessel systems as cell models for studying trophoblast physiology

Master Thesis

Faculty of Science, University of Bern

handed in by

Roman Bächler

February 2021

Supervision:

Prof. Dr. Christiane Albrecht

Institute of Biochemistry and Molecular Medicine (IBMM), Bühlstrasse 28, 3012 Berne, Switzerland

Table of contents

List of abbreviations

CTB	Cytotrophoblast
STB	Syncytiotrophoblast
DMEM	Dulbecco's Modified Eagle's Medium
FBS	Fetal Bovine Serum
BSA	Bovine serum albumin
hCG	human chorionic gonadotropin
kDa	kilo Dalton
PBS	Phosphate buffered saline
DPBS	Dulbecco`s Phosphate buffered saline
rpm	Revolutions per minute of rotor
RT	Room temperature (20-25°C)
DMEM-HG	DMEM high glucose medium (4.5g/l glucose)
CK-7	Cytokeratin-7
ZO-1	Zonula occludens-1
E-cadherin	Epithelial cadherin
CALHM4	Calcium homeostasis modulator 4
SC-1	Syndecan-1
DAPI	4′,6-diamidino-2-phenylindole
AF488	Alexa Fluor® 488
AF594	Alexa Fluor® 594
PDMS	Polydimethylsiloxane
ELISA	Enzyme-linked immunosorbent assay
EIA	Enzymatic immunoassays
RIA	Radioimmunoassay
DMSO	Dimethyl sulfoxide
dH2O	Sterile distilled water
APTES	3-Aminopropyltriethoxysilane

Abstract

The prediction of drug effects before human clinical trials is the fundamental part of drug screening and discovery processes. To reduce the steadily increasing costs of drug discovery processes and human disease- related research as well as the research on animals, there is an urgent need to develop more predictive tissue models. Growing knowledge about interactions between cells and their environment enable the construction of 3D organ-on-a-chip models. Organ-on-a-chip technologies enable high fidelity organ function *in vitro* and are outmatching conventional 2D- and animal - models regarding their reproducibility of physiological processes.

In this thesis a first step towards a placenta-on-a-chip model was made by the adaption of a microfluidic system for endothelial cells for the application in BeWo trophoblast cells. In addition, the static cultivation of the BeWo cells in chamber slides was optimized with the aim of being able to compare these two systems for morphological and secretory differences In the course of this evaluation, differentiation time course experiments of cytotrophoblast (CTB-) BeWo cells to syncytiotrophoblast (STB-) BeWo cells, in the static and the microfluidic system were carried out. In order to analyze morphological differences, the trophoblast specific biomarkers cytokeratin-7 (CK-7), zonula occludens-1 (ZO-1), E-cadherin (E-cad), as well as the calcium homeostasis modulator 4 (CALHM4) and syndecan-1 (SC-1) were stained and then evaluated with a fluorescence scanner microscope and by confocal microscopy. To assess secretory differences, the human chorionic gonadotropin (hCG-) – secretion of the BeWo cells was measured in both setups using an ELISA.

After numerous optimization steps it was possible to cultivate the trophoblast cell line BeWo in the microfluidic system under flow for a maximum of 24 hours. The exposure of the BeWo cells to the flow resulted in a bundling of keratin filaments as well as an increased nuclear size. In the static chamber slide system, morphological alterations over the time course of 88h culturing time were observed in STB-BeWo cells where differentiation was induced by treatment with Forskolin. During the differentiation process, in both systems an enlargement of the nuclei and in the static system also a reorganization of the cytoskeleton and breakdowns of the junctional proteins ZO-1 and E-cad were observed. The CALHM4 staining revealed not only a membraneous, but also an intracellular localization of this protein which is reminiscent of intermediate

filaments. With regards to the SC-1 staining, a signal increase over the course of differentiation as well as structural changes were found. Concerning the structural changes, it was observed that the SC-1 staining signal seemed cloudy and distributed over the whole cells in the Forskolin stimulated BeWo cells whereas it appeared granulated and localized closer to the cell membrane in undifferentiated BeWo cells. The ELISA quantification revealed an elevation of hCG secretion with increasing differentiation of the BeWo cells in the static system; hCG secretion in the microfluidic chip system was not detectable.

In summary the morphological findings propose a successful differentiation of the BeWo cells after stimulation with Forskolin in both systems. In addition, in the static system the differentiation process could be confirmed by the increased hCG secretion in STB-BeWo compared to CTB-BeWo cells. The enlargement of the nuclei in the microfluidic chip system by the flow, suggests that the flow triggers the differentiation process of the BeWo cells. The second apparent effect that the flow exerted on the BeWo cells, namely the keratin filament bundling, may be explained by the fact that the BeWo trophoblast cells render themselves more resistant to the mechanical influences of shear stress. Based on the results of the CALHM4 stainings it could be speculated that CALHM4 belongs to the mechanosensitive channels that are known to interact with the cytoskeleton in response to the signal of a mechanically gated channel. The results of the SC-1 staining suggest a functional relevance of this structure in STB-BeWo cells as for example in the regulation of permeability and transport mechanisms.

In conclusion, with this work the first steps were made to cultivate the BeWo trophoblast cells for a limited time in the microfluid chip and indications of morphological changes induced by the flow were identified. This sets the stage for future studies aiming at establishing a placenta-on-a-chip model.

Acknowledgement

I would first like to thank my thesis supervisors Prof. Dr. Christiane Albrecht and Prof. Dr. Robert Rieben who made this master thesis work possible. Since most of the work was carried out in the laboratory of Prof. Dr. Christiane Albrecht, I am especially grateful to her for all the time she took for providing me guidance and feedback throughout this project. I am also very thankful to Prof. Dr. Robert Rieben for giving me access to his laboratory and the fruitful discussions.

Also, I would like to thank my co-supervisors, Dr. Line Zurkinden, who guided me in the start phase of this project and especially Dr. Jonas Zaugg, who took over the supervision after. He had a very congenial way of passing on his wide-ranging theoretical and practical knowledge.

Further I would like to thank the members of the Albrecht group, particularly Michael Lüthi, Dr. Sampada Kallol, Dr. Edgar Ontsouka and Dr. Barbara Fuenzalida, who created a very pleasant working atmosphere and were always very helpful. Last but not least also a big thank you to the Rieben group members Dr. Nicoletta Sorvillo and Anastasia Milusev for the good cooperation and support.

1 Introduction

1.1 Human placenta

The placenta is a temporary organ that develops during pregnancy and connects the developing fetus via the umbilical cord to the uterine wall. It is highly specialized on tasks like nutrient uptake, thermo regulation, waste elimination and gas exchange via the mothers blood supply. In addition it releases hormones into the maternal and fetal circulation which support pregnancy and is needed to fight against internal infections (Gude et al., 2004). The placenta consists of fetal tissue which gets delivered after birth and maternal tissue. The fetal placenta that forms the fetus develops from the chorionic sac and the maternal placenta develops from the endometrium (Herrick & Bordoni, 2019). In the second half of pregnancy the chorionic villi on the fetal side are flooded by the intervillous space on the maternal side and those parts are separated through the placental barrier (see Figure 1). This enables the fetus to have an independent circulation and still be in exchange with the mother's circulation across the placental barrier (Kreuder et al., 2020).

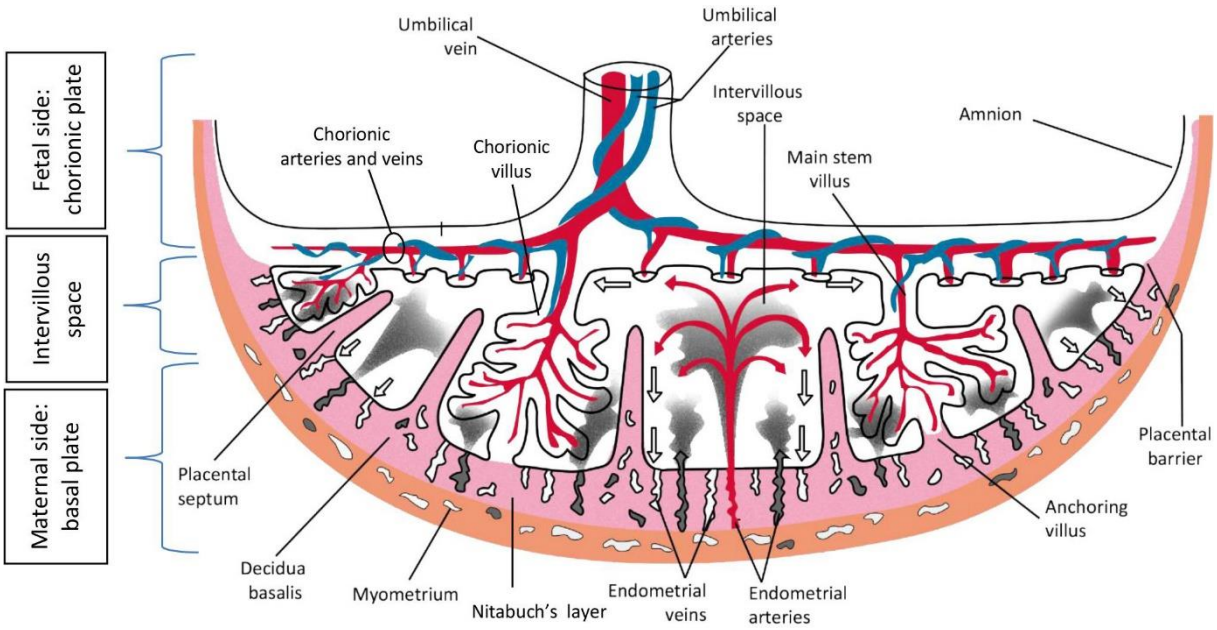

Figure 1: Schemata of the fetal- and maternal side of the placenta in the second half of pregnancy. Chorionic villi (fetal side) and flooded intervillous space (maternal side) are separated through the placental barrier (source: Jansen et al., 2020).

1.2 Cell populations of the human placenta

The placental barrier described in part 1.1 consists of endothelial cells on the fetal side and villous trophoblasts on the maternal side (see Figure 2) (Elad et al., 2014). Villous trophoblasts consist of two cell types: cytotrophoblasts that are undifferentiated and the fully differentiated syncytiotrophoblasts. There are cytotrophoblast progenitor cells that divide in an asymmetric way. One daughter cell retains its progenitor character while the other one is destined for differentiation. During the differentiation process a cytotrophoblast fuses with a syncytiotrophoblast and in this way its cell constituents are transferred to the syncytiotrophoblasts (Ahrendt & K.J. Buhling, 2006). The syncytiotrophoblasts form a epithelial like, continuous layer and cover the entire surface of the villous trees and are in direct contact with the maternal blood (Wang & Zhao, 2010). This layer forms a syncytium and is built from the underlying cellular cytotrophoblasts (Kudo et al., 2003). Fully developed villi are the functional unit of maternal-fetal nutrient transport and oxygen exchange (Wang & Zhao, 2010). Trophoblasts form the outer layer of a blastocyst that develops into a large part of the placenta and provide nutrients to the embryo. They are the first cells to differentiate from the fertilized egg and are formed during the first stage of pregnancy.

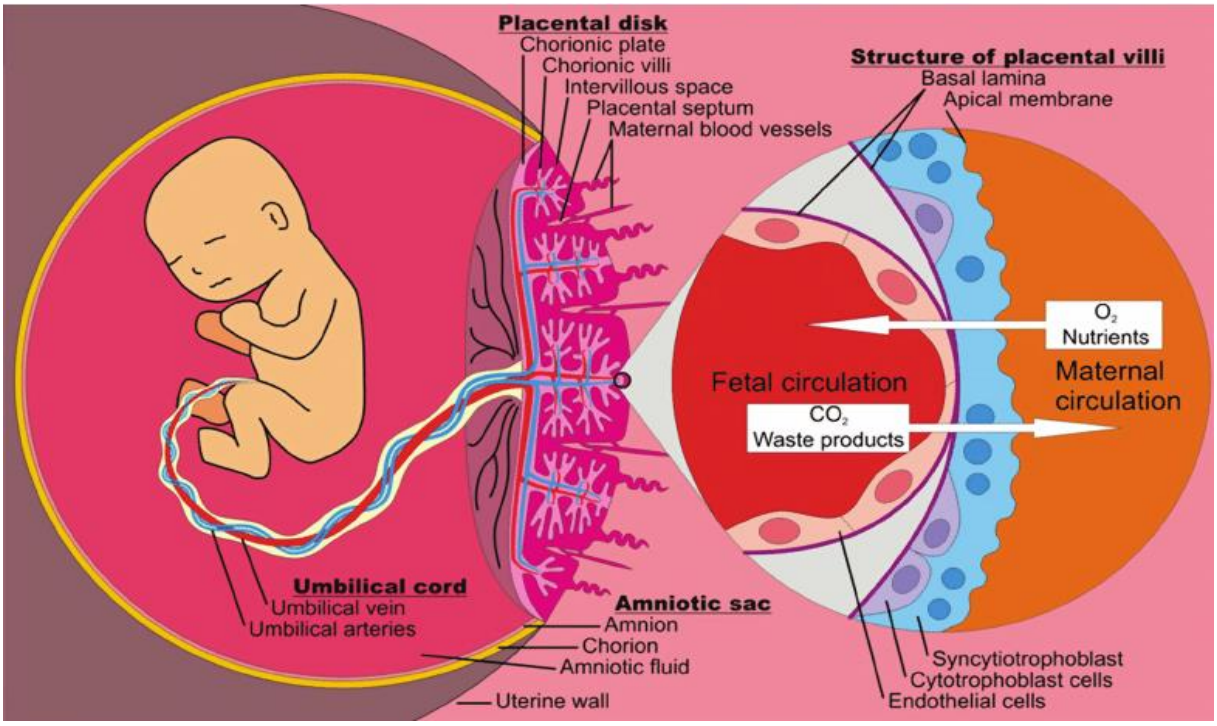

Figure 2: Overview of anatomy and morphology of the human placenta. The close up shows the surface of a placental villi which is covered by a monolayer of syncytiotrophoblasts with underlying cytotrophoblasts. This is the place where the exchange between mother and fetus occurs and is called placental barrier. (Source: https://www.uniaktuell.unibe.ch/2020/what_shapes_our_health_very_early_on/index_eng.html, accessed 21.01.20)

1.3 BeWo cell line

The BeWo cell line is an undifferentiated trophoblast cell line from a human carcinoma that was established in the year 1968 by Pattillo and Gey (Pattillo & Gey, 1968). BeWo cells are able to form a tight polarized monolayer and express microvilli at their apical surface similar to the human trophoblasts (Cerneus & Van Der Ende, 1991). Furthermore they secrete placental hormones including human chorionic gonadotropin, polypeptide hormones, estrogenic and pregestational steroids, estradiol and progesterone (https://www.sigmaaldrich.com/-catalog/product/sigma/-cb_-86082803?lang=de&region=DE, accessed 21.01.2021) BeWo cells can be used to mimic endocrine features and transport mechanisms of the human placenta. However most prominently BeWo cells are used as an *in-vitro* model for trophoblast intercellular fusion and differentiation (Burres & Cass, 1986). These processes can be triggered by the influence of certain inducers such as Forskolin and result in the formation of a syncytium (Rama & Rao, 2003). Based on this attributes, BeWo cells are chosen as a model for the establishment of a functional trophoblast cell layer in this thesis.

1.4 Organ-on-a-chip

Organ-on-a-chip is a microengineered *in-vitro* organ model that mimics the *in-vivo* environment of the respective organ physically and chemically (Kimura et al., 2018). They integrate microengineering, microfluidic technologies and biomimetic principles to create key features of specific human tissues and organs and their interactions (Zheng et al., 2016). Growing knowledge in this fields and about interactions between cells and their environment enable the construction of organ-on-a-chip models with increasing capability to reproduce high fidelity organ function *in-vitro* (Zhang & Radisic, 2017). Although most of the recently developed organ-on-a-chip systems cannot be considered as organs, they are able to mimic specific functional units of the respective organ. This provides a tool for the investigation of fundamental mechanisms in disease etiology, organogenesis and drug effects, improving preclinical safety and efficacy testing and is potentially serving as a replacement for animal testing (Zhang et al., 2018) (Zheng et al., 2016).

1.5 Placenta-on-a-chip

The most important function of the placenta is the exchange of endogenous and exogenous substances. This enables the supply of the fetus with oxygen and nutrients, the excretion of metabolic waste and protection against potentially harmfull agents. This exchange takes place at the placental barrier, as already described in part 1.1. Placental transport has so far been investigated by experimental systems including *in-vivo* animal models, ex vivo placental perfusion and *in-vitro* cell cultures. These methods usually fail to reconstitute physiological conditions of the human placenta, often show the lack of standardization and therefore a high lab-to-lab variability. The placenta-on-a-chip model represents a bioengineering approach that combines microfluidic and microfabrication technologies to recapitulate the organ-specific architecture and physiological microenvironment crucial to placental barrier function (Das C, Lucia MS, 2017). However, in the present thesis only a first step towards the establishment of a placenta-on-a-chip model was done by culturing the BeWo cells under microfluidic conditions. In that way the flow exhibits shear stress to the cells which was shown to regulate differentiation and physiology of syncytiotrophoblasts and extravillous trophoblasts (Brugger & Guettler, 2020).

1.6 Microscopy

During the work of this thesis, fluorescence confocal microscopy was used in addition to conventional fluorescence microscopy. In contrast to conventional fluorescence microscopy, confocal microscopy illuminates not the entire specimen at one time, but only a fraction. In the present work confocal microscopy was used to obtain high-resolution images of cell structures while conventional fluorescence microscopy with a scanner was used to get an overview of the staining results at a lower resolution.

1.6.1 Fluorescence microscopy

A cell biologist is interested to visualize specific cell structures to investigate them subsequently with a microscope. For that antibodies are used that bind specifically to appropriate structures. To visualize the binding location of the antibody a fluorescent molecule (fluorophore) is either bound directly to the antibody (direct immunofluorescence) or to second antibody which binds to the first antibody (indirect immunofluorescence). The fluorochrome can get excited by a lower wavelength and emits light with a longer wavelength what is called the Stokes shift. Using filters allows

the user of a fluorescent microscope to illuminate the specimen with one wavelength and filter the returning light to see only longer wavelength (Lichtman & Conchello, 2005).

1.6.2 Confocal microscopy

Confocal microscopy was pioneered by Martin Minsky during his Junior Fellowship at Harvard University in 1955 (M. Minsky, 1987). The idea of Minsky was to perform point-by-point image construction whereby only a point of light is sequentially focused sequentially across a specimen and some of the returning rays are collected. The illumination of only a single point at a time is avoiding most of the unwanted scattered light that is emitted if the entire specimen is illuminated at the same time. In addition, the light that returns from a specimen passes a second pinhole aperture that is rejecting rays that are not coming from the focal point. In modern confocal microscopes the key elements have stayed the same: the point-by-point illumination and the pinhole apertures. In the meantime advances in optics and electronics have been incorporated and led to improved speed, image quality and storage of generated images (Semwogerere & Weeks, 2005). There are two major techniques to discriminate in confocal microscopy: the image generation from reflecting light or from fluorescence by stimulating fluorophores (fluorescence confocal microscopy), that was used during this work (Nwaneshiudu et al., 2012).

1.7 ELISA

ELISA is the abbreviation of enzyme-linked immunosorbent assay and refers to an antibody-based detection method that is based on an enzymatic color reaction and thus belongs to the enzymatic immunoassays (EIA) (Patel & Gan, 2013). It is derived from the radioimmunoassay (RIA) that was first described by Berson and Yalow (Yalow & Berson, 1960). Because of safety concerns regarding the use of radioactivity, the radioisotope used in RIA was replaced by an enzyme which lead to the modern-day EIA and ELISA (Patel & Gan, 2013). The basic principle of the ELISA assay is the detection of an antigen by an antibody coupled to an enzyme, which converts added substrate and therefore causes a color reaction. However various types of ELISAs have been established with modifications to those basic principle (see Figure 3). There is a direct ELISA where the antibody is bound to a surface which is usually the bottom of a 96-well plate and afterwards directly detected by an enzyme coupled antibody. In

the indirect ELISA the primary antibody binds to the antigen is uncoupled but gets bound by an additional secondary antibody that is coupled to an enzyme (see Figure 3 at the very left). In the case of a sandwich ELISA a capture antibody is bound to a surface and binds an antigen to which in turn binds the secondary antibody, carrying the enzyme. The last type is called competitive ELISA where the antigen in the sample and the antigen bound to the surface compete with each other. The primary antibody is incubated first with the sample, containing the corresponding antigen and after the resulting antibody-antigen complexes are added to wells that have been coated with the same antigen. After this second incubation, unbound antibody is washed off. The more antigen that was in the sample, the more primary antibodies are not able to bind to the immobilized antigen (Patel & Gan, 2013). The ELISA assay is widely used as a diagnostic tool in medicine, as a quality control in various industries and also as an analytical tool in biomedical research.

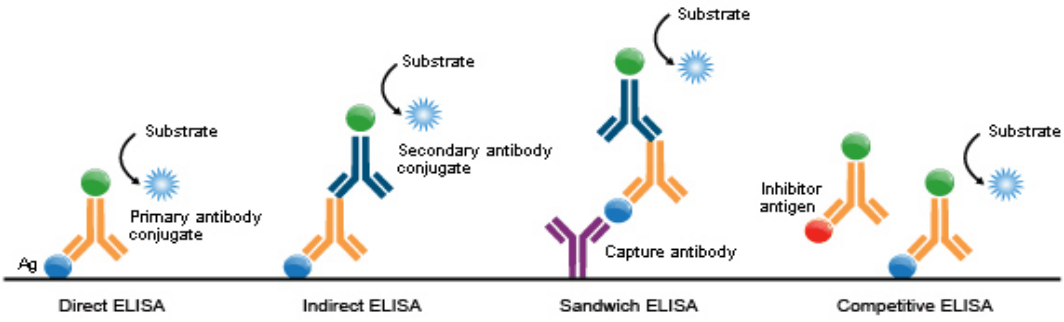

Figure 3: Schemata of the ELISA types "direct ELSIA", "indirect ELISA", "sandwich ELISA" and "competitive ELISA".(Source: http://www.abnova.com/support/resources.asp?switchfunctionid={70196CA1-59B1-40D0-8394-19F533EB108F}, accessed 21.01.2021)

In the present work the concentration of hCG secreted from the BeWo cells in the supernatant was measured with an ELISA. Thereby the sandwich ELISA technique was chosen which is 2-5 times more sensitive than direct or indirect ELISA and also highly specific since two antibodies are used against different epitopes of the same antigen (https://www.bio-rad-antibodies.com/blog/deciding-which-elisa-technique-is-right-for-you.html, accessed 30.01.20).

1.8 Human chorionic gonadotropin

Human chorionic gonadotropin (hCG) is a pregnancy glycoprotein hormone, mainly secreted by the syncytiotrophoblasts covering the chorionic villi. The maternal hCG concentration and glycan structure changes during pregnancy and is therefore widely used as a pregnancy marker in hospital and home settings (Guibourdenche et al.,

2010) (Berger & Sturgeon, 2014). It is known that the hCG secretion of trophoblasts is increasing during the differentiation to syncytyotrophoblasts (Handschuh et al., 2007), therefore it was measured in this thesis with an ELISA as a marker for functional differentiation of the BeWo cells.

1.9 Investigated cellular structures

In the present work the cellular structures CK-7, ZO-1, E-cad, SC-1 and CALHM4 were stained in the static-, respectively microfluidic system and visualized with conventional and confocal microscopy. CK-7, ZO-1 and E-cad were stained in order to evaluate cell growth and differentiation of the BeWo trophoblasts. SC-1, as a representative of the glycocalyx was stained in order to examine expressional differences under static or fluidic conditions as it was already observed for other glycocalyx constituents in the same microfluidic system for endothelial cells by the Rieben group (Luther, 2018). In addition, CALHM4 stainings were carried out and evaluated to gain novel insights of the trophoblastic expression of this structure which is largely unknown so far. The following paragraphs give background information about the aforementioned structures.

1.9.1 Cytokeratin-7

Cytokeratin-7 (CK-7) intermediate filament is a low molecular weight cytokeratin that is highly expressed throughout the trophoblast lineage (Haigh et al., 1999) (Frank et al., 2000) as well as in certain endothelial cell types (Huang et al., 2016). By the virtue of the exclusive CK-7- but absent vimentin expression, CK-7 is used as an accurate intracellular marker to assess the purity of isolated human placental villous trophoblasts by flow cytometry (Maldonado-estrada et al., 2004). For this application our group has the anti CK-7 in stock which could be used well for this thesis to see reorganization of the cytoskeleton in different culturing conditions.

1.9.2 Zonula occludens-1

Zonula occludens-1 (ZO-1) is a protein located at the cytoplasmatic membrane surface of intercellular tight junctions which regulate the paracellular pathway for the movement of ions and solutes. Tight junctions constitute together with adherence junctions and desmosomes the junctional cell complex (Aplin et al., 2009). It is clearly necessary that junctional proteins are involved in the process of syncytial formation, where CTBs fuse

to become STBs to form a tight materno-fetal barrier, which was also stated previously by Pidoux et al. (Pidoux et al., 2010).

1.9.3 Calcium homeostasis modulator 4

Calcium homeostasis modulators (CALHMs) are recently identified large-pore channels that allow the passage of ions and ATP in a voltage dependent manner. The CALHM family consists of six members (CALHM1-6) that are differently expressed throughout the human body. Despite the fact that they play crucial roles in human physiology and pathology the structure and function of CALHM proteins remain mostly unclear (Syrjanen et al., 2020). It was found that the three paralogs CALHM2, 4 and 6 are highly expressed in the human placenta while their role is unknown (Drożdżyk et al., 2020).

1.9.4 E-cadherin

E-cadherin (E-cad) is a Ca^{2+} dependent adhesion molecule that occurs predominantly in epithelial cells and belongs to the family of cadherins (Van Roy & Berx, 2008). Cadherins are essential for the establishment of the epithelial cell shape and maintenance of the differentiated epithelial phenotype (Braga, 2000). Further cadherins play a role in stabilizing cell-cell contacts, embryonic morphogenesis, maintaining cell polarity and signal transduction (Van Roy & Berx, 2008).

1.9.5 Syndecan-1

Syndecan-1 (SC-1) is a cell surface transmembrane heparan sulphate proteoglycan that is predominantly expressed on endothelial cells (Alexander et al., 2000). SC-1 binds to cell surface proteins, cytokines and chemokines and participates in a multitude of processes relevant to inflammation (Go, 2003). Syndecan-1 was found to be expressed in BeWo cells which was stated among others by Szabo et al. (Szabo et al., 2013), Prakash et al (Prakash et al., 2011) and can be looked up in the human protein atlas webpage https://www.proteinatlas.org/ENSG00000115884-SDC1/celltype, accessed 31.01.21)

1.10 Coating materials

The following paragraphs describe the coating materials that were used during the work of this thesis to enable the best possible adherence of the BeWo cells which was of particular importance in the microfluidic system.

1.10.1 Matrigel

Matrigel is a preparation of basement membrane proteins extracted from Engelbreth-Holm-Swarm (EHS) mouse sarcoma which is a tumor, rich in extracellular matrix proteins. The composition is approximately 60% Laminin, 30% collagen IV and 8% entactin and contains also heparan sulfate proteoglycan as well as other growth factors that occur naturally in EHS tumors (http://fscimage.fishersci.com/cmsassets/-downloads/segment/Scientific/pdf/BD/bd_cellculture_matrigel_faq.pdf, accessed 21.01.2021). This constituents make Matrigel to a reconstituted basement membrane that is similar to the decidual ECM insofar that it is rich in laminin and relatively poor in collagen (Tarrade et al., 2002).

1.10.2 Fibronectin

Fibronectin is a glycoprotein of the extracellular matrix that is involved in many physiological processes like cell adhesion, migration, growth and proliferation (Romberger, 1997). Fibronectin was found to be present as free filaments and coating collagen fibers in both, maternal and fetal plasma and throughout the stroma of chorionic villi (Amenta et al., 1986).

1.10.3 Collagen I

Collagen I is one of the most abundant collagens in the human body and the most widely used extracellular matrix protein for coating, facilitating cell attachment, differentiation and migration (Henriksen & Karsdal, 2016) (https://www.thermofisher.com/ch/en/home/life-science/cell-culture/organoids-spheroids-3d-cell-culture/extracellular-matrices-ecm/collagen-i-rat-bovine.html, accessed, 21.01.2021) Collagen I was found to be the basic structural unit of the human placenta, present in the form of cross-banded fibers (Amenta et al., 1986).

2 Hypothesis and specific aims

The aim of this Master project was to establish, adapt and characterize the microfluidic system (Rieben group) for trophoblast cells. Particularly, we wanted to analyze the benefits of a microfluidic system for the establishment of a functional trophoblast cell layer using a microscopic and a secretion approach. Conventional and confocal microscopy was used to characterize differences in cell growth and differentiation using trophoblast-specific biomarkers (CK-7, ZO-1 and E-cad). On the other hand, the effects of trophoblast culturing in a microfluidic system on their secretory capacity was assessed by the quantification of the trophoblast-specific differentiation marker hCG.

In this master thesis the following hypotheses were tested:

- The microfluidic system for endothelial cells (Rieben group) is adaptable for the application in BeWo trophoblast cells (Albrecht group).
- BeWo cells cultured under microfluidic as compared to static conditions exhibit differences in morphology and secretion capacity.

To test these hypotheses the following specific aims were defined:

1. To establish culture conditions optimal for BeWo cell differentiation in static conditions
2. To optimize the staining procedures for high resolution confocal microscopy of BeWo cell structures
3. To adapt the procedures of the endothelial cell microfluidic chip for the usage in BeWo cells
4. To characterize different expression patterns in cellular structures of BeWo cells cultured under static and microfluidic conditions
5. To measure hCG secretion of BeWo cells under static and microfluidic conditions

3 Material and methods

A complete list of used materials and devices can be found in the appendix.

3.1 BeWo Cell culture

The BeWo cells, used for the experiments, were between passage 27 and 36. They were cultured in complete medium composed of DMEM high glucose (4.5g/l glucose) supplemented with 10% FBS and Anti-Anti in a humidified incubator at 37°C and 5% CO_2. The BeWo cells were splitted with Trypsin (see 3.4) once or twice a week between 1:4 and 1:8 at 60 - 80% confluency. For storage the cells were frozen (see kryo conserving of cell cultures) and kept in liquid nitrogen.

3.2 Kryo conserving of cell cultures

First the cells were trypsinized and counted as described in part 3.5. After the cells were counted, they are centrifuged again at 1200 rpm for 5 minutes. In the meantime, the freezing medium composed of 90% FBS and 10% DMSO was prepared and cryo tubes that will be used were labelled with cell type, passage number, date and initials. After the centrifugation was finished the pellet was resuspended in freezing medium to receive the desired cell density. BeWo cells were frozen at 5 mio cells/ml. Then the cell suspension was distributed to the cryo tubes by adding 1ml per tube. Finally the filled cryo tubes were put into an Isopropanol racket that allows a slow cooling and frozen at -80°C. For longer storage the cryo tubes could be transferred to liquid nitrogen (-196°C) after they were frozen.

3.3 Reviving of kryo conserved cell cultures

To get the right frozen vial, the exact storage location of the favored cell line had to be noted down (LN_2 – tank / Tower No. / Box No. / Slot No.). The frozen vial was first held for approximately 30 seconds in the water bath at 37°C. After the partially thawed cells were washed out from the vial by adding warm complete growth medium and transferred to a 15mL Falcon tube where the volume was supplemented to 15mL with complete growth medium. The tube was centrifuged after for 5 minutes at 1200 rpm. The cell pellet was resuspended in 15mL complete growth medium and centrifuged again for 5 minutes at 1200 rpm in order to get rid of most of the DMSO from the freezing medium. Subsequently the pellet was resuspended in ca. 1mL complete

growth medium and transferred to a T75-flask with ca. 10mL prewarmed complete growth medium. Remaining cells in the tube were washed out from the tube with another ca. 1mL complete growth medium and were also transferred to the T75-flask. The cells were homogenously dissolved by slowly up and down pipetting the medium in the T75-flask. After the cells were evenly dispersed over the bottom of the flask. This was done by moving the flask first in a horizontal direction and after in a vertical one. In between the flask was kept still until the waves calmed down. Finally the flask was kept for ca. 10 minutes in the laminar flow so that the cells could adhere before it was transferred to the incubator at 37°C and 5% CO_2. Every flask was labelled with cell line, passage number, date and initials.

3.4 Cell culture splitting

First all the complete growth medium was removed from the flask containing the culture to be split. After the cells were washed with ca. 10mL DPBS in order to get rid of all FBS which inactivates Trypsin. If the cells were cultured in a T75-flask, 2mL 1x Trypsin was added to the flask and evenly distributed over the whole bottom. After the flask was placed in the in the incubator at 37°C and 5% CO_2 for at least 2 minutes whereby it is periodically checked for cell detachment. It is useful to accelerate the cell detachment by tapping the flask by hand at the side. As soon as all cells were detached 10mL of complete growth medium was added in order to inactivate the Trypsin. The cell suspension was transferred after to a 15mL tube where the volume was supplemented to 15mL with DPBS. Subsequently the tube was centrifuged at 1200 rpm for 5 minutes. After the pellet was resuspended in 10mL complete growth medium from which the desired amount was transferred into a new flask containing prewarmed medium and then the total volume was adjusted to 12mL in the case of a T75-flask (eg. for a 1:5 dilution 2mL of the cell suspension were transferred to a flask containing 10mL of prewarmed complete growth medium). Subsequently the cells were homogenously dissolved by slowly up and down pipetting the medium in the T75-flask. After the cells were evenly dispersed over the bottom of the flask. This was done by moving the flask first in a horizontal direction and after in a vertical one. In between the flask was kept still until the waves calmed down. Finally the flask was kept for ca. 10 minutes in the laminar flow so that the cells could adhere before it was transferred to the incubator at 37°C and 5% CO_2. Every flask was labelled with cell line, passage number, date and initials.

3.5 Cell counting

First the BeWo cells were trypsinized and pelleted as described in part 3.4. During centrifugation the Neubauer counting chamber was prepared. For that the Neubauer chamber and the glass cover was cleaned with 70% - EtOH and after the glass cover was placed in the center of the Neubauer chamber. When the centrifugation is done the cell pellet was dissolved in 1-3mL of complete growth medium, depending on the expected amount of cells. Then 10µL of the cell suspension was dissolved in 90µL Trypan blue. During both of these dilution steps extreme care must be taken in order to transfer only cell suspension from a cell suspension that is as homogeneous as possible. This was assured by continuously up and down pipetting during those steps. Then 10µL of Trypan blue – cell suspension was carefully pipetted into to the Neubauer using capillary forces. Finally the cells of all 4 squares were counted under the light microscope at 10X and subsequently the cell concentration was calculated with the following formula: (counted cells of all four squares x 10 x 10^4) / 4 = amount of cells per mL complete growth medium.

3.6 Microfluidic chip

The basic procedure for the establishment of a microfluidic chip experiment was taken over from the protocols of the Rieben group (see appendix: “microfluidics protocol”). The paragraphs 3.6.1 to 3.6.6 also include the adjustments in the respective working steps that have resulted from this work. The steps “Preparing the tubings” and “Connecting the pump” were not changed from the original procedure and therefore not described here.

3.6.1 In house production of chips

First the silicon elastomer and the curing agent were mixed in a proportion of 10:1. For one petri dish that results in 4 microfluidic chips (4 channels each) 35g silicon elastomer was mixed with 3.5g curing agent (see Figure 4). Those components needed to be mixed very well in a large weighing boat with a plastic spoon for at least 3 minutes. After the PDMS in the weighing boat was set under vacuum. Due to the vacuum the trapped air expanded and finally left the

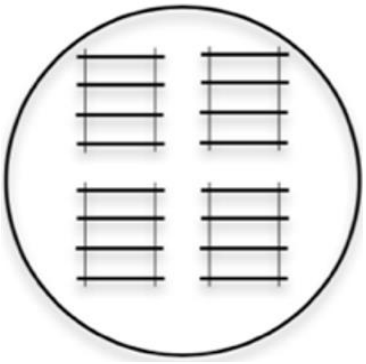

Figure 4: Schemata of one petri dish containing 4 microfuidic chips with 4 channels each.

PDMS. During this process the vacuum had to be released several times in order to prevent overflow of the PDMS due to the expansion. In the meantime mold needles (Ø 550µm =24G) and support needles (Ø 120µm= acupuncture needles) were prepared by cutting the steel part as close as possible to the plastic part. For one microfluidic chip (4 channels) 4 mold needles and 2 support needles were needed (compare Figure 4). After cutting the needles were put into a petri dish filled with Isopropanol until use. As soon as all air was released from the PDMS it was poured into a petri dish which was again put under vacuum to eliminate newly created air bubbles. Then first the support needles were placed on the bottom of the petri dish and after the mold needles were placed orthogonally on top of the support needles (compare Figure 4). The alignment of the needles could be further optimized with forceps as long as the PDMS is not cured. To cure the PDMS the petri dish was carefully placed into an incubator at 60°C and incubated overnight. On the next day the solidified PDMS was taken out of the petri dish and cut into four equal chips. After all needles were carefully removed with forceps. Next inlet and outlets of the channels were punched with a Ø 2.0mm biopsy puncher with a distance of 1cm in between. For this step care must have been taken to ensure that the punched holes are vertically and hit the channels. In a last step, the small channel wholes at the sides of the chip were closed using PDMS. For this 5g of PDMS was prepared as described above (whereby in this step it was not that important to remove the air that picky) and put with a 10µL pipette tip on the small channel holes which after got closed by the PDMS due to capillary forces. Here care must have been taken to ensure that no PDMS was put on the underside of the chip, otherwise the uneven surface would make bonding difficult. Finally, the chips got incubated again overnight at 60°C to cure the newly applied PDMS.

3.6.2 PDMS-bonding

The finished microfluidic chips resulting from the procedure described in part 3.6.1 was cut with a scalpel so that every single part contains a microchannel. Next the microfluidic chip parts were taped with one piece of scotch tape on the bottom side while the channel side was kept on top. Thereby a small space was left between the single microchannels. Then a glass slide was cleaned by wetting it with dH_2O, after with soap water, rinsed with dH_2O and with Isopropanol. After the glass slide was dried with a nitrogen gun, whereby it was carefully blown in the direction of the slide to avoid breaking it. Subsequently the microfluidic chip and the glass slide was placed in the

oxygen plasma cleaner. Then the oxygen tank, the vacuum pump, the pressure indicator and the plasma cleaner were turned on and it was waited until the pressure the pressure decreased until ca. 300 mTorr. As soon as this pressure was reached the O_2 valve was brought into position and it was waited until the pressure stabilizes at ca. 650 mTorr. Arrived there, plasma was turned on to a high level and it was incubated for 3 minutes under oxygen plasma. After 3 minutes the valve was opened slowly to let the pressure come out. As soon as the oxygen plasma cleaner could be opened microfluidic chip and glass slide were taken out and as quick as possible the microfluidic chip was turned over by holding on the tape and pressed onto the glass slide

3.6.3 Covalently cross-link Fibronectin and Collagen I to PDMS

The PDMS surface was turned from hydrophobic to hydrophilic by adding 5% APTES to the channels (silanization) immediately after bonding. After 20 min incubation at room temperature the channels were washed with dH_2O and treated with 0.1% Glutaraldehyde for 30 min at room temperature to provide a crosslinking substrate for extracellular matrix proteins. Next the channels were washed 3 times with dH_2O and replaced by 50µg/ml fibronectin in PBS and incubated for 1h at 37°C. Subsequently the channels were filled with 100µg/ml Collagen I in 0.02N Acetic acid without a washing step in between and incubated for 1.5h at room temperature. For both coatings the channel flipped after 5, 15, 30 and 45 minutes as described in 4.3.2 on p.49. Finally, the channels were filled with DMEM-HG complete medium and the whole microfluidic chip was placed in the incubator at 37°C to allow equilibration for at least 30 minutes before cell loading.

3.6.4 Coating with Matrigel

Matrigel needs to be utilized at 4°C during the whole application because it forms gel very quickly at room temperature. Therefore also tips, tubes and medium for dilution must be kept at 4°C. Matrigel was diluted 1:20 (ca. 12.2mg/mL) in cold DMEM-HG basal medium in a pre-cold tube. The diluted Matrigel was added 3 times to the channels using pre-cold tips and after the channel was incubated at 37° for 30 minutes to form the gel. After incubation the channel was flushed 3 times with DMEM growth medium and incubated for at least 30min filled with media at 37°C for equilibration.

3.6.5 Cell seeding

BeWo cells were harvested and adjusted to a cell density of 2 mio cells/ml. After this cell suspension that should be as homogeneous as possible was put dropwise into the inlets using a 200µl pipette. The drops were sucked through the microchannels via the outlets using also the 200µl pipette. After repeating this step 3 times the microfluidic chip was incubated first top facing down and after top facing up for 30 minutes each at 37°C. In between new cell suspension that was kept also at 37°C in the mean time was added the same way as the first time. After that 1h total adhering step the channels were washed in order to get rid of unattached cells. Because the pump got only connected on the next day the medium needed to be changed in the evening of the cell seeding day as well in the morning on the day the pump was connected.

3.6.6 Adaption of flowrate to physiological value

With following formula, it was calculated that a flowrate of 170µL/minute leads to a shear rate of 2 dyne/cm^2 in the present system:

$$\tau = \frac{4\mu\, Q}{\pi r\text{^}3}$$

τ	= shear rate	= 2 dyne/cm^2
µ	= viscosity	= ~ 1 for DMEM-HG
Q	= flow rate	= 170µL/minute
π	= Pi	= 3.12159
r	= radius	= 275µm

Because the flowrate depends not only on the rpm value entered at the pump but also on the tightness the pump heads get screwed to the pump (compare part 0), it had to be adjusted for every channel in every experiment. To do this, the flow through was collected for one minute in a 1ml tube and its volume was determined with a 200µl pipette. After that, adjustments had to be made up or down. Experience has shown that the pump had to be set to around 2 rpm to achieve a flow rate of 170µl.

3.7 Chamber slide time course culturing

A chamber slide consists basically of a single microscopic slide with one or more defined compartment defined by removable chambers. This allows to cultivate, fixate and stain of adherent cells similar to well plates. The advantage is that the chamber(s)

can be removed after staining which allows a better evaluation and side-by-side comparison under the microscope. In the present work 8-chamber glas slides from SPL® were used (see Figure 5).

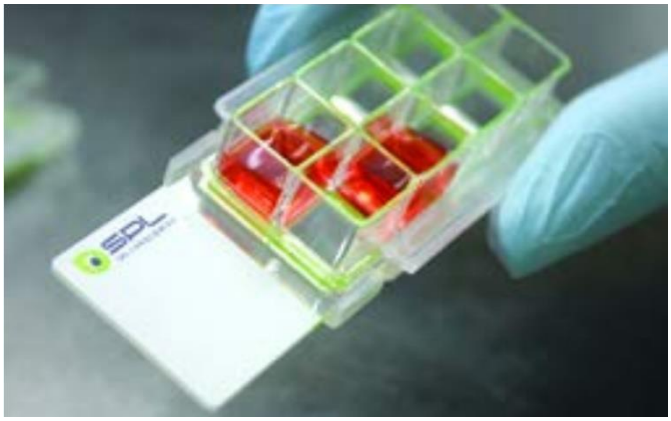

Figure 5: Picture of an SPL® 8-chamber slide. (source: https://www.amazon.com/SPL-Culture-Chamber-0-2-0-6-Treated/dp/B084GCHB5F)

First the BeWo cells were counted as described in part 3.5. Next the amount of BeWo cells and the volume that are needed was calculated. For one chamber 50`000 BeWo cells were seeded in 300µl DMEM-HG complete growth medium. For a time course experiment of 72h Forskolin stimulation 7 slides with 8 chambers each were needed (16h culturing without Forskolin and 40h, 64h, 88h once with and once without Forskolin). Therefore 2.8 x 10^6 BeWo cells were diluted in 16.8ml DMEM-HG complete growth medium. The cells suspension was then distributed to the chamber slides by adding 300µl per chamber. Thereby care was taken to keep the suspension homogeneous at all times by continuously pipetting up and down. Directly after seeding the chamber slides were not moved for 15 minutes to allow the BeWo cells to adhere evenly distributed before they were placed in the incubator at 37°C. On the next day after a growth phase of approximately 16h the first slide was fixated as described in part 3.9. For all other slides fresh media is added with 100µM Forskolin (see part 3.8) or without respectively. All slides were then successively fixed at the corresponding time points and stored at 4°C before they were stained all together (see part 3.10.

3.8 Forskolin stimulation

A stock solution of 100mM Forskolin in 95% EtOH was used for the Forskolin stimulation. This stock solution was then diluted 1:1000 in complete growth medium to receive a concentration of 100µM. In this way the solvent concentration on the cells was minimized. The complete growth medium with 100 µM Forskolin was added to the

cells in a chamber slide after they have grown without Forskolin for at least 16h or to the microfluidic chip already with the first media change (see part 3.6.5). The cells were incubated with the Forskolin in the chamber slide for 24h, 48h and 72h and in the microfluidic chip for 48h.

3.9 Cell fixation

First all of the complete growth medium was removed from the cells. Then they were washed 3 times with DPBS that was prewarmed to 37°C. Thereby the largest possible volume of DPBS is chosen, corresponding to the size of the culture vessel. While the DPBS from the last washing step is kept on the cells the 16% Formaldehyde stock solution gets diluted to 4%. For that 1 ampoule (1mL) and 3mL DPBS at 37°C is added to a 15mL Falcon tube. Then the DPBS is replaced by 4% Formaldehyde that is added at a volume that covers the cells generously and the cells are incubated for 20 minutes at room temperature. After the Formaldehyde is removed and the cells are washed 3 times with DPBS. The cells can now be stored in DPBS at 4°C.

3.10 Cell staining

Before the cells were stained they needed to be fixated (see 3.9). Depending on the location of the structures to be stained the cells first needed to be permeabilized. If intracellular structure were wanted to be stained a permeabilization step was needed (except for DAPI staining which can permeate through the membrane). For the permeabilization 0.5% Tween 20 in DPBS was added to the cells at a volume that covers the cells generously followed by an incubation step of 30 minutes at room temperature. After the permeabilization buffer was removed and the blocking solution which consists of 5% BSA and 0.5% Tween 20 in DPBS was added at the same volume to the cells. Then the cells were incubated with the blocking solution for 60 minutes at room temperature. In the meantime, the antibody dilutions could be done in the blocking solution. In order to safe antibody, for the dilutions always the smallest possible volume was chosen that was able to fully cover the cells. In general, the cells were incubated with the primary antibodies overnight for at least 12h at 4°C with gentle shaking. After the secondary antibodies were incubated with the cells for at least 1h at room temperature with gentle shaking followed by the incubation with DAPI for 20 minutes at room temperature with gentle shaking. All antibody and DAPI incubations were done in the dark. After each staining step the cells were washed with the

blocking/staining solution 3 times for 10 minutes with gentle shaking at room temperature in the dark.

3.11 Chamber slide mounting

The 8-chamber slide could be mounted after the chamber frame and the seal was removed from it. As a first step the whole area of the part that was needed to be mounted was covered with plenty of water in order to minimize the inclusion of air during mounting afterwards. Then 30µL of Vectashield® mounting media was pipetted on one side of the slide. Subsequently the coverslip was placed. The cover slip was first carefully brought into contact with the mounting media and then slowly dropped lengthways to displace the water underneath. Afterwards the remaining air below the coverslip could be displaced with careful pressure. For an optimal result the mounting media was first cured for 15 minutes at room temperature and after placed at 4°C to allow complete curing. For faster results it was also possible to cure the mounting media for approximately 45 minutes at room temperature. Regardless the procedure, the mounting media was always cured protected from light.

3.12 Fluorescence imaging

The fluorescence images of the present work were taken with the 3DHistech Slide scanner (Pannoramic 250 Flash II) or the Carl Zeiss confocal microscope (LSM 710 with Airyscan). The images were analysed and processed with the CaseViewer 2.4 software (scanner images) or the ZEN Imaging software (confocal images).

3.13 Nuclear size analysis

The nuclear size of BeWO cells was analyzed using ImageJ software. If images were compared with each other, every image need to be in the same format and taken at the same magnification. After the image was opened with the ImageJ software the color channels needed to be split, whereas only with the channel of the DAPI was proceeded. Next a binary picture was created by adjusting the threshold number to a reasonable value so that all nuclei appear in its full size in dark on a white background. In a next step the nuclei that are in close contact were separated in order to measure them as single objects using the watershed option. Finally, the particle analysis could be started whereas the lower size limit (pixel^2) had to be entered to exclude artifacts in the count. The counting results were exported and further proceeded in Excel.

4 Results

The following results part is divided into three sections. The first part concerns the static chamber slide system, the second one the microfluidic system and the third one the hCG secretion of the BeWo cells for both systems. For the two first parts the respective method establishment and after the staining and secretion results are shown. This setup basically reflects the procedure during the present work in which both systems were established so that they could be compared in terms of morphological and secretory aspects.

4.1 Chamber slides: Method establishment

The following chapter describes the results of the time course experiment method establishment in chamber slides which was done in order to compare this static system after to the microfluidic system. Additionally, it includes the results of the staining optimization that was done in chamber slides and used for both systems.

4.1.1 Comparable coating of BeWo cells using four different coating matrices

In order to find the most suitable coating for BeWo cells which later could also be used for microfluidic chips, different coating compositions are tried on glass slides. The same amount of BeWo cells was seeded to differently coated chambers (conditions listed in Table 1) or non-coated ones in duplicates whereas one of the duplicates was stimulated with Forskolin for 48h and the other one was kept unstimulated. The evaluation under the light microscope revealed, that the BeWo cells were able to grow on all coatings very well. There was no remarkable difference in adherence, growth or differentiation of the BeWo cells between different coatings and non-coated chambers. Based on this finding coatings were waived for upcoming chamber slide experiments in order to save time and money.

Table 1: Coating compositions applied to glass chamber slides in order to find best coating condition for BeWo cells regarding adherence and growth. The tested coating materials were Fibronectin, Collagen I and Matrigel.

Coating matrices	**Applied concentrations**
No coating	-
Fibronectin + Collagen I	0.05mgL + 0.1mg/mL
Collagen I	0.05mg/mL
	0.1mg/mL
	0.2mg/mL
Fibronectin	0.025mg/mL
	0.05mg/mL
	0.1mg/mL
Matrigel	0.1mg/mL
	0.2mg/mL

4.1.2 50`000 cells/chamber found to be most suitable seeding density for time course experiments

An optimal seeding density had to be found that is not too low to see intercellular interactions but also not too high in order to prevent overgrowth in time course experiments. In general, it was decided to seed the same amount of cells to all chambers in a time course experiment for chambers that will be stimulated with Forskolin or untreated control and for all. In this way also the cell proliferation could be assessed as an indication of the effectiveness of Forskolin which inhibits cell division. In this context cell amounts ranging from 30`000 up to over 60`000 cells were seeded in the chambers that comprise 0.98cm^2 whereas 50`000 cells/chamber were found to be most suitable. Different seeding results are depicted Figure 6. Figure 6 (A) shows a chamber with BeWo cells that were too sparsely seeded were no cell clusters were formed and therefore intercellular interactions cannot be evaluated. In addition, it was observed that BeWo cells that are lacking intercellular interactions with cells in close proximity to each other are slower in proliferation. Figure 6 (B) shows a chamber where BeWo cells were seeded at a too high density. Under this condition the cells overgrow within the first 48h which leads to multilayers and delamination at the edges.

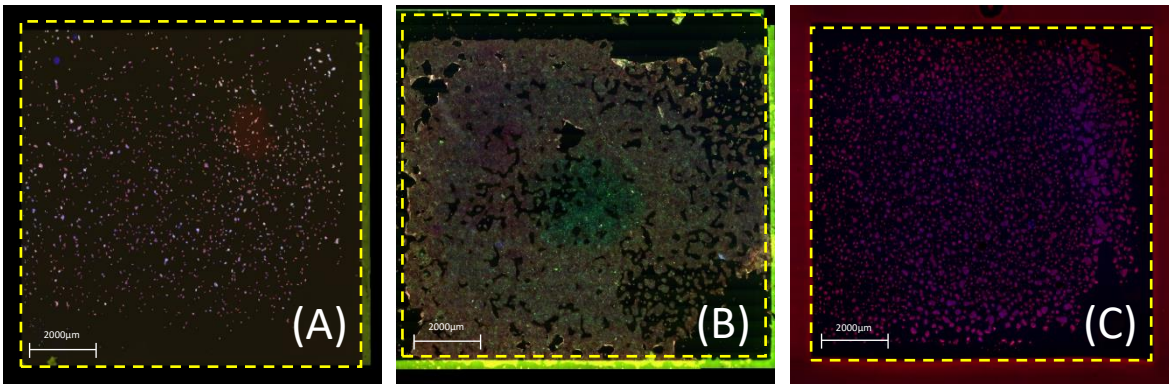

Figure 6: Scans of different seeding densities in chambers of a chamber slide. The yellow dashed line indicates the borders of the chambers. A) Scan of 30`000 cells seeded in a 0.98cm2 chamber after 48h of growth. Cells were stained for CK-7 (green), ZO-1 (red) and nuclei (blue) B) Scan of 60`000 cells seeded in a 0.98cm2 chamber after 48h of growth. Cells were stained for CK-7 (green), ZO-1 (red) and nuclei (blue) C) Scan of 50`000 cells seeded in a 0.98cm2 chamber after 48h of growth. Cells were stained for CALHM4 (red) and nuclei (blue). Picture: Histech scanner at 1X.

Overgrowing BeWo cells are extremely sensitive for delamination during fixation and staining and can easily get lost during those procedures. Beside of this issue, the scanner is not able to bring all cells in focus in one picture because 2D pictures are taken focusing on one focal plane. Figure 6 (C) shows a chamber with an optimal cell density where cell clusters as well as single cells can be observed (see close up in Figure 7) which allows a broader spectrum of investigations compared to the other two conditions discussed.

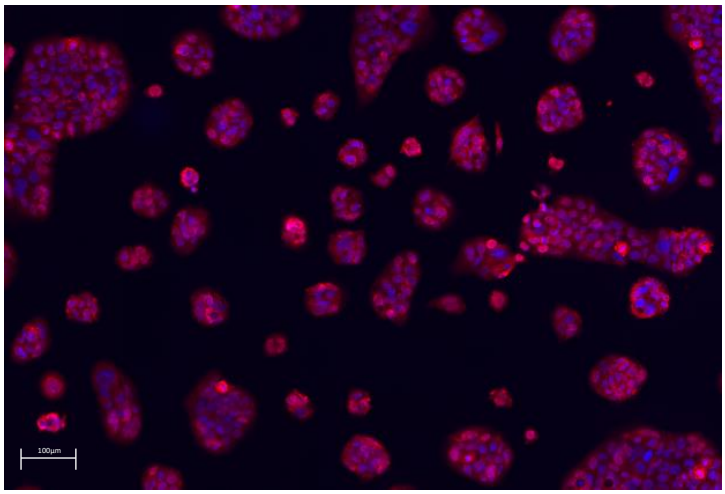

Figure 7: Closeup of Figure 6 (C) that shows a chamber with an optimal cell density where BeWo cell clusters as well as single cells can be observed. Cells were stained for CALHM4 (red) and nuclei (blue). Picture: Histech scanner 10X

4.1.3 15 minutes rest allow even cell distribution in chambers

Another aspect of an optimal seeding is that the cells adhere evenly distributed. To achieve this the slide must be held steady while the BeWo cells attach to the surface which was found out to happen within 15 minutes. Therefore, the chamber slide must not be moved within this time frame after seeding. A bad example where it was not kept to this time frame is depicted in Figure 8. Obviously, with this handling the BeWo cells aggregate in the center of the chamber.

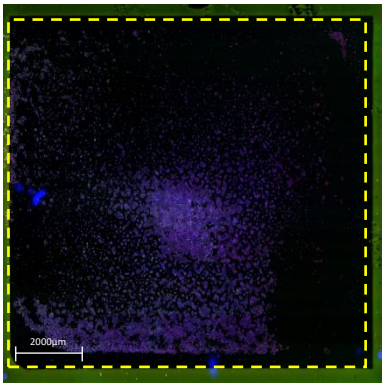

Figure 8: Scan of a chamber that show cell aggregation in its center. The yellow dashed line indicates the borders of the chambers. 50`000 cells were seeded in a 0.98cm^2 chamber. Cells were stained for CK-7 (green) and ZO-1 (red).

4.1.4 Organization of time course experiments on separate slides

In the first experiments, a Forskolin time course experiment was tried to fit on one single 8-chamber slide. In this setup the cells in chamber 1 and 5 were fixed after 24h culturing time, 2 and 6 after 48h, 3 and 7 after 72h and 4 and 8 after 96h (according to Table 2). Chamber 2, 3 and 4 were treated with Forskolin for 24h, 48h and 72h respectively whereas chambers 6-8 serve as controls for corresponding treatment time points. When following this procedure care must be taken to ensure that the cells that are still being cultured do not get contaminated by Formaldehyde which is toxic to cells. This risk was avoided by closing the chambers that are not fixed at respective time point with a tape during fixation and after fixation closing the fixed chambers.

Table 2: Setup of a Forskolin time course experiment with BeWo cells in an 8-chamber slide. BeWo cells were cultured for 24h, 48h, 72h and 96h with Forskolin or without respectively.

	24h culturing time	48h culturing time	72h culturing time	96h culturing time
8-chamber Slide	Chamber 1 No Forskolin	Chamber 2 24h Forskolin	Chamber 3 48h Forskolin	Chamber 4 72h Forskolin
	Chamber 5 No Forskolin	Chamber 6 No Forskolin	Chamber 7 No Forskolin	Chamber 8 No Forskolin

Another fact that became a problem was that during each time point fixation the whole chamber slide was left for at least 20 minutes outside of the incubator. Therefore, the cells cultured for 96h were standing outside of the incubator for 3 times 20 minutes before they are fixed themselves. As it turned out later this was the reason why the cells looked less viable and detached with increasing cultivation time. To get around this issue the time course was distributed to several chamber slides for further experiments. With this measure each chamber slide includes a single time point and stays in the incubator during the whole respective time course of Forskolin stimulation.

4.1.5 Intensified washing and blocking reduced staining background

The staining procedure was based on the staining protocol of Sampada Kallol (see “Staining protocol Sampada Kallol” in appendix). However certain optimizations have been made in order to achieve better results. One of them was to intensify the washing procedure. In Sampadas protocol the washing was performed by rinsing the cells 3 times with the staining solution. This procedure was optimized by prolonging each washing step to 10 minutes with gentle shaking. In general, during all incubation steps (permeabilization, blocking and antibody binding) gentle shaking was included in the protocol. Another adjustment concerns the staining solution itself. In the adopted protocol the blocking solution contains 5% BSA whereas this value has been reduced to 1% for the staining solution. Using the same solution with 5% BSA for blocking and staining let to reduced background signal by further minimizing unspecific antibody binding and kept things simpler by using only one solution for both steps.

4.1.6 Mounting medium plays critical role in staining imaging quality

Another factor that turned out to be critical for staining image quality was the choice of the mounting media. Initially Aquatex® was used to mount the chamber slides until it was observed that it hardly protects the fluophores from bleaching. This became particularly obvious when the live view of the Histech scanner software was used to

define the exposure time for the CK-7 staining (AF488). Within a few seconds the field of view apparently lost its intensity while it was illuminated. Figure 9 (A) shows a scan of a chamber of chamber slide where dark bleaching spots are visible in the CK-7 staining (AF488) at the places which were previously illuminated during live view. To assure this finding an experiment was set up where a strip of the chamber was first exposed to 2 seconds exposure time of the light source and after the whole area was scanned (see Figure 9 (B)). A bleaching path has clearly emerged there where the CK-7 staining (AF488) was previously exposed to the light source.

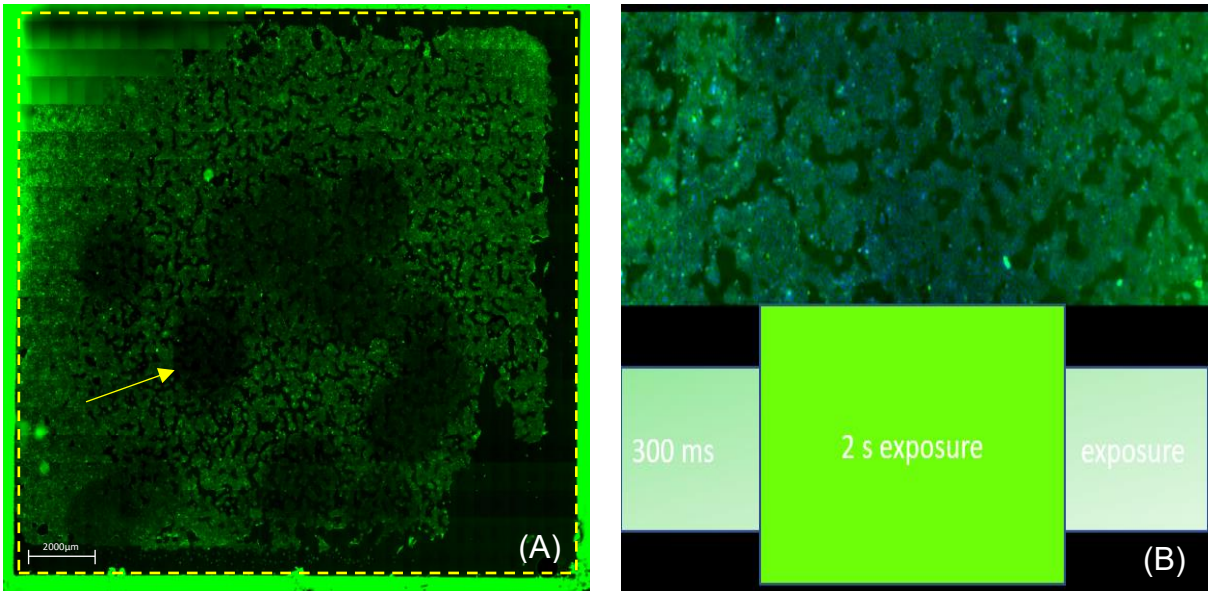

Figure 9: Scans of chamber slide chambers, mounted with Aquatex® that show bleaching of the Alexa Fluor 488 coupled to anti-CK-7 due to exposure to light of the HXP120 short-arc lamp of the Histech scanner. A) Visible are dark spots (bleached) in a scan (one is marked with a yellow arrow as an example) that were induced by exposure to the light source prior to the scan by using the live view function. The yellow dashed line marks the border of the chamber. B) Visible is a bleaching path that was induced by 2 second exposure of the staining to the light source prior to the scan. Cells were stained for CK-7 (green) and nuclei (blue). Picture: Histech scanner 1X.

In a next step the previously used Aquatex® mounting media was compared to Vectashield® mounting media. The resulting images (see Figure 10) show huge differences in quality. While in the picture of the Aquatex® mounted chamber, which appears very blurred, the light seems to be very strongly scattered, the Vectashield® mounting enabled a much clearer imaging (compare Figure 10 (A) and (B)).

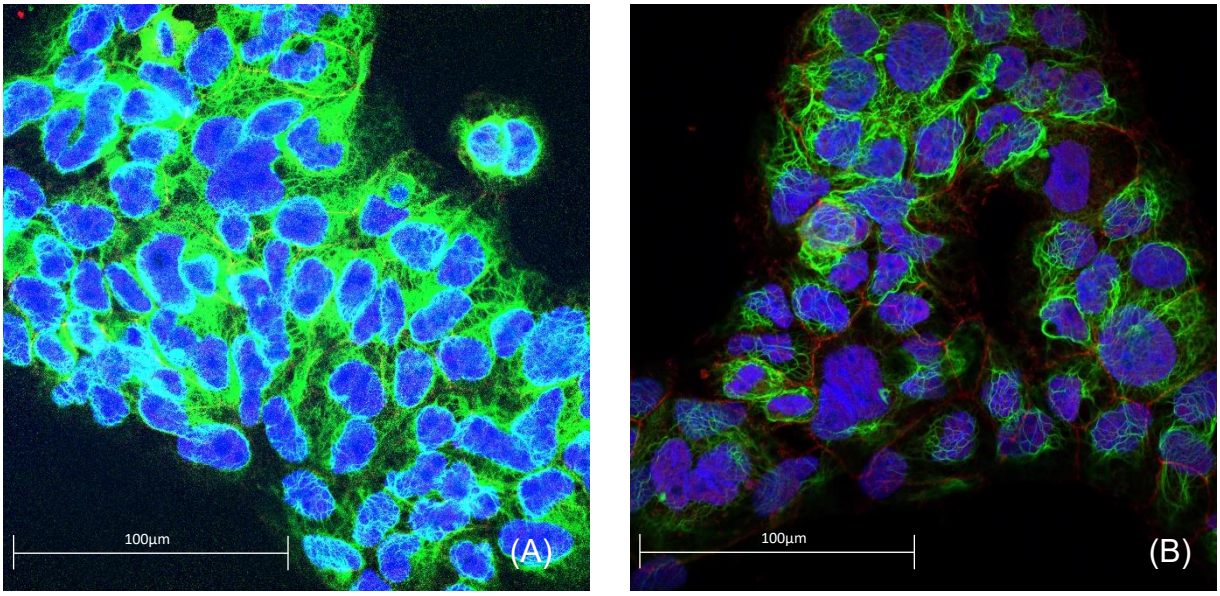

Figure 10: Confocal pictures that compare chamber slides with BeWo cells that were mounted with Aquatex®(A) or Vectashield® (B). Cells were stained for CK-7 (green), ZO-1 (red) and nuclei (blue). Picture: Zeiss confocal microscope 40X.

4.2 Chamber slides: Staining results

In this chapter the staining results are described that were obtained by staining of the cellular structures CK-7, ZO-1, E-cad, SC-1 and CALHM4 of the BeWo cells cultured in chamber slides.

4.2.1 CK-7

In some cases, it was observed that multiple nuclei are enclosed by the same cytoskeleton meshwork (see close ups in Figure 12). This observation can be made more often in the Forskolin stimulated BeWo cells than in the non-Forskolin stimulated ones. Additionally, nuclei of STB-BeWo cells turned out to be enlarged compared to the ones of CTB cells (see Figure 11). Forskolin seem to have an effect already within the first 24h as already at this time point multinucleated cells were observed within stimulated cells but not in the untreated control. The number of dividing cells captured on the scans is higher among non-Forskolin stimulated cells than among Forskolin stimulated cells.

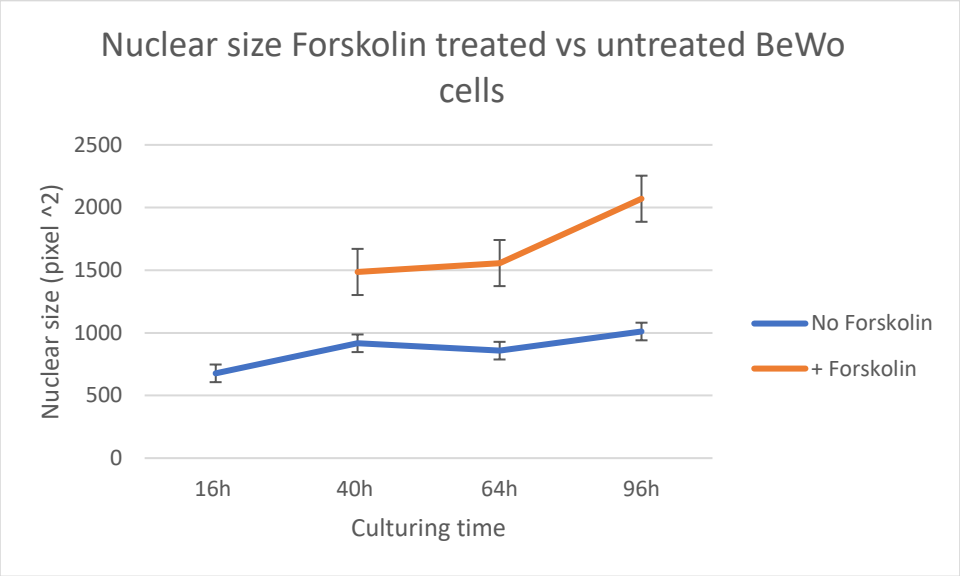

Figure 11: Graph showing nuclear size means of Forskolin treated vs untreated BeWo cells during time course. Nuclear size was measured in pixel^2 with ImageJ using time course images that are depicted in Figure 12.

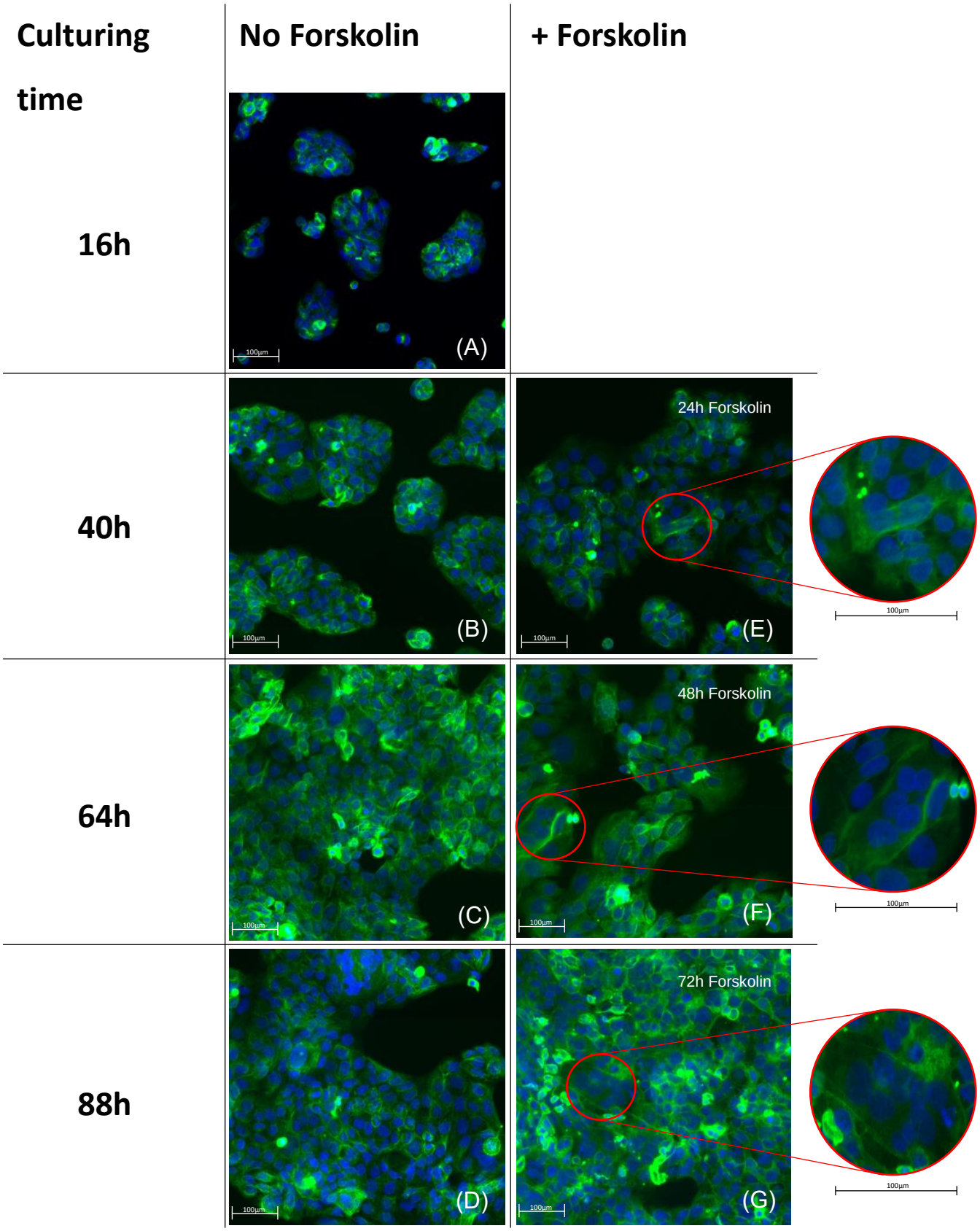

Figure 12: Differentiation of CTB-BeWo cells to STB-BeWo cells directed with Forskolin stimulation. Stimulated cells (A-D) are compared to unstimulated cells (E-G) with the same culturing time. Cells are stained for CK-7 (green) and nuclei (blue). For the marked areas in pictures E-G close ups were added to the right. Pictures: Histech Scanner 20X

The staining of CK-7 revealed that a large rearrangement of this filaments takes place during cell division. In Figure 13 (A) and (B), CTB-BeWo cells are depicted in their meta- respectively anaphase state. It seems like the CK-7 meshwork gets first disrupted in order to aggregate close to the cell membrane in bigger filaments during metaphase and after gets reorganized in an oval shape in direction of the two poles during anaphase.

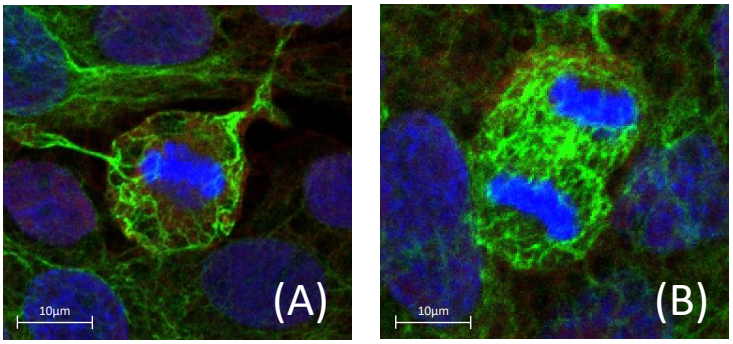

Figure 13: Confocal pictures showing the cytoskeletal organization of BeWo cells in their metaphase- (A) and anaphase -state (B). Cells were stained for CK-7 (green) and nuclei (blue). Pictures: Zeiss confocal microscope 40X.

Further it could be observed that the cytokeratin network spans several cells which becomes even clearer when looking at the confocal pictures of the CK-7 staining. In Figure 14, one example where the cytoskeleton spans over cell borders that are indicated by the ZO-1 staining is marked with a yellow circle.

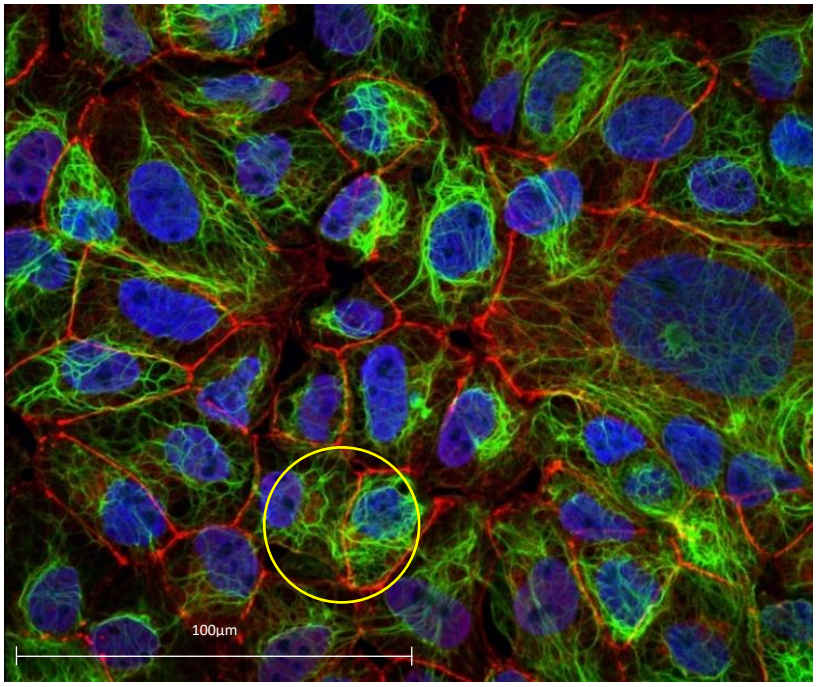

Figure 14: BeWo cells that were cultivated for 40h and stimulated for 24h with Forskolin. Cells were stained for CK-7 (green), ZO-1 (red) and nuclei (blue). The yellow circle marks an example where the cytoskeleton spans over cell borders that are indicated by the ZO-1 signal. Picture: Zeiss confocal microscope 40X.

4.2.2 ZO-1

It can be observed that during the time course (depicted in Figure 16) the specific intercellular ZO-1 staining signal increases with culturing time but decreases during the process of differentiation. During the process of cell fusion ZO-1 junctions are broken between fusing membranes as it is also shown in Figure 15. Circle number 1 possibly indicates an ongoing ZO-1 breakdown in the intercellular space between two fusing cells whereas circle number 2 marks multiple nuclei that are possibly enclosed by a single membrane as there is no ZO-1 signal visible between them.

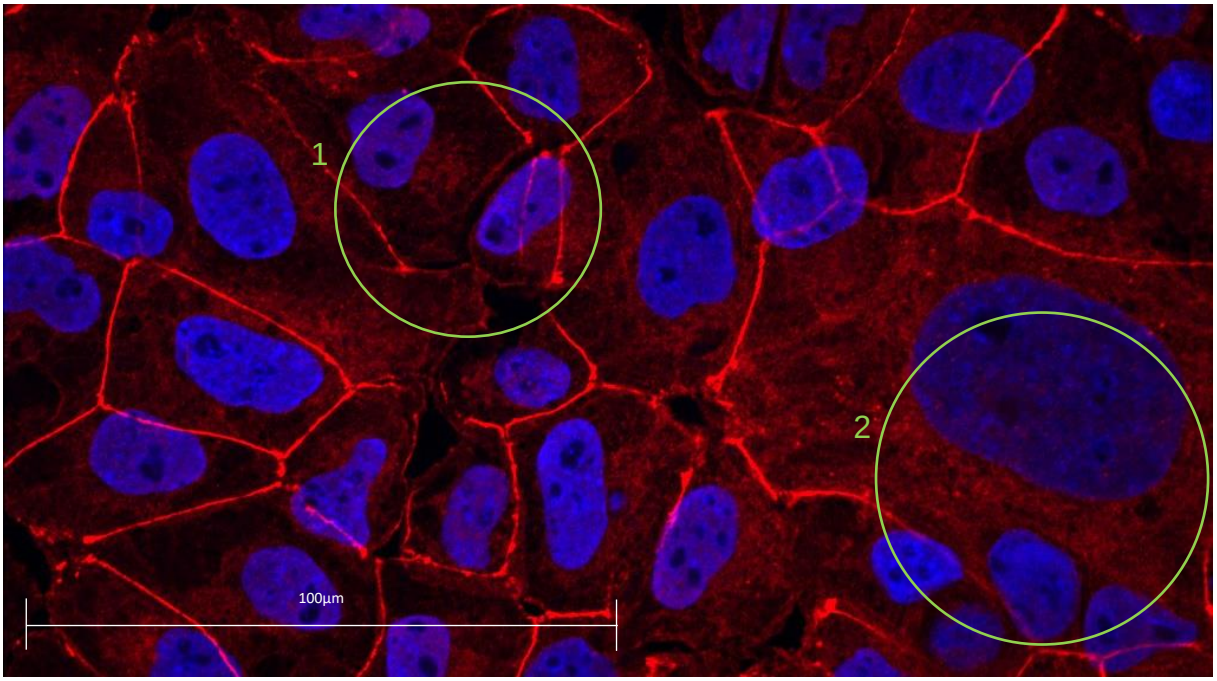

Figure 15: BeWo cells that were cultivated for 40h and stimulated for 24h with Forskolin. Cells were stained for ZO-1 (red) and nuclei (blue). Circle number 1 possibly indicates an ongoing ZO-1 breakdown in the intercellular space between two fusing cells whereas circle number 2 marks multiple nuclei that are enclosed by a single membrane. Picture: Zeiss confocal microscope 40X.

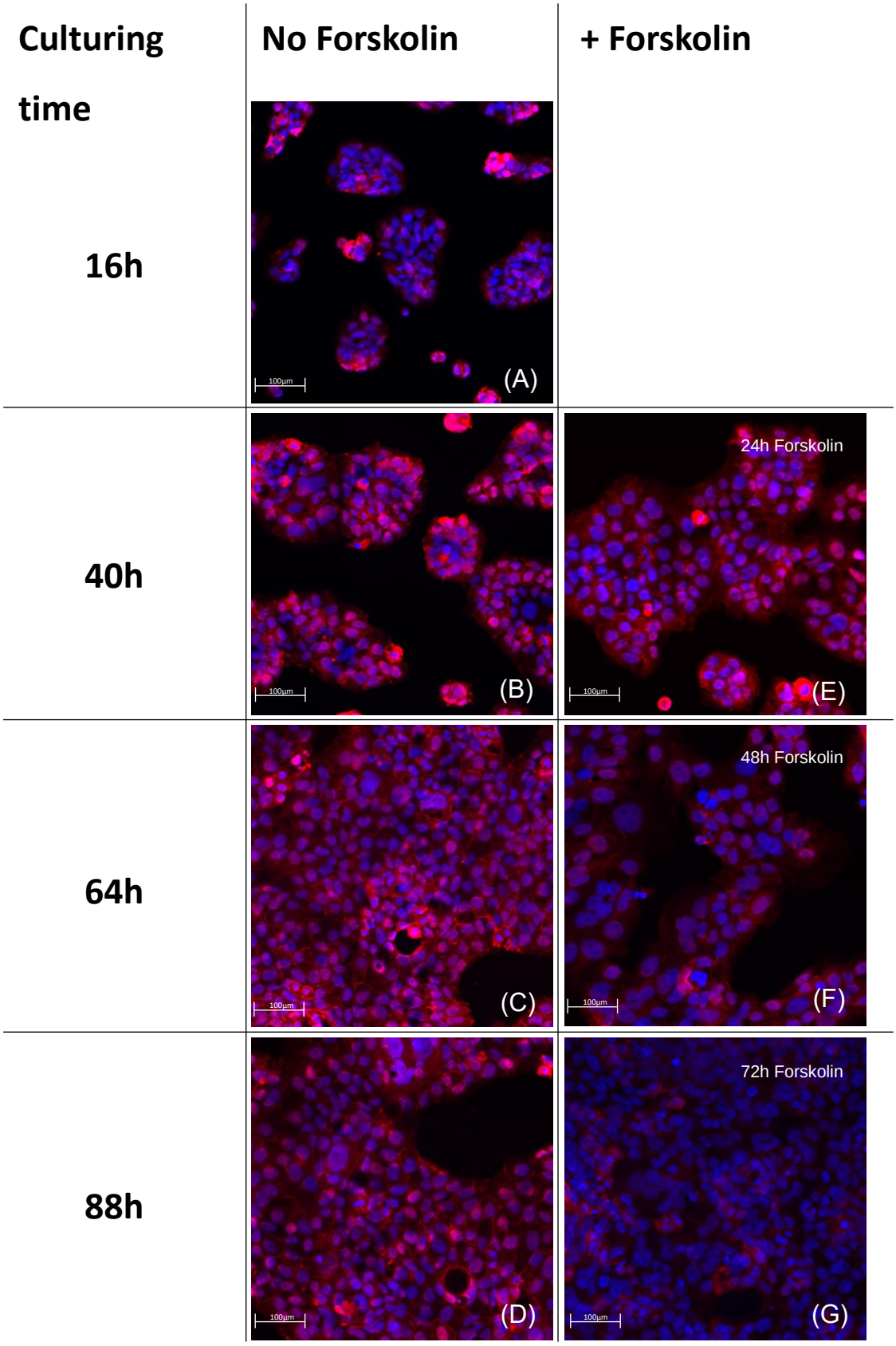

Figure 16: Differentiation of CTB-BeWo cells to STB-BeWo cells directed with Forskolin stimulation. Stimulated cells (A-D) are compared to unstimulated cells (E-G) with the same culturing time. Cells were stained for ZO-1 (red) and nuclei (blue). Pictures: Histech Scanner 20X.

4.2.3 CALHM4

The time course depicted in Figure 18 shows that the signal of the CALHM4 staining decreases with the time of culturing whereby this is happening faster in unstimulated cells compared to stimulated ones.

Furthermore, the signal is not only located at the membrane but also intracellularly. Looking at the staining with a higher magnification at the confocal microscope (Figure 17) this finding is strengthened. Additionally, the signal appears in a meshwork like structure that is reminiscent of the one of intermediate filaments.

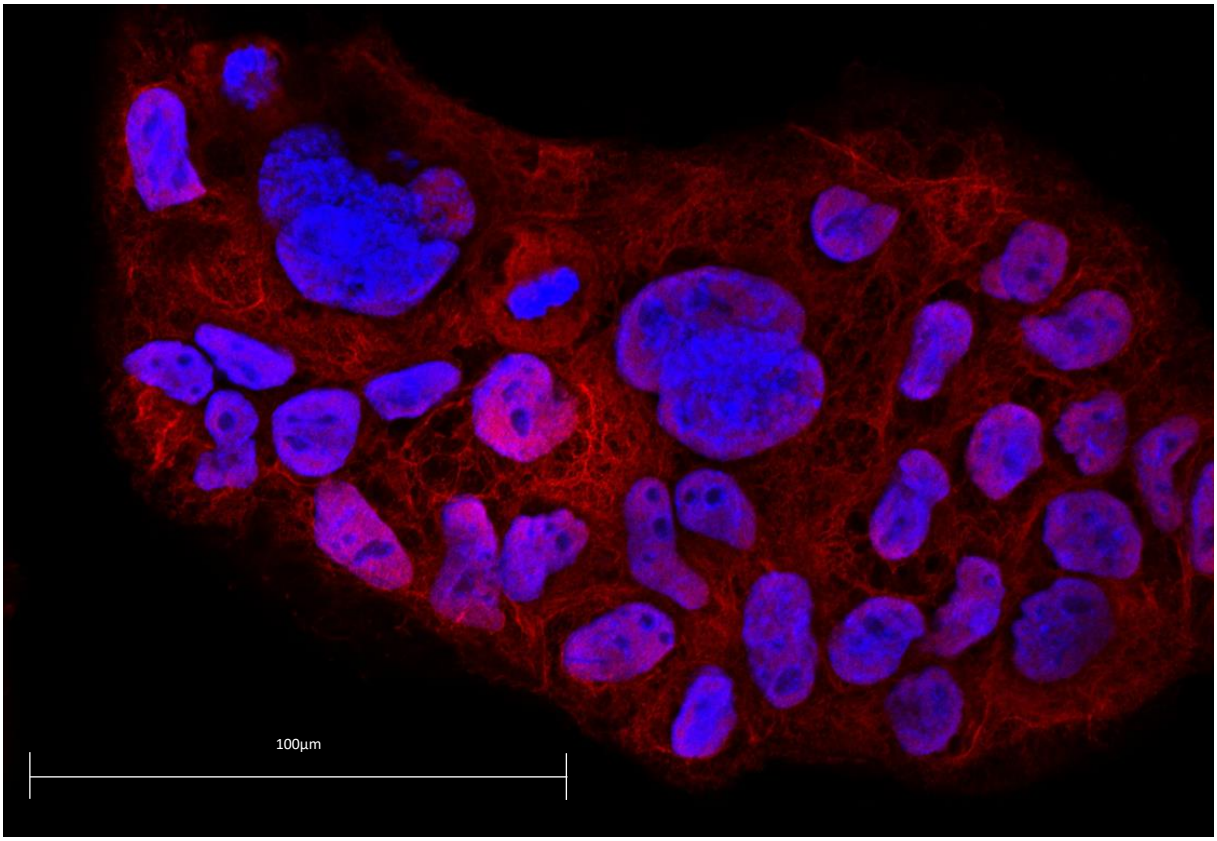

Figure 17: BeWo cells that were cultivated for 64h without Forskolin stimulation. Cells were stained for CALHM4 (red) and nuclei (blue). Picture: Zeiss confocal microscope 40X.

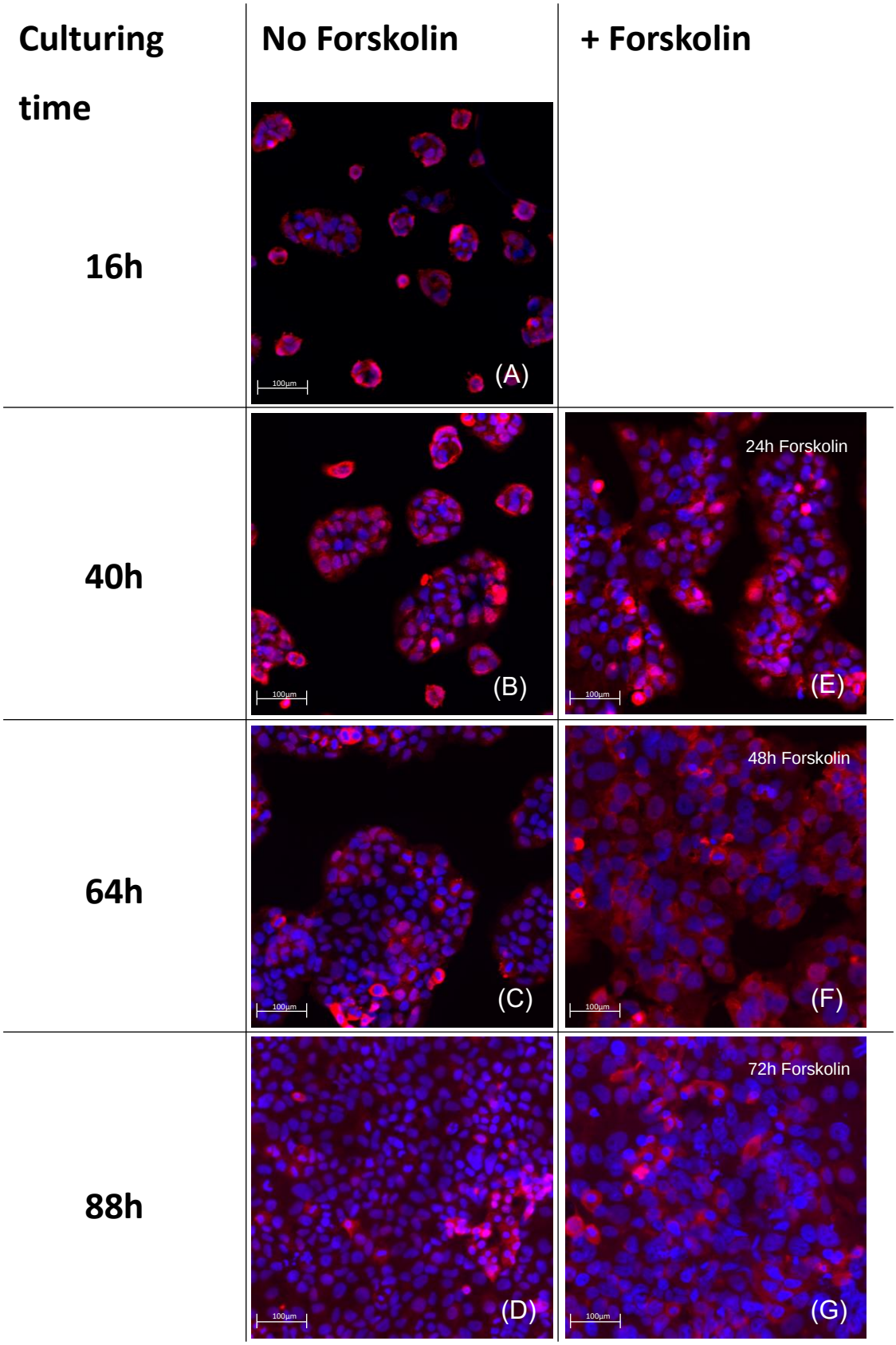

Figure 18: Differentiation of CTB-BeWo cells to STB-BeWo cells directed with Forskolin stimulation. Stimulated cells (A-D) are compared to unstimulated cells (E-G) with the same culturing time. Cells are stained for CALHM4 (red) and nuclei (blue). Pictures: Histech Scanner 20X.

4.2.4 E-cadherin

Looking at the E-cad staining pictures of the time course (Figure 20) a tendency similar to that of the ZO-1 staining appears. After 40h of culturing time the E-cad signal of the untreated BeWo cells stays at a similar level, whereas it is dropping for the untreated with increasing culturing time. The signal difference between 16h and after 40h+ indicates as with the ZO-1 that the number of E-cad junctions is still increasing after 16h. In contrast to the ZO-1 staining signal the E-cad staining signal appears more clustered which can be best observed in the confocal picture (Figure 19).

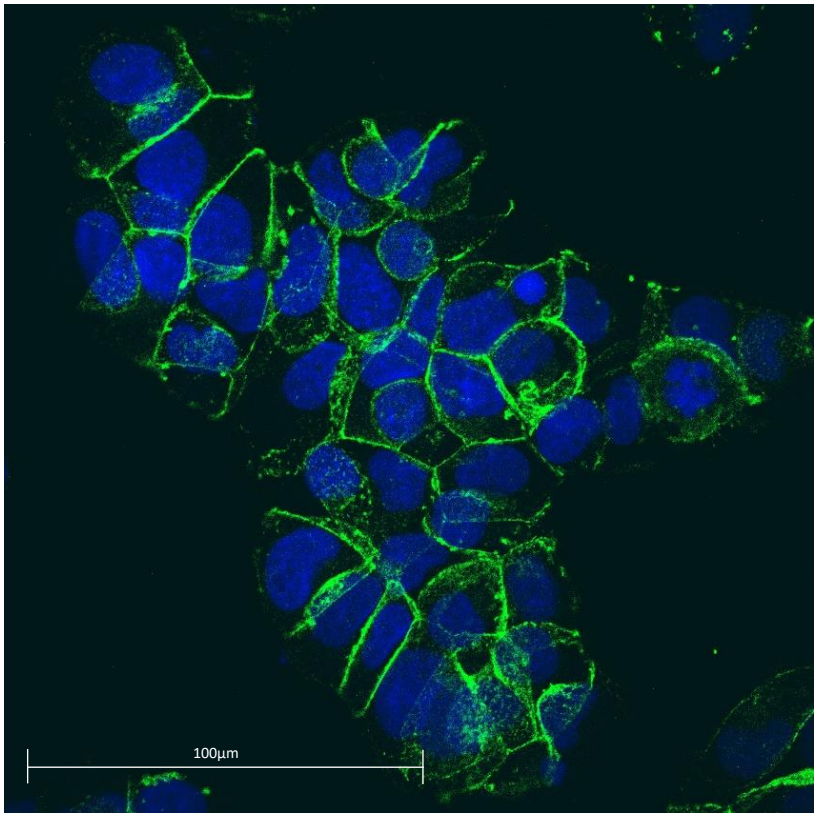

Figure 19: BeWo cells that were cultivated for 64h without Forskolin stimulation. Cells were stained for E-cad (green) and nuclei (blue). Picture: Zeiss confocal 40X.

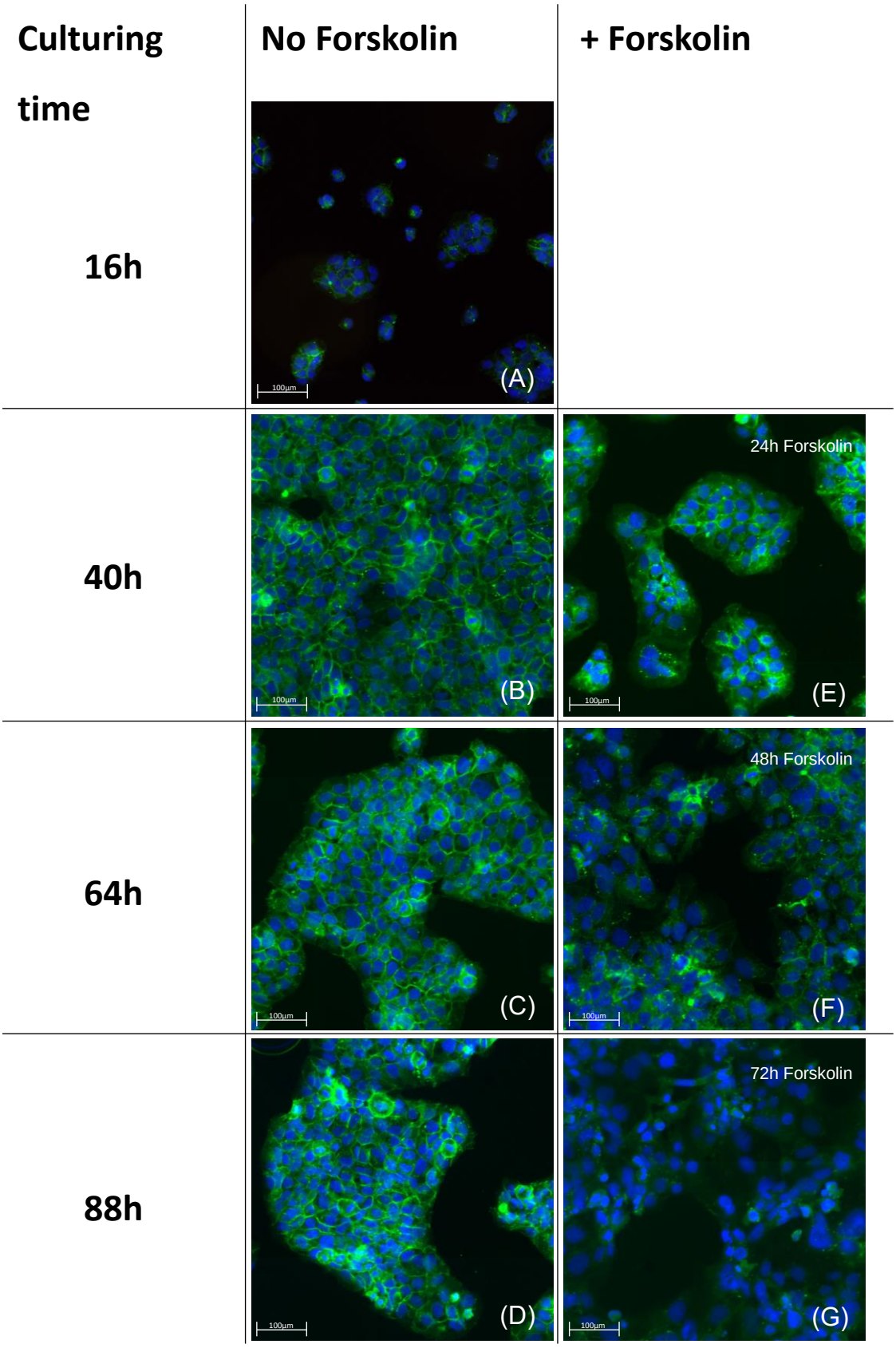

Figure 20: Differentiation of CTB-BeWo cells to STB-BeWo cells directed with Forskolin stimulation. Stimulated cells (A-D) are compared to unstimulated cells (E-G) with the same culturing time. Cells are stained for E-cad (green) and nuclei (blue). Pictures: Histech Scanner 20X.

Additionally, the pictures show strong dotted signal which occurs at a larger extent in Forskolin stimulated cells with a maximum at 48h of Forskolin stimulation (see also Figure 21).

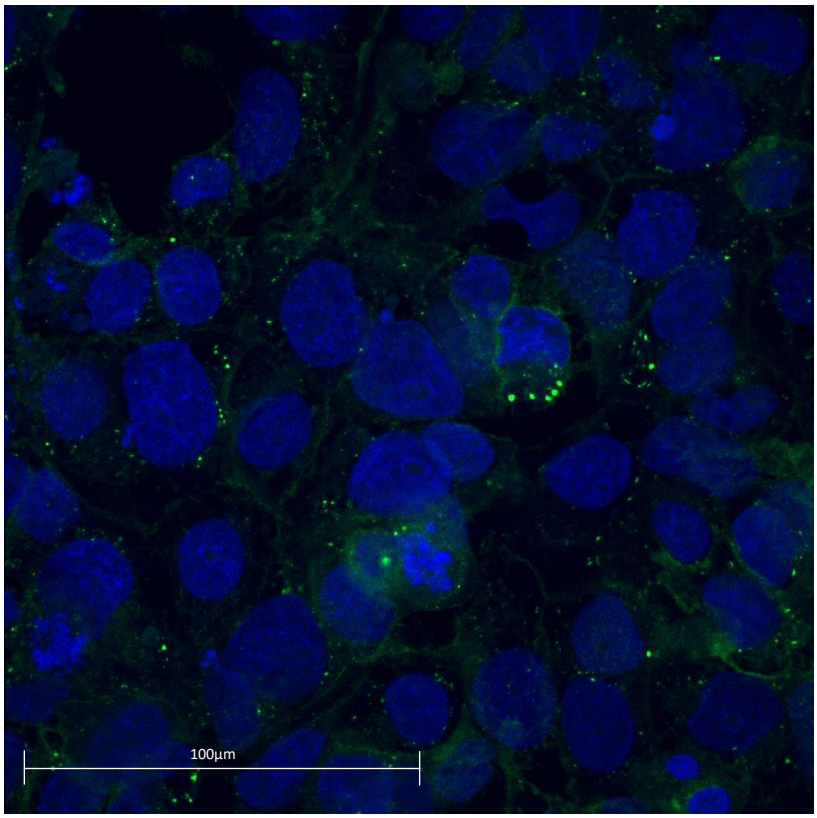

Figure 21: BeWo cells that were cultivated for 64h and stimulated for 48h with Forskolin. Cells were stained for E-cad (green) and nuclei (blue). The green dotted signal might come from extracellularly cleaved E-cad between two cells that underwent cell-cell fusion in the course of syncytialisation. Picture: Zeiss confocal microscope 40x.

4.2.5 Syndecan-1

The SC-1 staining of the time course created in general a more intense signal in the Forskolin stimulated BeWo cells (Figure 23 (E-G)) compared to unstimulated ones (Figure 23 (A-D)). However the staining depicted in Figure 23 (B) which shows unstimulated BeWo cells that were cultured for 40h does not fit into this overall image since there also an increased signal can be observed. In addition to the intensity also the structure of the staining signal varies. Whereas the staining signal in the Forskolin stimulated BeWo cells seems cloudy and distributed over the whole cells it appears more granulated and more localized to the cell membrane in undifferentiated BeWo cells which can be observed better at a higher magnification (see Figure 22).

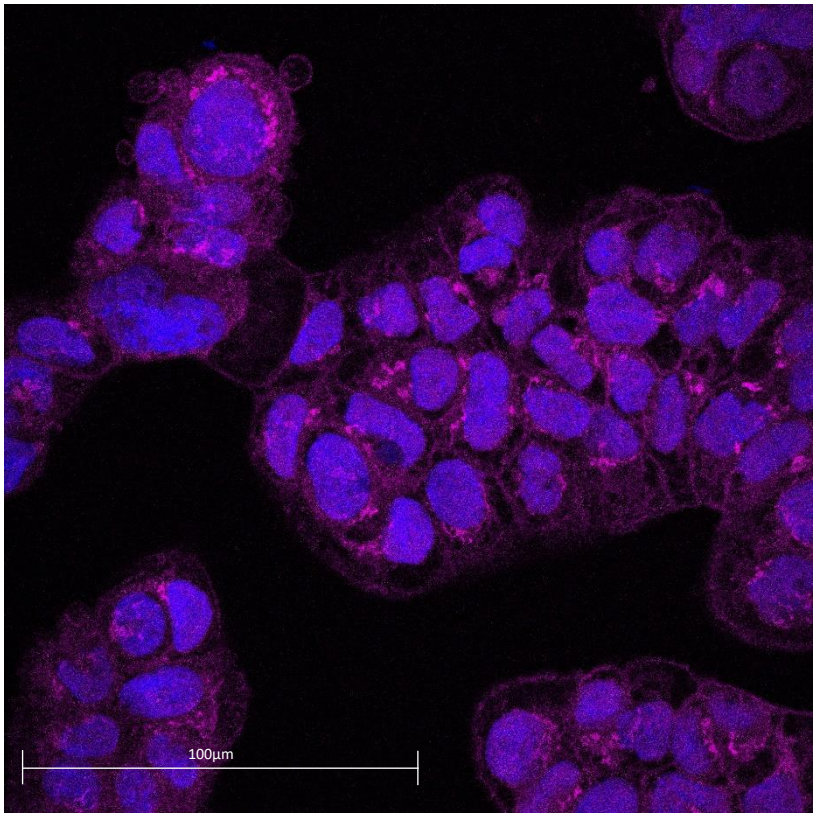

Figure 22: BeWo cells that were cultivated for 40h without Forskolin stimulation. Cells were stained for SC-1(magenta) and nuclei (blue). Picture: Zeiss confocal microscope 40X.

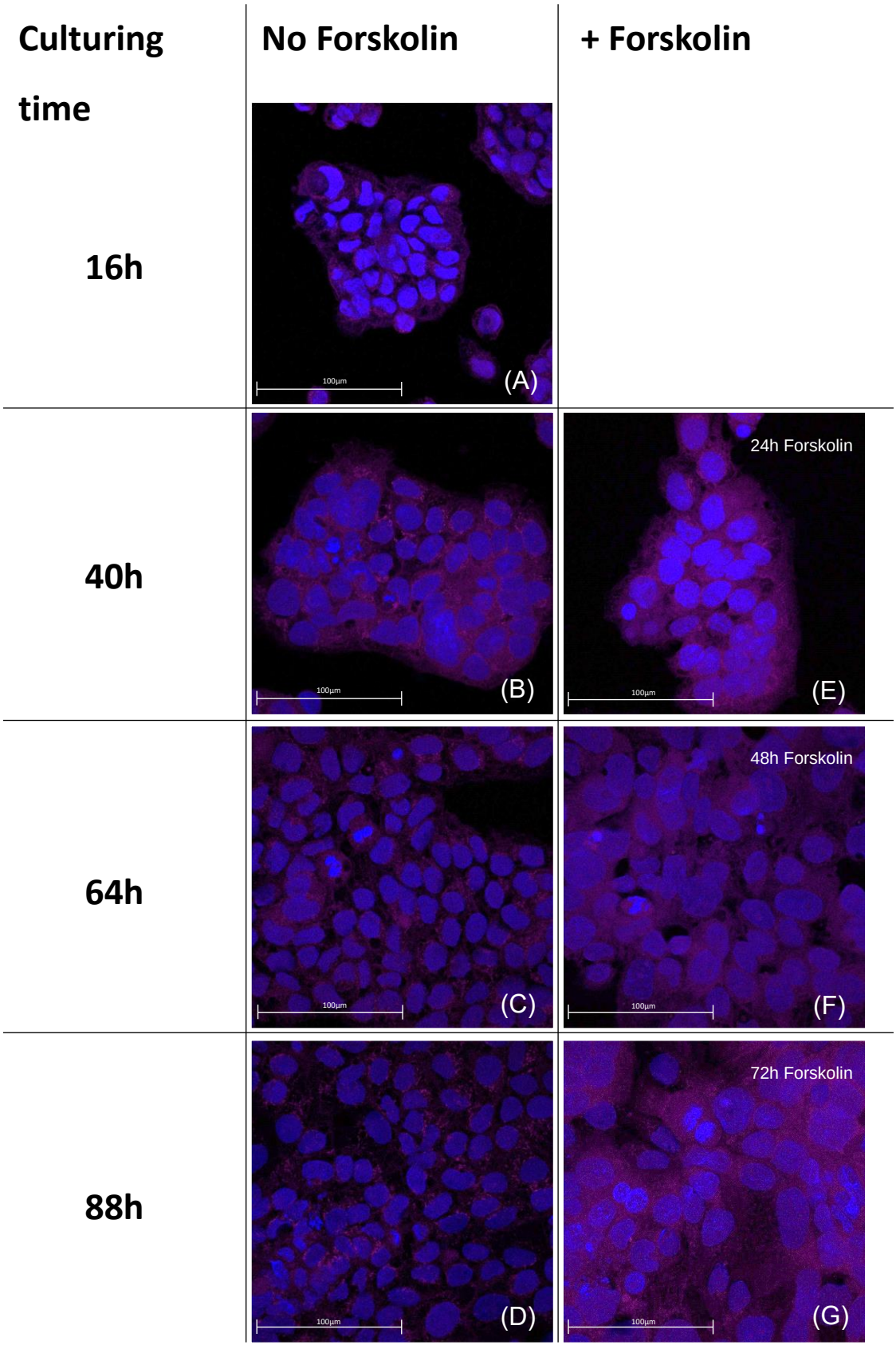

Figure 23: Differentiation of CTB-BeWo cells to STB-BeWo cells directed with Forskolin stimulation. Stimulated cells (A-D) are compared to unstimulated cells (E-G) with the same culturing time. Cells are stained for SC-1 (magenta) and nuclei (blue). Pictures: Zeiss confocal microscope 40X.

4.3 Microfluidic chip: Method establishment

The group of R. Rieben developed a close circuit microfluidic *in-vitro* system in which endothelial cells are cultured in 3D round section microchannels and subjected to physiological, pulsatile flow. One aim of the present work was to adapt this system to trophoblasts of the BeWo cell line. To achieve this goal some steps in the protocol of the Rieben group (see appendix “microfluidic protocol”) had to be supplemented or optimized. These changes are described in the course of the following chapter.

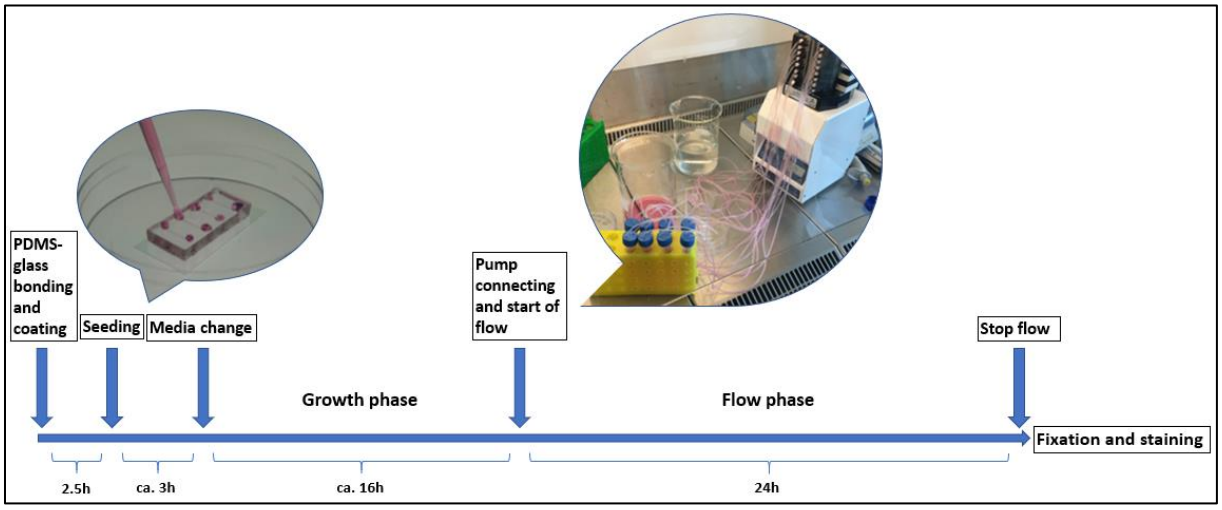

Figure 24: Principle sequence of a microfluidic chip experiment with BeWo cells. The procedure starts with the PDMS-glass bonding and microchannel coating. Next the BeWo cells are seeded and the medium is changed what initiates the growth phase. After ca. 16h growth phase the pump gets attached and the flow is started. Finally, the BeWo cells are fixated and stained after 24h of flow. Picture sources: Microfluidic chip: Sfriso et al. 2018 / pump: foto taken by B. Fuenzalida.

4.3.1 Fibronectin/Collagen I mix found to be best coating

The coating candidates tested for the microchannel coating were Matrigel, Fibronectin and Collagen I. In a first step channels are coated with a combination of Fibronectin and Collagen I, Fibronectin or Collagen I only and Matrigel to find out which coating works best for BeWo cells.

Figure 25 show confocal pictures of the micro channels coated with Collagen I, Fibronectin or combined, in which BeWo cells were stained with anti CK-7 (green) and nuclei (blue). The channel coated with Collagen I (A) as well as the one coated with Fibronectin (B) is lacking confluency after 24h of flow. It seems like cells did detach in patches. In contrast the channel coated with combined Fibronectin/Collagen I (C) showed a confluent channel after 24h flow. In the Matrigel coated channel hardly any cells were left after 24h of flow, for this reason no picture is shown at this point.

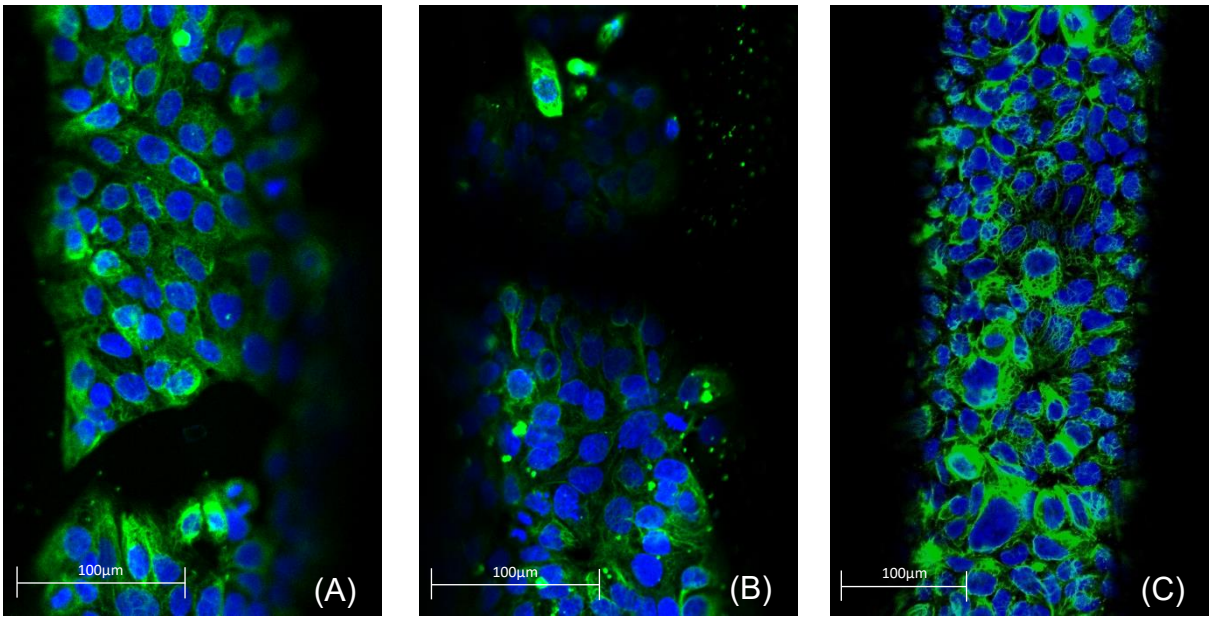

Figure 25: Microfluidic chip channels with BeWo cells after 24h flow that are differently coated. A) Coating: Collagen I 50ug/ml. B) Coating: Fibronectin 100ug/ml. C) Coating: Fibronectin 100ug/ml and Collagen I 50ug/ml. Cells were stained for CK-7 (green) and nuclei (blue).Picture: Zeiss Confocal 20x (A, B), 10X(C).

4.3.2 Orientation during coating has an impact on cell adherence

Figure 25 only show the bottom parts of a channel whereas the top part of the channels was neglected in this examination. With 10X at the confocal microscope it was possible to focus on the top part of a channel and it could be observed that this part was not close to confluency even if the bottom part was fully confluent. At a first thought it was assumed that the gravitation forces during growth phase could be the reason for this issue. Therefore an experiment was performed in which the microfluidic chip was kept top facing down (see Figure 26 (B)) during the growth phase between cell seeding and the start of flow. During this step the microfluidic chip was kept in a top facing up position so far (see Figure 26 (A)).

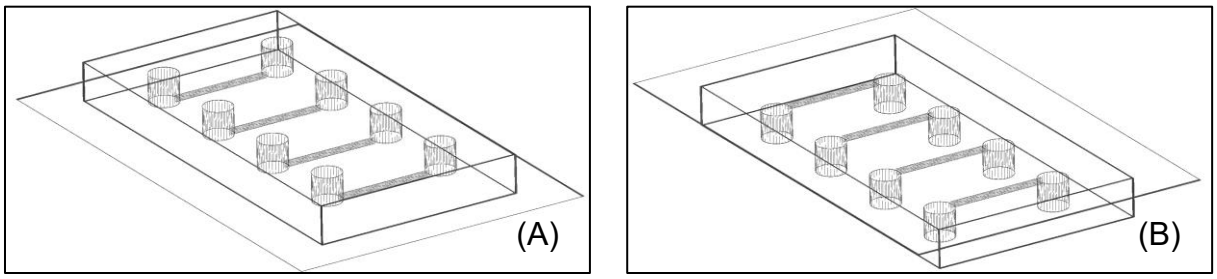

Figure 26: Representations of microfluidic chips in a top facing up (A) or top facing down (B) orientation. Source: Pictures of the microfluidic chips were taken from 3D models created with the Blender 3D software for windows.

With the assumption that gravitation is the cause of this unequal distribution an inverted microfluidic chip during growth phase would lead to the opposite result. However, this assumption could not be confirmed by the results as also in the inverted microfluidic

chip, only the bottom part (which was on top during growth phase) was confluent after growth phase. Next the orientation during the coating was considered as the cause. During coating the microfluidic chip was kept in a top facing up position for 1h (Fibronectin) plus 1.5h (Collagen I) which is a considerably long time for coating. This fact let to the conclusion that it could possibly lead to an uneven distribution of the coating due to gravitational forces. Consequently, an experiment was performed with 3 channels. The first one was kept top facing up, the second one top facing down and the third one was flipped several times during coating. Surprisingly the results validate the hypothesis that the orientation of the microfluidic chip influences the distribution of adherent cells after growth phase. Figure 27 show the three channels that were incubated at different orientations during coating.

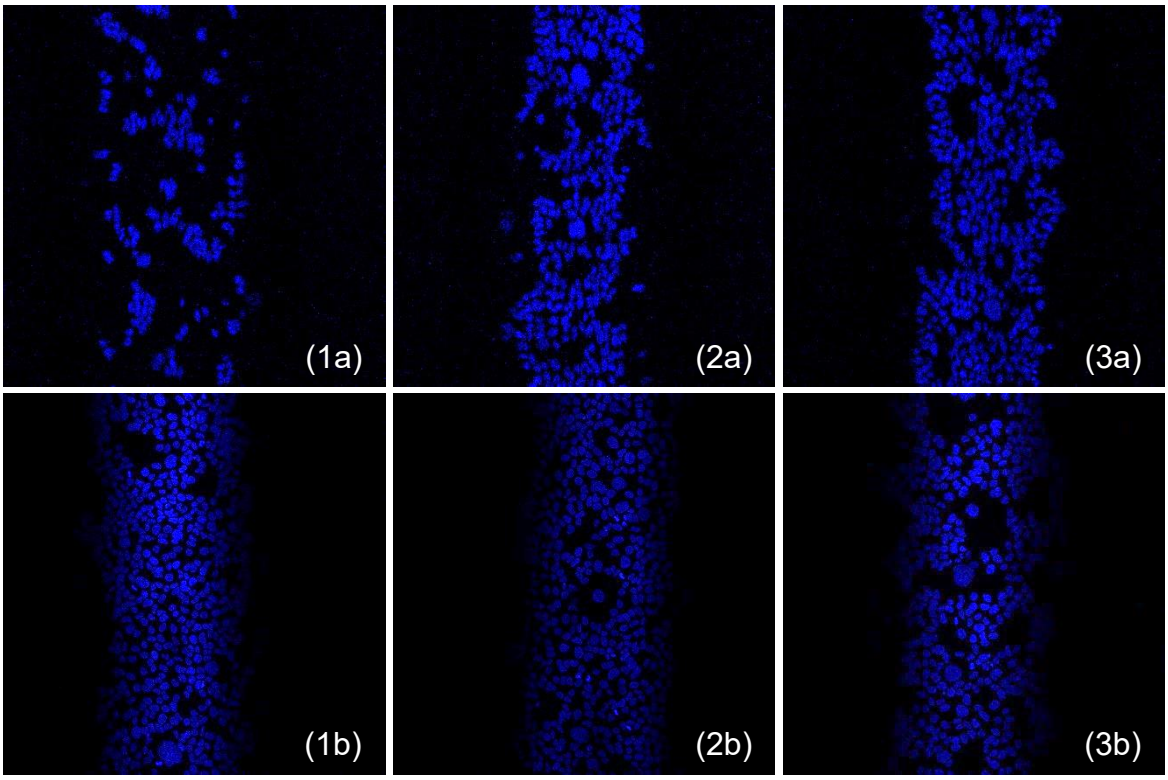

Figure 27: Nuclei staining of microfluidic channels after 24h culturing without flow that were kept in different orientations during coating with Fibronectin/Collagen I. 1) Top facing up coating: Top (1a) and bottom (1b) of the micro channel. 2) Top facing down coating: Top (2a) and bottom (2b) of the micro channel. 3) Turned while coating: Top (3a) and bottom (3b) of the micro channel.

Taking Figure 27 as references, ratios are calculated from counted nuclei of the top part divided by the bottom part of the channels (see Table 3).

Table 3: Ratios of counted nuclei of the top- or bottom -parts of the micro channels. Ratios were calculated from nuclei, counted from Figure 27.

Orientation while coating	**Ratio (top/bottom)**
Upside up	0.28
Upside down	0.88
Turning	1.18

Based on these results and verifying follow up experiments it is found to be advantageous to flip the microfluidic chip several times during coating. Therefore the microfluidic chip was flipped after 5, 15, 30 and 45 minutes of incubation time with Fibronectin or Collagen I (see Figure 28).

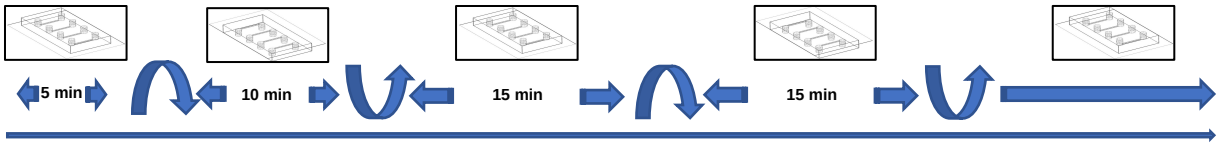

Figure 28: Microfluidic chip orientations during coating procedure. The microfluidic chip is flipped after 5, 15, 30 and 45 minutes of incubation time with Fibronectin or Collagen I. Source: Pictures of the microfluidic chips were taken from 3D models created with the Blender 3D software for windows.

4.3.3 Seeding density of 2 mio BeWo cells/mL with Forskolin stimulation found to be best condition

BeWo seeding densities of 0.5, 1, 2 and 3 mio BeWo cells/mL were tested. Additionally, these seeding densities were compared with and without Forskolin stimulation.
Evaluating the outcome of this comparisons (depicted in Figure 29) the seeding density of 2 mio BeWo cells/mL with Forskolin stimulation is found to be the best condition regarding the number of cells left in the microchannel after 24h of flow. Seeding densities of 0.5 and 1 mio BeWo cells/mL resulted in a clearly worse outcome whereas 3 mio BeWo cells/mL did not bring any improvement compared to 2 mio BeWo cells/mLwith Forskolin.

4.3.4 Longer adherence time and gentle handling lead to further improvements in confluency

In addition to the mentioned parameters also the seeding procedure itself and the handling was optimized. Whereas the Rieben group lets their endothelial cells adhere for only 10 minutes in a top facing up respectively down position (see appendix “microfluidics protocol”), 30 minutes on each side could improve the outcome for BeWo cells. Furthermore, better results could be achieved by using the pipette instead of the aspiration system to remove liquid through the outlet of the channels during seeding, media changes, fixation and staining. With this adaption the shearing rates to which the cells are exposed during the mentioned steps can be drastically reduced.

Figure 29: Confocal tile scans showing nuclei stainings (blue) of differently treated microchannels. A) Tile scan of a microchannel after 24h flow where 0.5 mio BeWo cells/ml were seeded and treated with Forskolin for 48h. B) Tile scan of a microchannel after 24h flow where 0.5 mio BeWo cells/ml were seeded. C) Tile scan of a microchannel after 24h flow where 1 mio BeWo cells/ml were seeded. D) Tile scan of a microchannel after 24h flow where 1 mio BeWo cells/ml were seeded and treated with Forskolin for 48h. E) Tile scan of a microchannel after 24h flow where 2 mio BeWo cells/ml were seeded. F) Tile scan of a microchannel after 24h flow where 2 mio BeWo cells/ml were seeded and treated with Forskolin for 48h. G) Tile scan of a microchannel after 24h flow where 3 mio BeWo cells/ml were seeded. H) Tile scan of a microchannel after 24h flow where 3 mio BeWo cells/ml were seeded and treated with Forskolin for 48h.

4.3.5 Specific staining only possible with directly labelled antibodies

For some reason that could not be verified the indirect staining in the microfluidic chip in which secondary antibodies are used was always problematic. Only the staining with directly labeled antibodies let to a satisfying signal noise ratio whereas indirect staining resulted in high background signal. An example, showing this issue is depicted in Figure 30. The figure shows the split color channels of a multi staining where the cells were stained for nuclei (blue), CK-7 (green) and ZO-1 (red). Only the ZO-1 staining which was performed with a secondary antibody (anti rabbit AF594) led to an unspecific staining signal with high background intensity. In contrast both, the primary anti ZO-1 antibody as well as the secondary anti rabbit AF594 led to specific staining results in the chamber slide stainings (compare part 4.2.2 on p. 39).

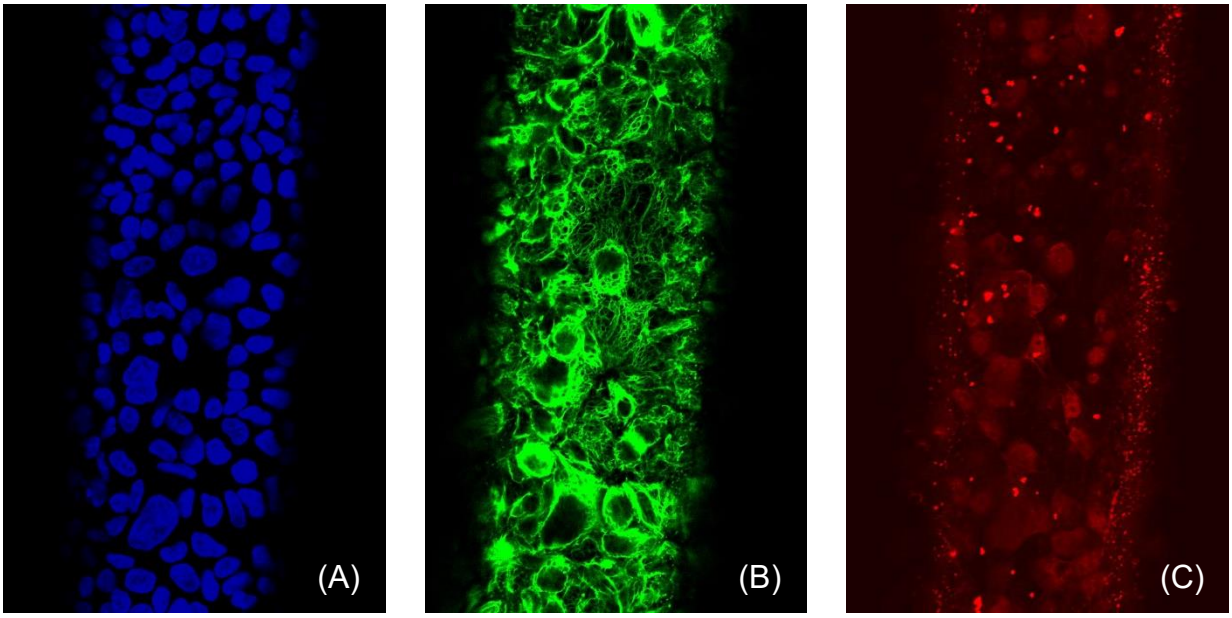

Figure 30: Splitted color channels of an image of BeWo cells in a microchannel. Cells were stained for A) nuclei (blue), B) CK-7 (green) and C) ZO-1 (red). BeWo cells were not treated with Forskolin and exposed to flow for 24h. Picture: Zeiss Confocal 20X.

4.3.6 Microchannel mounting with Vectashield® improves image quality

After staining the microchannels were commonly kept in DPBS. It was found out, that the Vectashield® mounting media is well suited for mounting the channel and can improve the staining pictures remarkably. Figure 31 present E-cad and nuclei staining pictures of the same micro channel, that was first kept in DBPS (Figure 31 (A)) and after mounted with Vectashield® (Figure 31 (B)). Obviously, the intensity of a signal that can be expected from an E-cad staining (compare with pictures of chamber slide E-cad stainings in chapter 4.2.4 on p. 43) could have been amplified by the mounting with Vectashield®.

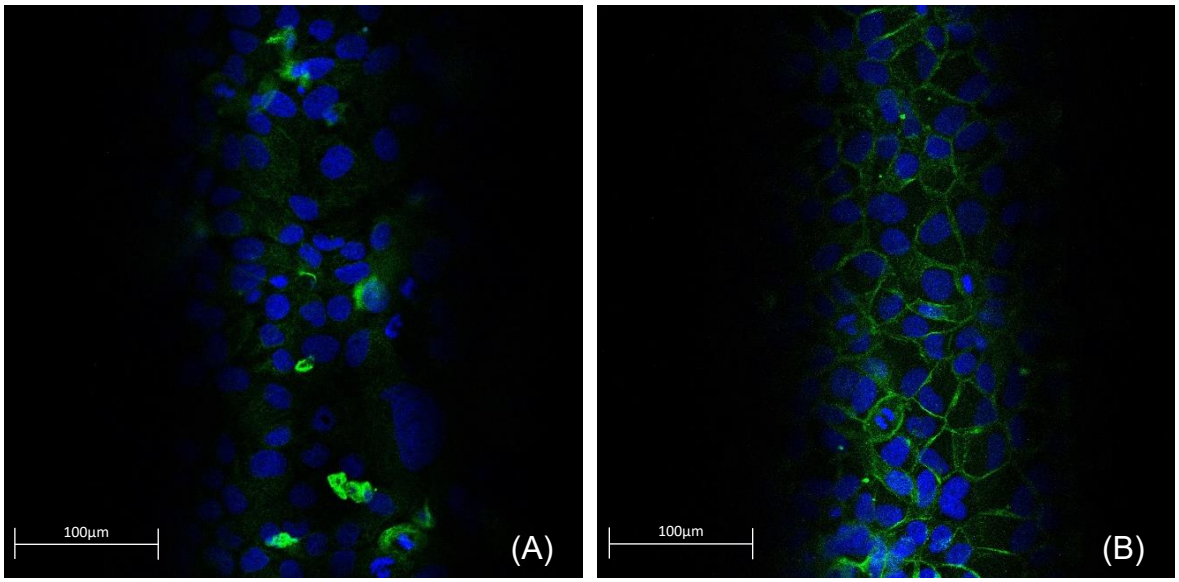

Figure 31: Microfluidic chip channel that was kept in DPBS (A) and after mounted with Vectashield® mounting media (B) after 24h flow and Forskolin stimulation. Cells were stained for E-cad (green) and nuclei (blue). Pictures: Zeiss confocal 20X.

4.4 Microfluidic chip: Staining results

In this chapter the staining results are described that were obtained by the staining of the cellular structures CK-7 and E-cad of the BeWo cells in the microfluidic chip.

4.4.1 CK-7

It can be observed that in the non-Forskolin stimulated cells that are depicted in Figure 32 (A), dividing BeWo cells are captured in the image whereas this is not the case for flow- and or Forskolin-stimulated cells (examples are indicated by yellow arrows in Figure 32 (A)). Further, it seems as if the cytokeratin filaments are organized in thicker bundles in the BeWo cells that were stimulated with flow (compare Figure 32 (B) with (A). This effect seems to be even more evident under Forskolin stimulation in addition to the flow (compare Figure 32 (C) with (B).

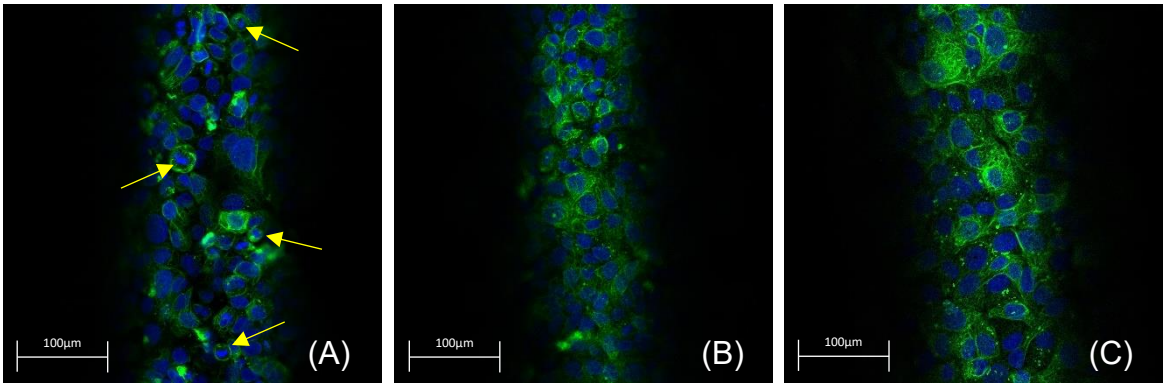

Figure 32: Comparison of CK-7stainings from BeWo cells of differently treated micro channels. A) Condition: No flow / No Forskolin, dividing cells are indicated by yellow arrows. B) Condition: 24h flow / No Forskolin. C) Condition: 24h flow / + Forskolin. Cells were stained for CK-7 (green) and nuclei (blue). Picture: Zeiss confocal 20X.

In addition, the nuclear size increased with flow- respectively flow- and Forskolin-treatment of the BeWo cells (see Figure 33).

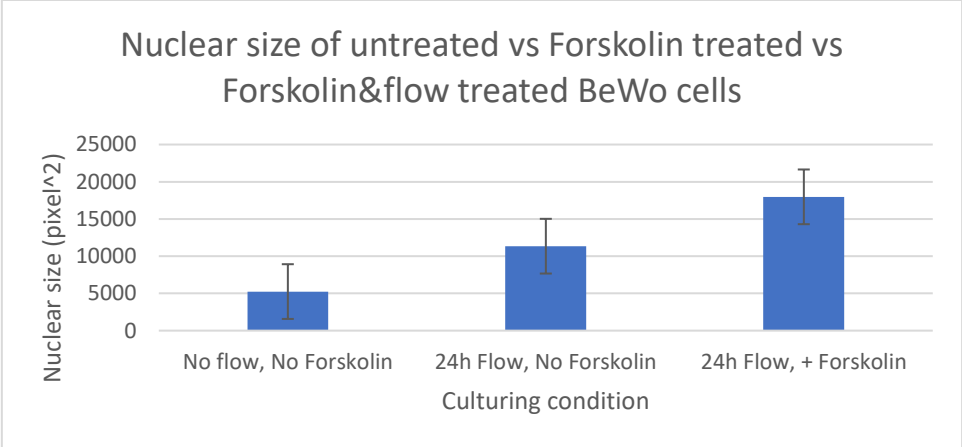

Figure 33: Graph showing nuclear size means of untreated vs Forskolin treated vs Forskolin & flow treated BeWo cells in a microfluidic chip experiment. Nuclear size was measured in pixel^2 with ImageJ using time course images that are depicted in Figure 32.

4.4.2 E-cadherin

Figure 34 (B) show E-cad junctions between some of the Forskolin stimulated cells that are partially broken down after 24h of flow (indicated by yellow arrows). Also, in the non-Forskolin stimulated channel (Figure 34 (A) this incident can be observed albeit to a lesser extent.

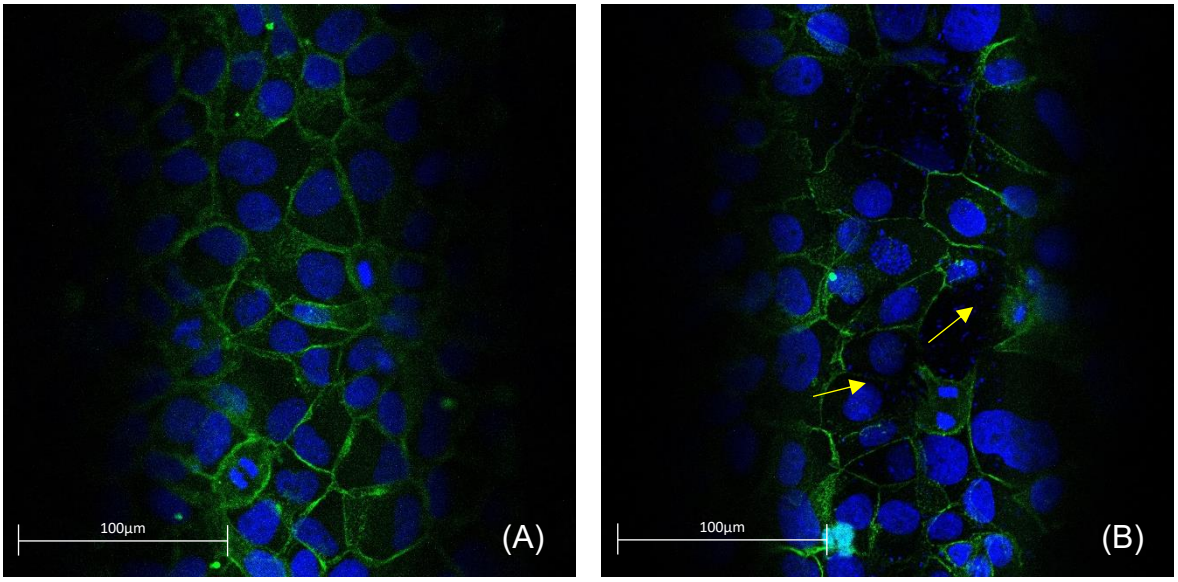

Figure 34: Comparison of E-cad junctions between BeWo cells from differently treated microchannels. A) Condition: 24h flow / No Forskolin. B) Condition: 24h flow / + Forskolin. Cells were stained for E-cad (green) and nuclei (blue), examples for E-cad breakdowns are indicated by yellow arrows. Picture: Zeiss confocal 20X.

4.5 hCG-ELISA

Supernatant samples of the static chamber slide system and the microfluidic chip system were collected during Forskolin time course experiments and the hCG concentration in those samples was determined with a sandwich ELISA. The hCG concentration was only detectable in the chamber slide samples whereas the concentration felt below the detection limit in the microfluidic chip samples.

4.5.1 Chamber slides hCG-ELISA results

The BeWo cells were cultured in chamber duplicates for 24h to 96h whereas supernatant samples were taken every 24h as shown in Figure 35. After 24h of Forskolin stimulation (30h culturing time) the media was changed for all duplicates and therefore the secretion time for the 48h Forskolin sample was only 24h respectively 48h for the 72h sample.

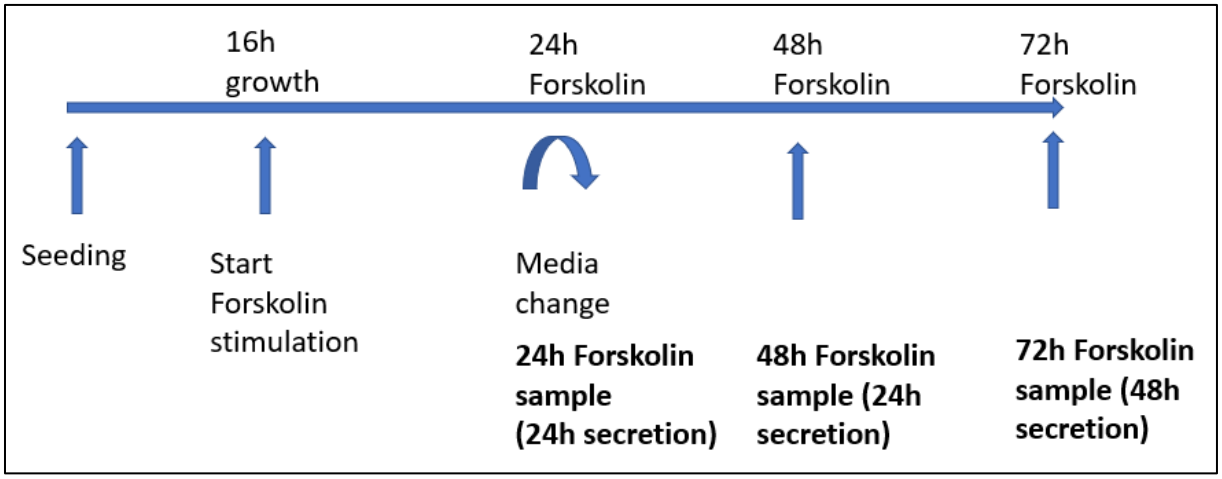

Figure 35: Supernatant sampling sequence for the chamber slide hCG-ELISA. The first sample was taken after 16h of growth and 24h of Forskolin stimulation, the second one after 16h of growth and 48h of Forskolin stimulation and the third one after 16h of growth and 72h of Forskolin stimulation.

The results of the chamber slides hCG-ELISA are shown in Figure 36. Whereas the hCG concentration stayed at the same level in the supernatant of the non-Forskolin treated BeWo cells during the time course of the experiment it raised in the ones of the Forskolin treated BeWo cells. There the hCG concentration raised for 230% from the 24h compared to the 72h samples which was found to be significant by a T-Test at a significance level of $\alpha<0.05$.

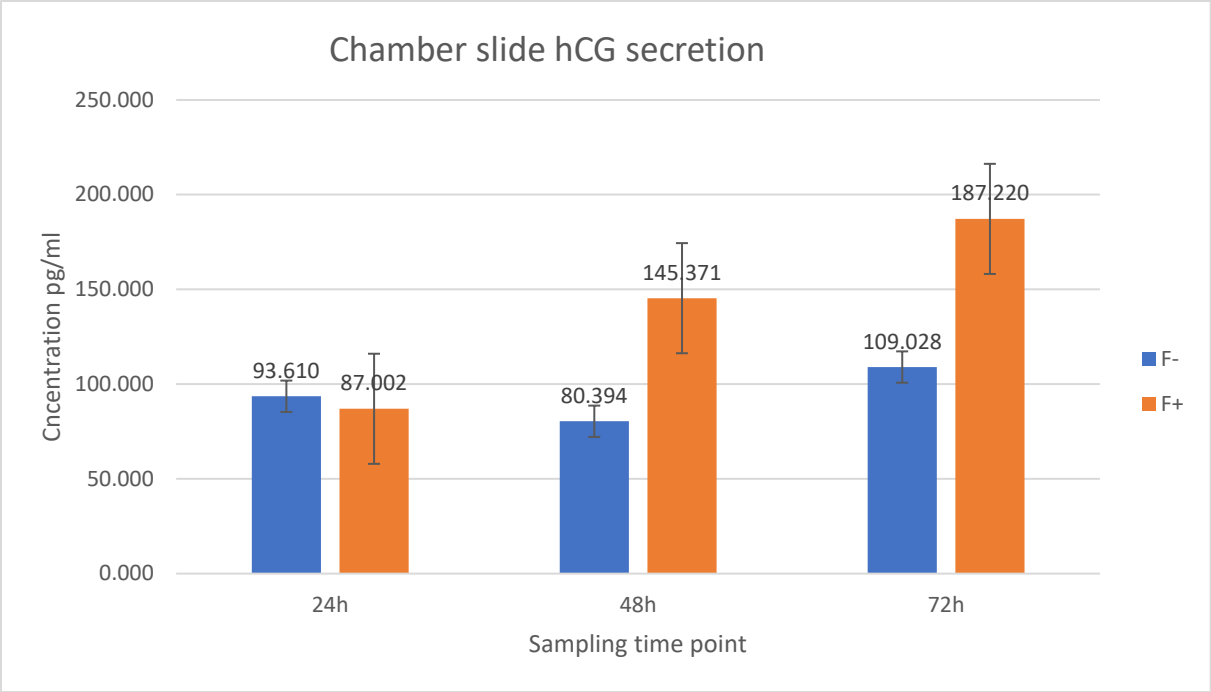

Figure 36: Graph showing hCG concentrations in pg/mL in supernatants samples of chamber slides at respective culturing time points of Forskolin vs Non-Forskolin treated BeWo cells.

4.5.2 Microfluidic chip hCG-ELISA results

The hCG concentration felt below the detection limit in the microfluidic chip samples that was calculated from the standard curve (see Figure 37).

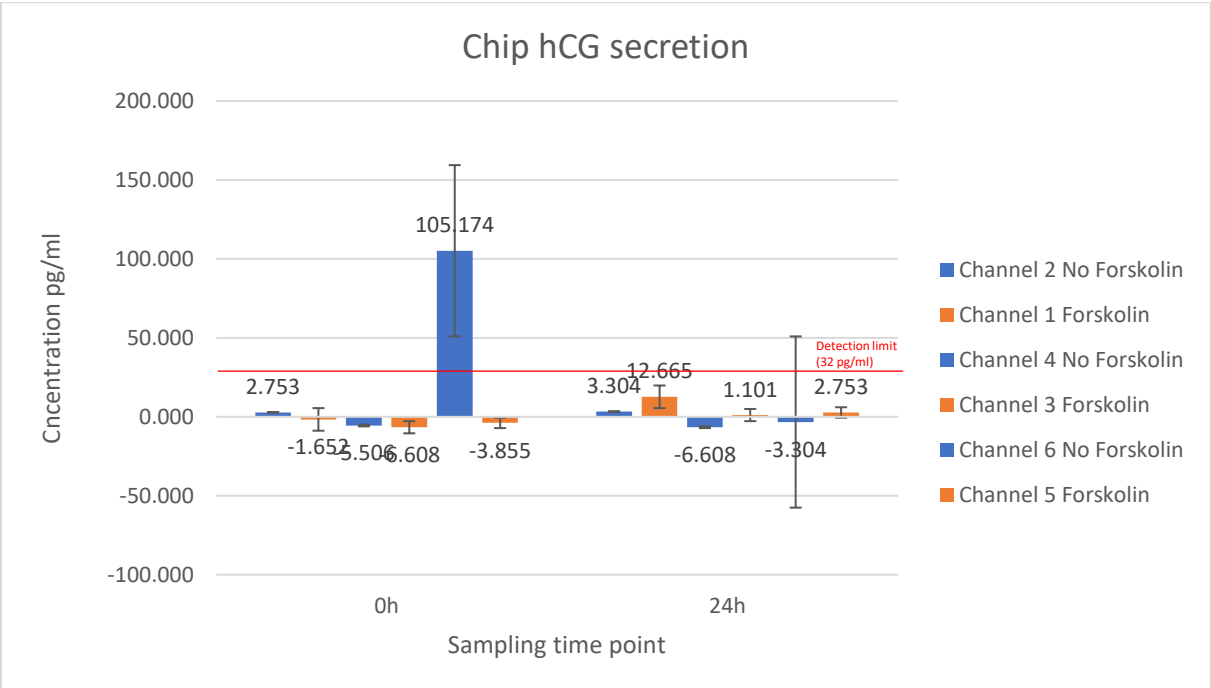

Figure 37: Graph showing hCG concentration in pg/mL in supernatants samples of microfluidic chips at respective culturing time points of Forskolin vs Non-Forskolin treated BeWo cells. The calculated detection limit of 32 pg/ml is drawn in in red.

5 Discussion

5.1 Chamber slides: Staining results

5.1.1 CK-7

It could be observed that the nuclei of STB-BeWo cells were enlarged compared to the nuclei of CTB-BeWo cells. It was already stated by Huppertz et al. that nuclei of syncytial trophoblasts exhibit a large and ovoid shape, show different levels of aging and do not longer show any proliferative activity (Berthold Huppertz, 2018). This enlargement could be the result of the increased heterochromatization that was found in the nuclei of syncytiotrophoblasts (B. Huppertz, 2010). The heterochromatization in turn is expected to lead to rearrangement of euchromatic chromosomal regions into heterochromatic nuclear compartments, in turn leading to repression of the expression of specific genes eg. for proliferation. However, it was also stated that the nuclei of syncytiotrophoblasts return to a smaller and denser morphology after 3-4 weeks after syncytialisation (B. Huppertz, 2010). The number of dividing cells captured on the scans is higher among non-Forskolin stimulated cells than among Forskolin stimulated cells. This observation further supports the assumption that the Forskolin was effective as expected to downregulate cell proliferation with ongoing differentiation (Pascale Gerbaud et al., 2015).

A superficial examination of the literature could lead to the conclusion that cytokeratin as a component of intermediate filaments are present intracellularly (Herrmann et al., 2007) and connected to desmosomes which is required for mechanical stability and intercellular coherence (Hatzfeld et al., 2017). However this is not what was observed in the confocal picture (Figure 14 in part 4.2.1 on p. 38). Looking at this picture it became obvious that the cytoskeleton spans several cells whereas the cell borders could be verified by the ZO-1 staining. Interestingly a recent publication was found that states that keratins interconnect desmosomes in the intercellular space and polymerize into filaments next to desmosomes in murine blastocysts (Moch et al., 2020). Taking this statement as a basis the keratins connect the desmosomes not only intracellularly through the cytoplasm but also intercellularly which could lead to the uninterrupted signal that was observed in the confocal picture of the CK-7. In this context it would be interesting to locate also the desmosomes in a combi-staining including the desmosomes, the cytokeratin and the tight junctions.

5.1.2 ZO-1

The observed ZO-1 staining signal increase with culturing time in non-Forskolin stimulated BeWo cells could lead to the assumption that the tight junctions are not completely established after first 16h but rather further develop during 88h. Furthermore, ongoing breakdowns of ZO-1 in the intercellular space between fusing cells in the course of syncytialisation could be observed. Other studies have already shown that a knockdown of ZO-1 in primary trophoblast cell culture even leads to decreased cell-cell fusion and subsequent trophoblast differentiation (Pidoux et al., 2010). It is a big logistical challenge to get all proteins at the right time at the correct place for cell-cell fusion and it seems that ZO-1 plays a crucial role in this process.

5.1.3 CALHM4

The CALHM4 staining resulted in a signal that is not only located at the cellular membranes but also intracellularly. Confocal pictures revealed that meshwork like structures were stained that are reminiscent for intermediate filaments. Literature states that the CALHM4 channel consists of an extracellular-, a transmembrane- and a cytoplasmic -domain (Syrjanen et al., 2020), however no physical interaction with the cytoskeleton is found so far. A hypothesis to explain this observation could be that CALHM4 channels interact between mechanically gated channels and the cytoskeleton. This could happen in a way that an increased intracellular Ca^{2+} concentration as a result of the activation of mechanically gated channels leads to an activation of the CALHM4 channel. Upon activation the CALHM4 channel could be cleaved from the membrane and binds to the cytoskeleton in order to cause a corresponding reaction to the mechanical stimulus at the target location. This thesis suggests that CALHM4 belongs to the mechanosensitive channels that are known to interact with the cytoskeleton in response to the signal of a mechanically gated channel (Martinac, 2014). The CALHM4 signal decrease over culturing time could be explained in this way by the fact that in the first time period after seeding more mechanosensing takes place in the course of cell-ECM as well as cell-cell communication during adherence and reorganization of the cells on the new substrate. However, this thesis is only an initial indication that would be interesting to verify with corresponding follow-up experiments using the patch-clamp method.

5.1.4 E-cadherin

The E-cad staining revealed an increase of those structures in the non-Forskolin stimulated BeWo cells between 16h and 40h of culturing time and after the signal stays at a similar level until 88h. This finding suggests, that the E-cad boundaries were established after 40h of culturing time. In contrast, the signal was continuously dropping in the Forskolin stimulated BeWo cells with increasing culturing time. The signal drop in the Forskolin stimulated cells over a time course was already stated in literature that says that the fusion of BeWo cells is accompanied by a progressive breakdown of E-cad boundaries (Coutifaris et al., 1991). The observed E-cad clustering is supposed to be mediated by *cis* and *trans* interactions and to be stabilized in turn by α-catenin which provides a bridge to the actin cytoskeleton (Indra et al., 2018). Further Gerbaud et al stated that cadherin clustering mediates the so called commitment stage that trophoblasts do undergo prior to fusion and after initiates cell fusion at the right time and the right place (P. Gerbaud & Pidoux, 2015).

The strong dotted signal that could be observed occurs at a larger extent in Forskolin stimulated cells with a maximum at 48h of Forskolin stimulation. This signal may come from extracellularly cleaved E-cad between two cells that underwent cell-cell fusion in the course of syncytialisation. The extracellular cleavage of E-cad could already be observed in the context of epithelial cell extrusion (Grieve & Rabouille, 2014). The processes of cell extrusion and cell fusion are comparable to one another in the way that in both processes existing bonds between the cells must first be broken. It would be interesting to measure the concentration of cleaved E-cad in the supernatant of stimulated vs unstimulated cells in a subsequent experiment.

5.1.5 Syndecan-1

Looking at the literature SC-1 was found to be expressed on the apical surface of the syncytiotrophoblast layer in the human placenta (Hofmann-Kiefer et al., 2013). In addition it was already stated that SC-1 is expressed on BeWo cells whereas it is upregulated during differentiation to STB-BeWo cells (Prakash et al., 2011). The general observation that was made in chapter 4.2.5 that the SC-1 staining signal was increased in the Forskolin stimulated cells therefore goes along with previous studies. The function of the placental glycocalyx is stated to be likely wide ranging including the regulation of permeability and transport mechanisms of the syncytiotrophoblasts (Martin et al., 1974). In this context it makes sense that the glycocalyx is of lesser

importance on cytotrophoblasts but its expression is upregulated during the formation of a syncytium which represents a tight diffusion barrier.

Further it could be observed that the SC-1 staining signal seems cloudy and distributed over the whole cells in the Forskolin stimulated BeWo cells whereas it appears more granulated and more localized to the cell membrane in undifferentiated BeWo cells. As described in literature, the integrity of lipid rafts is essential for the clustering and biological activity of SC-1 on cell surfaces (Burbach et al., 2003) (Paris et al., 2008). At this point the literature on lipid grafts in trophoblasts becomes sparse. However an interplay was found between two proteins whereas one regulates the expression of lipid grafts and the other one cytoskeleton reorganization in BeWo cells during differentiation (Rashid-Doubell et al., 2007). Together with the general finding that lipid rafts are involved in numerous signal transduction processes (Schmitz & Grandl, 2008) it appears likely that their constitution changes during trophoblast differentiation.

5.2 Microfluidic chip: Method establishment

5.2.1 Fibronectin/Collagen I mix found to be best coating

Fibronectin/Collagen I was tried because it is already in use for the present system by the Rieben group, carrying out their experiments with porcine endothelial cells (Sfriso et al., 2018). The Rieben group uses Fibronectin combined with Collagen I to coat for endothelial cells and this coating also turned out to be the most suitable among the tested coatings for BeWo trophoblast cells. Matrigel was chosen as a coating because it was previously used by S. Kallol for Transwell coating using primary trophoblasts (Kallol et al., 2018). Even tough Matrigel serves evidently as a suitable coating material for trophoblasts experiments, it turned out as an unsuitable coating material for the chip microchannels. Possibly the Matrigel was just applied at a too high concentration that formed a too thick layer which among other things could limit the diameter of the channel and therefore increase the shearing rates at the same flow rate. In a publication Matrigel at 2.5mg/mL was used to fill microgaps of 15µM (Chaw et al., 2007). Therefore, it is conceivable that the usage of Matrigel at 12.2mg/mL could lead to a significant decrease of the 550µM diameter channel that was used in this experiment.

5.2.2 Seeding density of 2 mio BeWo cells/mL with Forskolin stimulation found to be best condition

The seeding density in the microfluidic chip experiment is defined by the number of cells suspended in 1 mL medium that is added to the microfluidic channel. With a higher seeding density, the risk increases that the cells form clumps and get detached in patches, while with a too low one just not enough cells are able to adhere in order to form a confluent layer after growth phase. 2 mio BeWo cells/mL were found to be best regarding microchannel confluency after 24h flow. The Rieben group usually uses 1 mio BeWo cells/mL for their endothelial cells. In the literature densities of 4 mio BeWo cells/mL (Zhu et al., 2018) and 5 mio BeWo cells/mL (Pemathilaka et al., 2019) were applied for microfluidic chips, whereas those are not directly comparable to the present system due to a way bigger size and a cuboid flat bottom channel geometry. It was observed that the stimulation of BeWo cells with Forskolin in the microchannels brings an advantage regarding the confluency level after application of 24h flow. Looking at nature it was stated that as the gestation progresses the syncytiotrophoblast increasingly adhere directly to the basement membrane which provides strong

adhesive and structural support for the syncytium throughout gestation (Aplin et al., 2009). In contrast to the physiological situation where cytotrophoblasts are in between the overlying syncytiotrophoblast and the basement membrane, in the microfluidic chip model only a monolayer of CTB-BeWo cells is present which differentiates to STB-BeWo cells. Therefore, in the microfluidic chip model there is more space available for the syncytiotrophoblasts to adhere to the basement membrane unhindered which could conceivably lead to a strongly adherent syncytium. However, looking at the literature there seems to be a large gap regarding the knowledge about the role of adhesion molecules in regulating villous epithelial integrity and growth.

5.2.3 Flow rate adapted to physiological value

It is conceivable that the shear stress exerted under physiological conditions on extravillous trophoblasts is different than the one on aortic endothelial cells. In the human supraceliac aorta a directional pulsatile flow exerts shear rates on the endothelial cells ranging from 3.5±0.8 dyn/cm^2 at rest to 6.2±0.5 dyn/cm^2 during exercise (Taylor et al., 2002). In contrast in the human placenta the maternal blood circulates in the intervillous space and exerts only shear rates ranging from 0.5±0.2 to 2.3±1.1 dyn/cm^2 on the surface of terminal placental villi (Lecarpentier et al., 2016). Based on this data a shear rate of 2 dyn/cm^2 was chosen for the microfluidic chip experiments during the present work.

5.2.4 Specific staining only with directly labelled antibodies

For some reason specific staining signals in the microfluidic chip could only be achieved with directly labelled antibodies but not with the usage of labelled secondary antibodies. Possibly the secondary antibodies (anti mouse or rabbit) just possess a crossreactivity potential with the coating materials Collagen I (bovine) and Fibronectin (human). However, this presumption could not be verified with a secondary antibody only control due to limited experimental capacities. The staining process in general could probably have been optimized through better washing. The microfluidic chip could have been reconnected to the pump for the washing process in order to wash for a longer time with a large volume of washbuffer. However, the stainings were always carried out in the Albrecht Lab where no pumps were available and therefore this washing procedure could never be tried out.

5.2.5 Microchannel mounting with Vectashield® improves image quality

It was found out that the microchannels of the microfluidic chip can be mounted with Vectashield® mounting media which improved staining imaging and is well applicable. Before the channels were just left in DPBS. Vectashield® mounting media has a low refractive index of 1.45 (https://vectorlabs.com/vectashield-mounting-medium-with-dapi.html#documents, accessed 21.02.2021) compared to DPBS (1.7828) (Barroso et al., 2019). Beside of that the Vectashield® mounting media inhibits photobleaching of fluorescent dyes (https://vectorlabs.com/vectashield-mounting-medium-with-dapi.-html#documents, accessed 21.02.2021) and does not dry out compared to DPBS. Therefore, specimens mounted with Vectashield® mounting media can be stored for long term at 4°C protected from light.

5.3 Microfluidic chip: Staining results

5.3.1 CK-7

It could be observed that for the non-Forskolin stimulated cells, dividing cells were captured in the image whereas this was not the case for Forskolin stimulated cells. This finding supports the assumption that the Forskolin stimulation was effective as already discussed in part 5.1.1 on p. 60. In addition to that the nuclear size increased in BeWo cells treated with Forskolin and flow compared to untreated BeWo cells. The finding that nuclear size increases with the duration of Forskolin stimulation was also made for the chamber slide stainings and is another confirmation of the effectiveness of the Forskolin stimulation (as discussed in part 5.1.1 on p.60) in the microfluidic chip. Further also the flow alone without Forskolin led to an enlarged nuclear size. Looking at the literature it was stated by Sanz et al. that fluid shear stress triggers trophoblast differentiation (Sanz et al., 2019). Therefore, possibly the flow led to an accelerated differentiation of the BeWo cells even without Forskolin stimulation.

Additionally, the finding was made, that the cytokeratin filaments appear in thicker bundles in the BeWo cells that were exposed to flow whereas this effect seems to be reinforced if the cells were stimulated with Forskolin in addition to the flow. Looking at the literature no information concerning this observation was found for trophoblast cells. However, Flitney et al. stated an increased keratin intermediated filament bundling in endothelial cells upon flow exposition in flow chambers (Flitney et al., 2009). Additionally, Flitney et al. performed particle tracking microrheology to measure the viscoeleastic properties of the keratin intermediate filaments which led to the result

that the stiffness is increased after bundling. In his study it was argued that the increased stiffness can be viewed as a protective mechanism that enables cells to better resist the potentially damaging effects of external mechanical forces. White et al. identified an upregulation of cytokeratin 18 mRNA in BeWo cells by Forskolin stimulation and suggested that this upregulation supports the rearrangement of the intermediated filaments in preparation of trophoblast fusion (White et al., 2009). It is therefore conceivable that the forskolin stimulation could also support the rearrangement of the cytokeratin filament bundling. In that way it could be explained that the Forskolin stimulation strengthens the cytokeratin bundling induced by the flow as it was observed. However, it would be very interesting to verify this observation the microfluidic chip with BeWo cells with an examination at the ultrastructural level with electron microscopy.

Comparing the cell shape that could be estimated from the cytokeratin staining no clear differences could be determined between the cells that are kept under flow or not. It could be shown by Liu et al. that trophoblast cells exhibit extension in the direction of flow (Liu et al., 2008). However, the applied shear stress in his study ranged from 7.5 to 30 dyne/cm2 therefore the shear stress of 2dyn/cm^2, chosen in the experiments of the present study to mimic physiological conditions, could have been just too low to induce those dramatic changes in cell morphology.

5.3.2 E-cadherin

It seems that the E-cad junctions between some of the cells were already partially broken down at the time point of fixation which is expected to happen during cell differentiation (as already described in part 5.1.4). Since also in the non-Forskolin stimulated channel some cell fusion happened, it could be assumed that those fusions of the non-Forskolin stimulated cells were induced by the flow. This finding goes along the literature that states that fluid shear stress triggers trophoblast differentiation (as discussed in part 5.3.1). However, the comparison between non-Forskolin stimulated cells with and without flow is missing at this point to verify this assumption.

5.4 Recommendations for further optimization of the microfluidic chip for trophoblasts

When considering the growth conditions of trophoblasts under physiological conditions, the microfluidic chip model does not appear to be ideal in several aspects. The chip consists of microchannels that allow the cells to adhere in a tubular structure as it is typical for the physiological growth of vascular endothelial cells for which the chip was designed. Vascular endothelial cells line the inside of blood vessels while villous trophoblasts stretch over the chorionic villi. Apart from the aforementioned differences in orientation, villous trophoblasts and the underlying fetal endothelial are supposed to crosstalk. Literature states that these interactions include an upregulations of key players in apoptosis in trophoblasts by the endothelial cells (Kuo et al., 2019) and vice versa an upregulation in angiogenic gene expression in endothelial cells by the trophoblasts (Troja et al., 2014). In order to mimic the physiological environment of these cells in the placenta, co-culturing of these cell types appears to be crucial. Further the co-cultivation would allow to reconstitute the multilayered structure of the placental barrier as already done by Zhu et al. (Zhu et al., 2018). Thereby two channels that are separated from one another by a porous membrane, allowing the growth of trophoblasts on one side and endothelial cells on the other. In addition to the study of trophoblast physiology under flow, this system could also be used for example to investigate transport mechanisms across the placental barrier.

5.5 hCG-ELISA

5.5.1 Chamber slides hCG-ELISA results

Whereas the hCG concentration stayed at the same level in the supernatant of the non-Forskolin treated BeWo cells during the time course of the experiment it raised in the ones of the Forskolin treated BeWo cells for 230% from the 24h compared to the 72h samples. Among others it was shown by Handschuh et al. that the hCG secretion is increasing in a primary villous cytotrophoblast culture during its differentiation to syncytiotrophoblasts (Handschuh et al., 2007). Thus, the results agree with the preliminary studies in the literature and are confirming the effectiveness of the Forskolin stimulation. Additionally, it would have been interesting to distinguish between different hCG isoforms as it is known that STBs produce less of the hyperglycosylated isoform of hCG than CTBs (Kovalevskaya et al., 2002). Nevertheless, the hCG measurements are a further indication in addition to the staining results that the BeWo cells in culture have undergone a differentiation induced by the Forskolin. However, they also indicate that the differentiation of CTB-BeWo cells to STB-BeWo cells is still ongoing after 48h and it remains unclear if it is completed after 72h.

5.5.2 Microfluidic chip hCG-ELISA results

Whereas significant hCG concentration differences could be measured in the chamber slide samples this was not the case for the microfluidic chip samples. There the concentration just felt below the detection limit of 32pg/ml that was calculated using the standard curve. This circumstance is not surprising as the cell-to-growth medium ratio was roughly 20`000 times lower in the samples of the microfluidic chip compared to the samples of the chamber slides. The medium volume should not be changed in further experiments to not risk a poorer supply of the cells. A possibility to solve this issue could be that the hCG in the samples get concentrated for example with protein concentrators with a cut off below 36.7 kDa which is the molecular mass of hCG (Canfield et al., 1987).

6 Conclusion and outlook

The microfluidic system for endothelial cells is adaptable to a certain extent for the use in BeWo trophoblast cells. After various adjustments it was possible to cultivate the BeWo cells under flow for a maximum of 24 hours. Longer exhibitions were so far not possible as the cells detached from the microchannel. In the static system it was observed that the BeWo cells continued to develop morphological differences over a culturing time of 88h. Changes in the course of differentiation included an enlargement of the nuclei, reorganization of the cytoskeleton as well as a breakdown of the junctional proteins ZO-1 and E-cad. The CALHM4 staining suggested not only a membraneous but also an intracellular location, structurally reminiscent of intermediate filaments. Based on these findings it could be speculated that CALHM4 represents a mechanosensitive channel and interacts with the cytoskeleton. The SC-1 staining revealed a tendency to increase during differentiation. Taking into account that the syncytium represents a tight diffusion barrier and SC-1 is expected to be involved in trophoblasts regulation of permeability and transport mechanisms, these results make sense and are promising. Considering the ongoing differentiation of the BeWo cells during the 88h culturing time in the static chamber slide system it is a shame that the experiments in the microfluidic chip system were limited to 24 hours of flow. However, despite of the short incubation time on the microfluidic chip system, there are indications that the flow still affected the BeWo cells. These effects were a bundling of the keratin filaments, which may be explained by a greater resistance to external mechanical forces, as well as an enlargement of the nuclei indicating an accelerated differentiation process of the BeWo trophoblast cells due to the flow. With regards to the secretion of hCG, clear differences between differentiated and undifferentiated BeWo cells emerged in the static system. Unfortunately, hCG levels in the supernatant of cells that were cultivated under flow felt below the detection limit of the ELISA, due to the low cell-to-growth medium ratio and the associated strong dilution of hCG.

The knowledge about the cultivation of trophoblasts that was gained during this work could be applied for the development of a micro fluidic system that comes closer to the physiology of the human placenta. A model system of the placental barrier as a functional unit of the placenta could be approached by coculturing the trophoblasts with endothelial cells. This system would include two channels that are separated from one another by a porous membrane, allowing the growth of trophoblasts on one side and

endothelial cells on the other. This setup would allow to reconstitute the multilayered structure of the placental barrier and could be considered as a placenta-on-a-chip model. Beside investigations of trophoblast physiology under flow, this system would allow to examine, for example, transport processes across the placental barrier, secretion of hormones or exosomes, cellular responses upon viral infection like through SARS-CoV-2 or under inflammatory conditions.

Due to time restrictions and the COVID19 pandemic, optimization of the microfluidic system with trophoblasts was limited. Nevertheless, this work was a decisive first step towards the cultivation of trophoblasts under fluidic conditions and the resulting know-how could contribute to the establishment of a placenta-on-a-chip model and in turn to minimize costs and animal experimentation.

7 List of references

Ahrendt, H. ., & K.J. Buhling. (2006). Reproduktionsmedizin und Endokrinologie. *Journal of Reproductive Medicine and Endocrinology*, *1*(3), 194–201. http://www.kup.at/kup/pdf/9658.pdf

Alexander, C. M., Reichsman, F., Hinkes, M. T., Lincecum, J., Becker, K. A., Cumberledge, S., & Bernfield, M. (2000). *Syndecan-1 is required for Wnt-1-induced mammary tumorigenesis in mice*. *25*(july), 329–332.

Amenta, P. S., Gay, S., Vaheri, A., & Martinez-Hernandez, A. (1986). The Extracellular Matrix is an Integrated Unit: Ultrastructural Localization of Collagen Types I, III, IV, V, VI, Fibronectin, and Laminin in Human Term Placenta. *Topics in Catalysis*, *6*(2), 125–152. https://doi.org/10.1016/S0174-173X(86)80021-8

Aplin, J. D., Jones, C. J. P., & Harris, L. K. (2009). Adhesion Molecules in Human Trophoblast - A Review. I. Villous Trophoblast. *Placenta*, *30*(4), 293–298. https://doi.org/10.1016/j.placenta.2008.12.001

Barroso, Á., Radhakrishnan, R., Ketelhut, S., Schnekenburger, J., & Kemper, B. (2019). *Refractive index determination of buffer solutions from visible to near-infrared spectral range for multispectral quantitative phase imaging using a calibrated Abbe refractometer*. https://doi.org/10.1117/12.2509221

Berger, P., & Sturgeon, C. (2014). Pregnancy testing with hCG - future prospects. *Trends in Endocrinology and Metabolism*, *25*(12), 637–648. https://doi.org/10.1016/j.tem.2014.08.004

BeWo Cell Line human 86082803 | *Sigma-Aldrich*. (n.d.). Retrieved January 4, 2021, from https://www.sigmaaldrich.com/catalog/product/sigma/cb_86082803?lang=de&region=DE

Braga, V. (2000). Epithelial cell shape: Cadherins and small GTPases. *Experimental Cell Research*, *261*(1), 83–90. https://doi.org/10.1006/excr.2000.5050

Brugger, B. A., & Guettler, J. (2020). *Go with the Flow — Trophoblasts in Flow Culture*.

Burbach, B. J., Friedl, A., Mundhenke, C., & Rapraeger, A. C. (2003). Syndecan-1 accumulates in lysosomes of poorly differentiated breast carcinoma cells. *Matrix Biology*, *22*(2), 163–177. https://doi.org/10.1016/S0945-053X(03)00009-X

Burres, N. S., & Cass, C. E. (1986). Density-dependent inhibition of expression of syncytiotrophoblastic markers by cultured human choriocarcinoma (BeWo) cells. *Journal of Cellular Physiology*, *128*(3), 375–382. https://doi.org/10.1002/jcp.1041280305

Canfield, R. E., O'Connor, J. F., Birken, S., Krichevsky, A., & Wilcox, A. J. (1987). Development of an assay for a biomarker of pregnancy and early fetal loss. In *Environmental Health Perspectives* (Vol. 74, pp. 57–66). National Institute of Environmental Health Sciences. https://doi.org/10.1289/ehp.877457

Cerneus, D. P., & Van Der Ende, A. (1991). Apical and basolateral transferrin receptors in polarized BeWo cells recycle through separate endosomes. *Journal of Cell Biology*, *114*(6), 1149–1158. https://doi.org/10.1083/jcb.114.6.1149

Chaw, K. C., Manimaran, M., Tay, F. E. H., & Swaminathan, S. (2007). Matrigel coated polydimethylsiloxane based microfluidic devices for studying metastatic and non-metastatic cancer cell invasion and migration. *Biomedical Microdevices*, *9*(4), 597–602. https://doi.org/10.1007/s10544-007-9071-5

Coutifaris, C., Kao, L. C., Sehdev, H. M., Chin, U., Babalola, G., Blaschuk Strauss, O. W. J. F., Ishikawa, A., Omata, W., Ackerman, W. E., Takeshita, T., Vandré, D. D., & Robinson, J. M. (1991). Cell fusion mediates dramatic alterations in the actin cytoskeleton, focal adhesions, and E-cadherin in trophoblastic cells. *Cytoskeleton*, *113*(4), 241–256. https://doi.org/10.1002/cm.21165

Das C, Lucia MS, H. K. and T. J. (2017). A microphysiological model of the human placental barrier. *Physiology & Behavior*, *176*(3), 139–148. https://doi.org/10.1016/j.physbeh.2017.03.040

Drożdżyk, K., Sawicka, M., Bahamonde-Santos, M. I., Jonas, Z., Deneka, D., Albrecht, C., & Dutzler, R. (2020). Cryo-EM structures and functional properties of calhm channels of the human placenta. *ELife*, *9*, 1–27.

https://doi.org/10.7554/eLife.55853

Elad, D., Levkovitz, R., Jaffa, A. J., Desoye, G., & Hod, M. (2014). Have We Neglected the Role of Fetal Endothelium in Transplacental Transport? *Traffic*, *15*(1), 122–126. https://doi.org/10.1111/tra.12130

Flitney, E. W., Kuczmarski, E. R., Adam, S. A., & Goldman, R. D. (2009). Insights into the mechanical properties of epithelial cells: the effects of shear stress on the assembly and remodeling of keratin intermediate filaments. *The FASEB Journal*, *23*(7), 2110–2119. https://doi.org/10.1096/fj.08-124453

Frank, H. G., Genbacev, O., Blaschitz, A., Chen, C. P., Clarson, L., Evain-Brion, D., Gardner, L., Malek, A., Morrish, D., Loke, Y. W., & Tarrade, A. (2000). Cell culture models of human trophoblast - Primary culture of trophoblast - A workshop report. *Placenta*, *21*(SUPPL.1), S120–S122. https://doi.org/10.1053/plac.1999.0528

Gerbaud, P., & Pidoux, G. (2015). Review: An overview of molecular events occurring in human trophoblast fusion. *Placenta*, *36*(S1), S35–S42. https://doi.org/10.1016/j.placenta.2014.12.015

Gerbaud, Pascale, Taskén, K., & Pidoux, G. (2015). Spatiotemporal regulation of cAMP signaling controls the human trophoblast fusion. *Frontiers in Pharmacology*, *6*(SEP), 1–14. https://doi.org/10.3389/fphar.2015.00202

Go, M. (2003). Syndecans in inflammation. *Protogeneia, Inc, Münster, Germany*, 575–591. https://doi.org/10.1096/fj.02-0739rev

Grieve, A. G., & Rabouille, C. (2014). Extracellular cleavage of E-cadherin promotes epithelial cell extrusion. *Journal of Cell Science*, *127*(15), 3331–3346. https://doi.org/10.1242/jcs.147926

Gude, N. M., Roberts, C. T., Kalionis, B., & King, R. G. (2004). Growth and function of the normal human placenta. *Thrombosis Research*, *114*(5-6 SPEC. ISS.), 397–407. https://doi.org/10.1016/j.thromres.2004.06.038

Guibourdenche, J., Handschuh, K., Tsatsaris, V., Gerbaud, P., Leguy, M. C., Muller, F., Evain Brion, D., & Fournier, T. (2010). Hyperglycosylated hCG is a marker of

early human trophoblast invasion. *Journal of Clinical Endocrinology and Metabolism*, *95*(10), 240–244. https://doi.org/10.1210/jc.2010-0138

Haigh, T., Chen, C. P., Jones, C. J. P., & Aplin, J. D. (1999). Studies of mesenchymal cells from 1st trimester human placenta: Expression of cytokeratin outside the trophoblast lineage. *Placenta*, *20*(8), 615–625. https://doi.org/10.1053/plac.1999.0441

Handschuh, K., Guibourdenche, J., Tsatsaris, V., Guesnon, M., Laurendeau, I., Evain-Brion, D., & Fournier, T. (2007). Human Chorionic Gonadotropin Expression in Human Trophoblasts from Early Placenta: Comparative Study Between Villous and Extravillous Trophoblastic Cells. *Placenta*, *28*(2–3), 175–184. https://doi.org/10.1016/j.placenta.2006.01.019

Hatzfeld, M., Keil, R., & Magin, T. M. (2017). Desmosomes and Intermediate Filaments: Their Consequences for Tissue Mechanics. *Pubmed*. https://doi.org/10.1101/cshperspect.a029157

Henriksen, K., & Karsdal, M. A. (2016). Type I Collagen. In *Biochemistry of Collagens, Laminins and Elastin: Structure, Function and Biomarkers*. Elsevier Inc. https://doi.org/10.1016/B978-0-12-809847-9.00001-5

Herrick, E. J., & Bordoni, B. (2019). Embryology, Placenta. In *StatPearls*. StatPearls Publishing. http://www.ncbi.nlm.nih.gov/pubmed/31869098

Herrmann, H., Bär, H., Kreplak, L., Strelkov, S. V., & Aebi, U. (2007). Intermediate filaments: From cell architecture to nanomechanics. In *Nature Reviews Molecular Cell Biology* (Vol. 8, Issue 7, pp. 562–573). Nature Publishing Group. https://doi.org/10.1038/nrm2197

Hofmann-Kiefer, K. F., Chappell, D., Knabl, J., Frank, H. G., Martinoff, N., Conzen, P., Becker, B. F., & Rehm, M. (2013). Placental syncytiotrophoblast maintains a specific type of glycocalyx at the fetomaternal border: The glycocalyx at the fetomaternal interface in healthy women and patients with HELLP syndrome. *Reproductive Sciences*, *20*(10), 1237–1245. https://doi.org/10.1177/1933719113483011

Huang, X., Lüthi, M., Ontsouka, E. C., Kallol, S., Baumann, M. U., Surbek, D. V., & Albrecht, C. (2016). Establishment of a confluent monolayer model with human primary trophoblast cells: Novel insights into placental glucose transport. *Molecular Human Reproduction*, *22*(6), 442–456. https://doi.org/10.1093/molehr/gaw018

Huppertz, B. (2010). IFPA Award in Placentology Lecture: Biology of the placental syncytiotrophoblast - Myths and facts. *Placenta*, *31*(SUPPL.), S75–S81. https://doi.org/10.1016/j.placenta.2009.12.001

Huppertz, Berthold. (2018). Human placentation. In *Encyclopedia of Reproduction* (Second Edi, Vol. 2). Elsevier. https://doi.org/10.1016/B978-0-12-801238-3.64926-7

Indra, I., Choi, J., Chen, C. S., Troyanovsky, R. B., Shapiro, L., Honig, B., & Troyanovsky, S. M. (2018). Spatial and temporal organization of cadherin in punctate adherens junctions. *Proceedings of the National Academy of Sciences of the United States of America*, *115*(19), E4406–E4415. https://doi.org/10.1073/pnas.1720826115

Jansen, C. H. J. R., Kastelein, A. W., Kleinrouweler, C. E., Van Leeuwen, E., De Jong, K. H., Pajkrt, E., & Van Noorden, C. J. F. (2020). Development of placental abnormalities in location and anatomy. *Acta Obstetricia et Gynecologica Scandinavica*, *99*(8), 983–993. https://doi.org/10.1111/aogs.13834

Kallol, S., Huang, X., Müller, S., Ontsouka, C. E., & Albrecht, C. (2018). Novel insights into concepts and directionality of maternal–Fetal cholesterol transfer across the human placenta. *International Journal of Molecular Sciences*, *19*(8). https://doi.org/10.3390/ijms19082334

Kimura, H., Sakai, Y., & Fujii, T. (2018). Organ/body-on-a-chip based on microfluidic technology for drug discovery. In *Drug Metabolism and Pharmacokinetics* (Vol. 33, Issue 1, pp. 43–48). Japanese Society for the Study of Xenobiotics. https://doi.org/10.1016/j.dmpk.2017.11.003

Kovalevskaya, G., Genbacevl, O., Fisher, S. J., Caceres, E., & O'Connor, J. F. (2002).

Trophoblast origin of hCG isoforms: Cytotrophoblasts are the primary source of choriocarcinoma-like hCG. *Molecular and Cellular Endocrinology*, *194*(1–2), 147–155. https://doi.org/10.1016/S0303-7207(02)00135-1

Kreuder, A. E., Bolaños-Rosales, A., Palmer, C., Thomas, A., Geiger, M. A., Lam, T., Amler, A. K., Markert, U. R., Lauster, R., & Kloke, L. (2020). Inspired by the human placenta: a novel 3D bioprinted membrane system to create barrier models. *Scientific Reports*, *10*(1), 1–14. https://doi.org/10.1038/s41598-020-72559-6

Kudo, Y., Boyd, C. A. R., Sargent, I. L., & Redman, C. W. G. (2003). Hypoxia alters expression and function of syncytin and its receptor during trophoblast cell fusion of human placental BeWo cells: Implications for impaired trophoblast syncytialisation in pre-eclampsia. *Biochimica et Biophysica Acta - Molecular Basis of Disease*, *1638*(1), 63–71. https://doi.org/10.1016/S0925-4439(03)00043-7

Kuo, C.-Y., Shevchuk, M., Opfermann, J., Guo, T., Santoro, M., Fisher, J. P., & Kim, P. C. (2019). Trophoblast-endothelium signaling involves angiogenesis and apoptosis in a dynamic bioprinted placenta model. *Biotechnology and Bioengineering*, *116*(1), 181–192. https://doi.org/10.1002/bit.26850

Lecarpentier, E., Bhatt, M., Bertin, G. I., Deloison, B., & Salomon, L. J. (2016). *Computational Fluid Dynamic Simulations of Maternal Circulation : Wall Shear Stress in the Human Placenta and Its Biological Implications*. 1–18. https://doi.org/10.1371/journal.pone.0147262

Lichtman, J. W., & Conchello, J. A. (2005). Fluorescence microscopy. *Nature Methods*, *2*(12), 910–919. https://doi.org/10.1038/nmeth817

Liu, W., Fan, Y., Deng, X., Li, N., & Guan, Z. (2008). Effect of flow-induced shear stress on migration of human trophoblast cells. *Clinical Biomechanics*, *23*(SUPLL.1), S112–S117. https://doi.org/10.1016/j.clinbiomech.2007.07.004

Luther, F. (2018). *Usage of a Microfluidic System to Investigate the Endothelial Glycocalyx in vitro*.

M. Minsky. (1987). Memoir on Inventing the Confocal Scanning Microscope. *Scanning*, *10*(1 988), 128–138.

Maldonado-estrada, J., Menu, E., & Roques, P. (2004). *Evaluation of Cytokeratin 7 as an accurate intracellular marker with which to assess the purity of human placental villous trophoblast cells by flow cytometry*. *286*, 21–34. https://doi.org/10.1016/j.jim.2003.03.001

Martin, B. J., Spicer, S. S., & Smythe, N. M. (1974). Cytochemical studies of the maternal surface of the syncytiotrophoblast of human early and term placenta. *The Anatomical Record*, *178*(4), 769–785. https://doi.org/10.1002/ar.1091780408

Martinac, B. (2014). Biochimica et Biophysica Acta The ion channels to cytoskeleton connection as potential mechanism of mechanosensitivity ☆. *BBA - Biomembranes*, *1838*(2), 682–691. https://doi.org/10.1016/j.bbamem.2013.07.015

Moch, M., Schwarz, N., Windoffer, R., & Leube, R. E. (2020). The keratin–desmosome scaffold: pivotal role of desmosomes for keratin network morphogenesis. *Cellular and Molecular Life Sciences*, *77*(3), 543–558. https://doi.org/10.1007/s00018-019-03198-y

Nwaneshiudu, A., Kuschal, C., Sakamoto, F. H., Rox Anderson, R., Schwarzenberger, K., & Young, R. C. (2012). Introduction to confocal microscopy. *Journal of Investigative Dermatology*, *132*(12), 1–5. https://doi.org/10.1038/jid.2012.429

Paris, S., Burlacu, A., & Durocher, Y. (2008). Opposing roles of syndecan-1 and syndecan-2 in polyethyleneimine-mediated gene delivery. *Journal of Biological Chemistry*, *283*(12), 7697–7704. https://doi.org/10.1074/jbc.M705424200

Patel, K. R., & Gan, S. D. (2013). Enzyme Immunoassay and Enzyme-Linked Immunosorbent Assay Homology Medicines Enzyme Immunoassay and Enzyme-Linked Immunosorbent Assay. *Article in Journal of Investigative Dermatology*, 12. https://doi.org/10.1038/jid.2013.287

Pattillo, R. A., & Gey, G. O. (1968). The Establishment of a Cell Line of Human Hormone-synthesizing Trophoblastic Cells in Vitro. *Cancer Research*, *28*(7), 1231–1236.

Pemathilaka, R. L., Caplin, J. D., Aykar, S. S., Montazami, R., & Hashemi, N. N. (2019). Placenta-on-a-Chip: In Vitro Study of Caffeine Transport across Placental Barrier Using Liquid Chromatography Mass Spectrometry. *Global Challenges*, *3*(3), 1800112. https://doi.org/10.1002/gch2.201800112

Pidoux, G., Gerbaud, P., Gnidehou, S., Grynberg, M., Geneau, G., Guibourdenche, J., Carette, D., Cronier, L., Evain-Brion, D., Malassiné, A., & Frendo, J. L. (2010). ZO-1 is involved in trophoblastic cell differentiation in human placenta. *American Journal of Physiology - Cell Physiology*, *298*(6), 1517–1526. https://doi.org/10.1152/ajpcell.00484.2008

Prakash, G. J., Suman, P., & Gupta, S. K. (2011). Relevance of syndecan-1 in the trophoblastic BeWo cell syncytialization. *American Journal of Reproductive Immunology*, *66*(5), 385–393. https://doi.org/10.1111/j.1600-0897.2011.01017.x

Rama, S., & Rao, A. J. (2003). Regulation of growth and function of the human placenta. In *Molecular and Cellular Biochemistry* (Vol. 253, Issues 1–2, pp. 263–268). Springer. https://doi.org/10.1023/A:1026076219126

Rashid-Doubell, F., Tannetta, D., Redman, C. W. G., Sargent, I. L., Boyd, C. A. R., & Linton, E. A. (2007). Caveolin-1 and Lipid Rafts in Confluent BeWo Trophoblasts: Evidence for Rock-1 Association with Caveolin-1. *Placenta*, *28*(2–3), 139–151. https://doi.org/10.1016/j.placenta.2005.12.005

Romberger, D. J. (1997). Fibronectin. *International Journal of Biochemistry and Cell Biology*, *29*(7), 939–943. https://doi.org/10.1016/S1357-2725(96)00172-0

Sanz, G., Daniel, N., Aubrière, M. C., Archilla, C., Jouneau, L., Jaszczyszyn, Y., Duranthon, V., Chavatte-Palmer, P., & Jouneau, A. (2019). Differentiation of derived rabbit trophoblast stem cells under fluid shear stress to mimic the trophoblastic barrier. *Biochimica et Biophysica Acta - General Subjects*, *1863*(10), 1608–1618. https://doi.org/10.1016/j.bbagen.2019.07.003

Schmitz, G., & Grandl, M. (2008). Update on lipid membrane microdomains. *Current Opinion in Clinical Nutrition and Metabolic Care*, *11*(2), 106–112. https://doi.org/10.1097/MCO.0b013e3282f44c2c

Semwogerere, D., & Weeks, E. R. (2005). Confocal Microscopy. *Encyclopedia of Biomaterials and Biomedical Engineering*. https://doi.org/10.1081/E-EBBE-120024153

Sfriso, R., Zhang, S., Bichsel, C. A., Steck, O., Despont, A., Guenat, O. T., & Rieben, R. (2018). 3D artificial round section micro-vessels to investigate endothelial cells under physiological flow conditions. *Scientific Reports*, *8*(1), 1–13. https://doi.org/10.1038/s41598-018-24273-7

Syrjanen, J. L., Michalski, K., Chou, T. H., Grant, T., Rao, S., Simorowski, N., Tucker, S. J., Grigorieff, N., & Furukawa, H. (2020). Structure and assembly of calcium homeostasis modulator proteins. *Nature Structural and Molecular Biology*, *27*(2), 150–159. https://doi.org/10.1038/s41594-019-0369-9

Szabo, S., Xu, Y., Romero, R., Fule, T., Karaszi, K., Bhatti, G., Varkonyi, T., Varkonyi, I., Krenacs, T., Dong, Z., Tarca, A. L., Chaiworapongsa, T., Hassan, S. S., Papp, Z., Kovalszky, I., & Than, N. G. (2013). Changes of placental syndecan-1 expression in preeclampsia and HELLP syndrome. *Virchows Archiv*, *463*(3), 445–458. https://doi.org/10.1007/s00428-013-1426-0

Tarrade, A., Goffin, F., Munaut, C., Lai-Kuen, R., Tricottet, V., Foidart, J.-M., Vidaud, M., Frankenne, F., & Evain-Brion, D. (2002). Effect of Matrigel on Human Extravillous Trophoblasts Differentiation: Modulation of Protease Pattern Gene Expression1. *Biology of Reproduction*, *67*(5), 1628–1637. https://doi.org/10.1095/biolreprod.101.001925

Taylor, C. A., Cheng, C. P., Espinosa, L. A., Tang, B. T., Parker, D., & Herfkens, R. J. (2002). *In Vivo Quantification of Blood Flow and Wall Shear Stress in the Human Abdominal Aorta During Lower Limb Exercise*. https://doi.org/10.1114/1.1476016

Troja, W., Kil, K., Klanke, C., & Jones, H. N. (2014). Interaction between human placental microvascular endothelial cells and a model of human trophoblasts: Effects on growth cycle and angiogenic profile. *Physiological Reports*, *2*(3), 244. https://doi.org/10.1002/phy2.244

Van Roy, F., & Berx, G. (2008). The cell-cell adhesion molecule E-cadherin. *Cellular*

and Molecular Life Sciences, *65*(23), 3756–3788. https://doi.org/10.1007/s00018-008-8281-1

Wang, Y., & Zhao, S. (2010). *Cell Types of the Placenta*. https://www.ncbi.nlm.nih.gov/books/NBK53245/

White, L. J., Declercq, W., Arfuso, F., Charles, A. K., Dharmarajan, A. M., & Charles - AdrianCharles, A. K. (2009). *Function of caspase-14 in trophoblast differentiation*. https://doi.org/10.1186/1477-7827-7-98

Yalow, B. R. S., & Berson, S. A. (1960). *IOtQDIDE INSULIN-I IODIDEhE ,;,/*. 11–13.

Zhang, B., Korolj, A., Lai, B. F. L., & Radisic, M. (2018). Advances in organ-on-a-chip engineering. In *Nature Reviews Materials* (Vol. 3, Issue 8, pp. 257–278). Nature Publishing Group. https://doi.org/10.1038/s41578-018-0034-7

Zhang, B., & Radisic, M. (2017). Organ-on-A-chip devices advance to market. In *Lab on a Chip* (Vol. 17, Issue 14, pp. 2395–2420). Royal Society of Chemistry. https://doi.org/10.1039/c6lc01554a

Zheng, F., Fu, F., Cheng, Y., Wang, C., Zhao, Y., & Gu, Z. (2016). Organ-on-a-Chip Systems: Microengineering to Biomimic Living Systems. In *Small* (Vol. 12, Issue 17, pp. 2253–2282). Wiley-VCH Verlag. https://doi.org/10.1002/smll.201503208

Zhu, Y., Yin, F., Wang, H., Wang, L., Yuan, J., & Qin, J. (2018). Placental Barrier-on-a-Chip: Modeling Placental Inflammatory Responses to Bacterial Infection [Research-article]. *ACS Biomaterials Science and Engineering*, *4*(9), 3356–3363. https://doi.org/10.1021/acsbiomaterials.8b00653

8 Illustration index

9 Table index

10 Appendix

10.1 List of used devices and materials

10.1.1 Devices

Confocal microscope	- Carl Zeiss, LSM 710 with Airyscan
Slide scanner	- Histech, Panoramic 250 Flash II
Light microscope	- Leica, DMi1
Plasma cleaner	- Harrick Plasma, Plasma Cleaner
Peristaltic pump	- Gilson, minipuls 3

10.1.2 Materials

BeWo b30 subclone	- Donated by Dr Alan L. Schwartz, Washington University School of Medicine, USA
DMEM 4.5 g/L D-glucose	- Gibco, 32430-027
0.05 % Trypsin-EDTA (1x)	- Gibco, 25300
DPBS	- Sigma, D8537
Anti-Anti 100 x	- Gibco, 15240-062
DMSO	- Sigma, D4540-500ML
FBS	- Sigma, F7524
Silicon Elastomer (PDMS)	- Dow corning, 2401673921
Curing Agent	- Dow corning, 240001673921
APTES	- Sigma Aldrich, A3648 – 100m
Glutaraldehyde 25%	- Sigma, G-6257

Matrigel	- BD Biosciences, 356234
Hu Plasma Fibronectin 1 mg/ml	- Merck, FC010
CollagenI Bovine 5mg/ml	- Gibco, A10644-01
Needles 0.55 x 25mm	- Braun, 4657675
Needles 0.12 x 30mm	- Seirin, Acupuncture Needle
Chamber culturing slides 8-well	- SPL, 30108
Formaldehyde 16%	- Thermo Scientific, 28906
Tween 20	- Sigma, P1379-500ML
Rabbit ZO-1 antibody	- Invitrogen, 61-7300
Mouse anti cytokeratin 7 antibody conj. AF488	- Novusbio, NBP2-47940AF488
Mouse anti E-Cadherin antibody conj. AF488	- Novusbio, NBP1-42793AF488
Mouse anti Syndecan-1 antibody conj. AF647	- Santa Cruz biotechnology, INC., sc-12765 AF647
Rabbit anti CALHM4	- Pinea (serum from rabbit 3)
DAPI	- Sigma, D9542
Aquatex® mounting media	- Merck Millipore, 108562
VECTASHIELD® Antifade Mounting with DAPI	- Vector laboratories,H1200-10Medium
Human hCG (intact) ELISA Kit	- Sigma, RAB0092

10.2 Protocols

10.2.1 Staining protocol Sampada Kallol

Permeabilisation

- Ad DPBS with 0.5% Tween 20 to the cells
- Incubate for 30 minutes at room temperature

Blocking

- Ad DPBS with 5% BSA and 0.5% Tween 20 to the cells
- Incubate at room temperature for 60minutes

Staining

- Ad primary antibody diluted in DPBS with 1% BSA and 0.5% Tween 20 to the cells
- Incubate at 4°C for at least 3 hours
- Ad secondary antibody (if needed) diluted in DPBS with 1% BSA and 0.5% Tween 20 to the cells
- Incubate at 4°C for at least 1 hour
- Ad DAPI diluted 1:5000 in DPBS with 1% BSA and 0.5% Tween 20 to the cells
- Incubate at 4°C for 30 minutes

10.2.2 Microfluidics protocol

Chip making

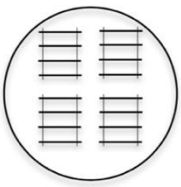

1. Mix Silicon Elastomer and Curing agent (from ARTORG) in proportion 10:1
   Example for 1 Petri dish (4 microchips):
   Silicon Elastomer: 35g, Curing Agent: 3.5g
2. Mix well the two components with a plastic spoon for 3-5 min
3. Vacuum to remove air bubbles. Release vacuum before overflow!
4. Clean needles (Ø 550µm =24G) with Isopropanol, and leave them to dry (on a tissue)
5. Transfer liquid PDMS (ok if still has some bubbles) into a petri dish (Ø 60 mm) and vacuum it to remove further air bubbles.
6. Vacuum the petri dishes until there are no air bubbles left.
7. Place support needles (Ø 120µm= acupuncture needles) on the bottom of the Petri dish.
8. Place mold needles (Ø 550µm) orthogonally on top of support needles.
9. Carefully transfer the Petri dish into the incubator (60°C). Pay attention that the needles do not move!
10. Cure overnight at 60°C (check that the Petri dish is placed on a flat surface).
11. Remove the solidified PDMS and cut four equal chips.
12. Remove the needles with forceps (Ø 550µm and Ø 120µm) store the 550µm needles (reusable) and discard the small needles
13. Punch holes, distance 1cm (use a ruler), as inlets and outlets using Ø 2.0 mm biopsy puncher. Be sure that the punched holes hit the channels and are vertical!!
14. Small channel holes have to be closed, prepare 5g PDMS as described above and with a 10ul pipette tip put a small drop of PDMS on the side of the chip to close the channel hole. Be careful to not put any PDMS on the underside of the chip (where the channels

are) otherwise the uneven surface would make bonding difficult. Cure overnight @60°C.
15. Chips can be stored at this point, tape the structures to protect them from dust.

PDMS-Glass bonding

1. Cut a chip (place it with the inlet/outlet holes towards the underside and the channel towards the top) in four parts with a scalpel. Every single part must contain a microchannel.
2. Tape a PDMS chip with scotch tape on the bottom side while keeping the channel side on top and leave a small space between the channels.
3. Clean a glass slide by wetting it with dH_2O, then with soap water, rinse with dH_2O and finally with Isopropanol.
4. Dry the glass slide with a nitrogen gun, blow along the short edge of the slide in direction of the slide to avoid breaking it.
5. Place PDMS-Chip & glass slide into the Oxygen Plasma Cleaner.
6. Turn on Oxygen Tank, Vacuum pump, Pressure Indicator and Plasma Cleaner.
7. Make sure O_2 valve is in the initial position
8. Wait the pressure decreases until ca. 300 mTorr, turn the O_2 valve into position.
9. Wait until the pressure stabilizes at ca. 650 mTorr.
10. Turn on plasma to a high level for glass-PDMS bonding. Leave 3min under oxygen plasma.
11. Open the valve to let pressure come out, be careful to do this slowly!
12. Turn the chips over by holding on to the tape and the PDMS chip in the center of the glass slide and gently press them onto the slide.

Covalently cross-link Fibronectin and Collagen I to PDMS

Work under the chemical hood or laminar flow hood. Discard the waste properly! APTES and Glutaraldehyde are toxic! Each channel can hold 50ul of liquid, so for one chip with 4 channels use a 200ul pipette set to 200ul and distribute the liquid evenly between the channels.

1. After oxygen-plasma bonding, modify the PDMS surface immediately by filling the microchannels with 5% APTES (the shorter the time between plasma oxygen treatment and APTES, the more APTES-groups will bind to the surface) for 3x times and the 3rd time leave it for 20 min.
2. Wash channels 3x with sterile distilled water.
3. Replace the water with 0.1% Glutaraldehyde 3x, leave for 30min.
4. Wash 3x with sterile distilled water
5. Replace the water with 50µg/ml fibronectin in PBS 3x, incubate 60min @ 37°C
6. Fill directly 100µg/ml Collagen-I in 0.02M Acetic acid 3x and leave it in the laminar flow @ RT for 1.5 hours.
7. Add cell culture medium (DMEM Glutamax for porcine cells and Cascade-200 for human cells) with 4% dextran and 1% BSA and place the Petri dish with the chip in the 37°C incubator for 30 min or longer before cell loading.

Cell seeding

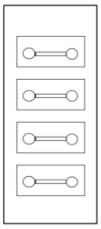

1. Prepare cell culture medium (DMEM Glutamax for porcine cells and Cascade-200 for human cells) with 4% dextran and 1% BSA
2. Harvest the cells of interest and adjust cell density at 10^6/ml by adding cell culture medium supplemented with dextran and BSA.

3. Put 3x cell suspension using 200µl pipette (10^6cells/ml) into the inlet, remove and add another drop into inlet and outlet. Be sure to have a single cell suspension, avoid cell clumps!
4. Place the microfluidic chip upside down in the incubator and leave it for 10min. The cells should have enough time to attach to the surface (Fix the glass slide with a tape to the petri dish)
5. Aspirate the unattached cells and add new cells (two drops, one each on inlet and outlet are enough). Incubate the chip on upright for 10min.
6. Check the chip under the microscope, cells should not be moving anymore.
7. Wash the channels with 4% dextran/ 1% BSA medium to get rid of unattached cells.
8. Wait until cells are confluent (normally next day) and change the medium 2 times per day (when not connected to pump). Change the medium in the morning after seeding before connecting to the pump.

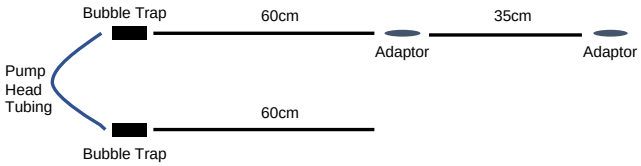

<u>Preparing the tubings</u>

There are PVC pump tubes (to connect the chip to the pump) and silicon pump head tubings (run inside of the pump around the rotor) as well as adapters to connect pump tubes to other pump tubes and to the chip and bubble traps. Tubings and adaptors can be used multiple times, pump head tubings are only used twice.

1. Cut for every channel (4 per chip) two 60cm and one 35cm pieces of PVC pump tubes (Art. Nr:10361). Make sure to not stretch the tubings while cutting in order to get the right length!
2. Attach one bubble trap each to both of the 60cm tubes (this is where they will be connected to the pump head tubings)
3. Connect one 60cm piece to one 35cm piece via an adapter and add another adapter to the free end of the 35cm tube. If the tubings are new, wash once with dH2O and put into an autoclaved beaker submerged in dH2O or if the tubings have been used once first wash once with EtOH and then with dH2O and proceed as with the new tubings. Use ca. 10ml of dH2O per tubing to wash. The tubings are then autoclaved on the same settings as any other liquids.
4. Wash the pump head tubings (4 per chip) with 5ml dH_2O, 5ml EtOH and again 5ml dH_2O and place them in an autoclaved beaker with aluminium foil on top.
5. Cool clave the pump head tubings (“microwave in U1”) 1x8min without foil cover and 1x8min with foil cover. Keep until day of chip connecting.

<u>Connecting the pump (4 tubings)</u>

1. Connect pulsatile pump when the cells are confluent.
2. Prepare 1 50ml falcon tube with dH_2O, 1 50ml falcon tube with PBS and one 50ml falcon tube for the waste.
3. Under the hood: connect the pump head tubings to the bubble traps, there is now one long tube with 60cm tubing – bubble trap – pump head tubing – bubble trap – 60cm tubing – adapter – 35cm tubing – adapter.
4. Put the pump head tubing into the pump around the rotor, place one end with the 60cm tube into the 50ml falcon used for flushing (first dH_2O, then PBS and lastly medium) and place the end with the 60cm + 35cm tube + adapter into the waste falcon tube.

5. Flush tubing with 30 ml of autoclaved dH_2O then with 30 ml of autoclaved PBS 1X with the pump settings on 10 RPM.
6. Check the tubing for leakage and continue flushing with 10-20ml 4% Dextran 1% BSA Medium.
7. Be sure that the medium runs through all the channels with the same speed (check how fast it drips out from the adapter end of the tubes). If not adjust the flow with the screws on the back of the pump.
8. Fill four 15ml Falcon tubes with 10 ml of sterile filtered (0.22um) 4% Dextran and 1% BSA Medium and insert the inlet and outlet of the tubings (ends without the adapters) into the holes drilled into caps of 15ml falcon tubes that have been autoclaved. Adjust the inlet at the level of 8ml and the outlet at 2 ml so that mixing of the medium is assured.
9. Take apart the 60cm + 35cm tubes at the adapter and insert the ends with the adapters in the inlet (adapter attached to the 60cm tube) and outlet (adaptor attached to the 35cm tube) of the microchannels.
10. Start the pump at 10 RPM (flow 860µl/min, shear stress = 21 dyn/cm2) or 7 RPM (flow 590µl/min, shear stress =15dyn/cm2)
11. Keep the desired RPM for 48h or 72h and change medium reservoir every day.

10.2.3 hCG ELISA protocol

Human hCG (intact) ELISA Kit

Sigma, RAB0092
https://www.sigmaaldrich.com/catalog/product/sigma/rab0092?lang=de&region=CH&cm_sp=Insite-_-caSrpResults_srpRecs_srpModel_rab0092-_-srpRecs3-1

Sandwich Assay Procedure

1. Bring all reagents and samples to room temperature (18–25 °C) before use. It is recommended that all standards and samples be run at least in duplicate.
2. Add 100 µL of each standard and sample into appropriate wells. Cover wells and incubate for 2.5 hours at room temperature or overnight at 4 °C with gentle shaking.
3. Discard the solution and wash 4 times with 1× Wash Solution. Wash by filling each well with Wash Buffer (300 µl) using a multi-channel Pipette or autowasher. Complete removal of liquid at each step is essential to good performance. After the last wash, remove any remaining Wash Buffer by aspirating or decanting. Invert the plate and blot it against clean paper towels.
4. Add 100 µL of 1× prepared Detection Antibody to each well. Cover wells and incubate for 1 hour at room temperature with gentle shaking.
5. Discard the solution. Repeat the wash procedure as in step 3.
6. Add 100 µL of prepared Streptavidin solution to each well. Cover wells and incubate for 45 minutes at room temperature with gentle shaking.
7. Discard the solution. Repeat the wash as in step 3
8. Add 100 µL of TMB One-Step Substrate Reagent (Item H) to each well. Cover wells and incubate for 30 minutes at room temperature in the dark with gentle shaking.
9. Add 50 µL of Stop Solution (Item I) to each well. Read at 450 nm immediately.

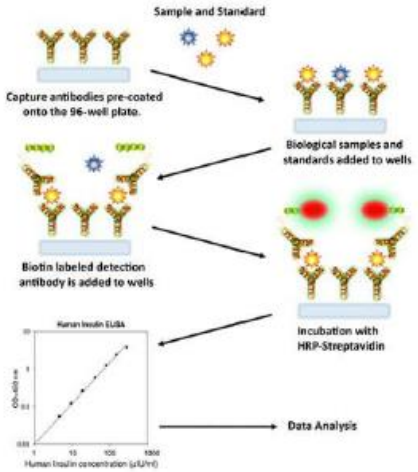

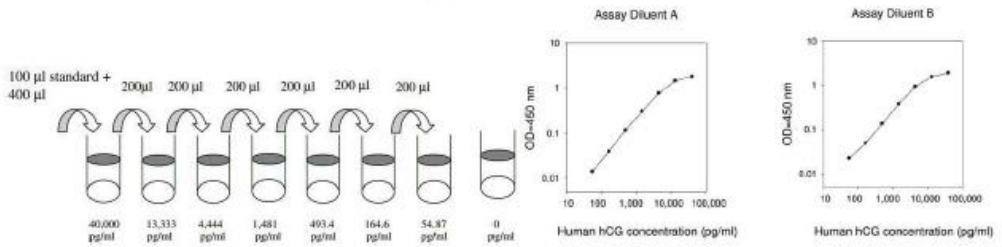

Certificate of Analysis

3050 Spruce Street, Saint Louis, MO 63103 USA
Tel: (800) 521-8956 (314) 771-5765 Fax: (800) 325-5052 (314) 771-5757

Product Name
Human hCG (intact) ELISA Kit
for serum, plasma, and cell culture supernatants

Product Number
RAB0092

Lot Number
1221D0234

Storage
Store the kit at -20°C. It remains active for up to 1 year. Avoid repeated freeze-thaw cycles. The reconstituted standard should be stored at -20°C or -70°C (-700C is recommended). Opened microplate strips or reagents may be store for up to 1 month at 2-8°C. Return unused wells to the pouch containing desiccant pack and reseal along entire edge.

Components

1. Human hCG Antibody-coated ELISA Plate (Item A) - RAB0092A-EA: 96 wells (12 strips x 8 wells) coated with anti-Human hCG.
2. 20x Wash Buffer (Item B) - RABWASH4
3. Lyophilized Human hCG Protein Standard (Item C) - RAB0092C-1VL
4. Biotinylated Human hCG Detection Antibody (Item F) - RAB0092D-1VL
5. HRP-Streptavidin (Item G) - RABHRP5
6. ELISA Colorimetric TMB Reagent (HRP Substrate, Item H) - RABTMB3
7. ELISA Stop Solution (Item I) - RABSTOP3
8. ELISA 1x Assay/Sample Diluent Buffer A (Item D1) - RABELADA-30ML
9. ELISA 5x Assay/Sample Diluent Buffer B (Item E1) - RABELADB-15ML

Assay/Sample Diluent Buffer – dilution (Preparation, Step 2)
Assay/Sample Diluent Buffer B (Item E1) should be diluted 5-fold with deionized or distilled water before use.

Sample Dilution - (Preparation, Step 3)
Assay/Sample Diluent Buffer A (Item D1) should be used for dilution of serum and plasma samples. 1x Assay/Sample Diluent Buffer B (Item E1) should be used for dilution of cell culture supernatant samples. The suggested dilution for normal serum/plasma is 2 - 10 fold.
* Please note that the levels of hCG may vary between different samples. Optimal dilution factors for each sample must be determined by the investigator.

Preparation of Standard - (Preparation, Step 4)
Briefly spin a vial of Item C. Add 400 µl Assay Diluent A (for serum/plasma samples) or 1X Assay Diluent B (for cell culture supernatants) into Item C vial to prepare a 200 ng/ml standard. Dissolve the powder thoroughly by a gentle mix. Add 100 µl hCG standard (200 ng/ml) from the vial of Item C, into a tube with 400 µl Assay Diluent A or 1X Assay Diluent B to prepare a 40,000 pg/ml standard solution. Pipette 400 µl Assay Diluent A or 1X Assay Diluent B into each tube. Use the 40,000 pg/ml standard solution to produce a dilution series (Figure 1). Mix each tube thoroughly before the next transfer. Assay Diluent A or 1 X Assay Diluent B serves as the zero standard (0 pg/ml).

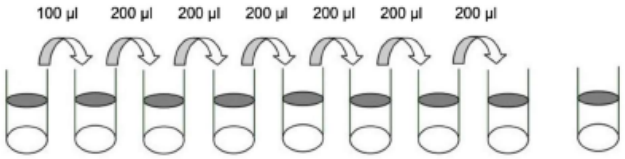

		Std1	Std2	Std3	Std4	Std5	Std6	Std7		Zero Standard
Diluent volume	Item C+ 400 µl	400 µl	400 µl	400 µl	400 µl	400 µl	400 µl	400 µl		400 µl
Conc.	200 ng/ml	40000 pg/ml	13333 pg/ml	4444 pg/ml	1481 pg/ml	493.4 pg/ml	164.6 pg/ml	54.87 pg/ml		0 pg/ml

Preparation of Biotinylated - Detection Antibody - (Preparation, Step 6)
Briefly spin the Detection Antibody vial (Item F) before use. Add 100 µl of 1x Diluent Buffer B (Item E1) into the vial to prepare a detection antibody concentrate. Pipette up and down to mix gently (the concentrate can be stored at 4°C for 5 days). The detection antibody concentrate should be diluted 80-fold with 1x Diluent Buffer B (Item E1) and used in Procedure, step 4.

Dilution of HRP-Streptavidin - Concentrate - (Preparation, Step 7)
Briefly spin the HRP-Streptavidin concentrate vial (Item G) and pipette up and down to mix gently before use, as precipitates may form during storage. HRPStreptavidin concentrate should be diluted 700-fold with 1x Diluent Buffer B (Item E1).
For example: Briefly spin the vial (Item G) and pipette up and down to mix gently. Add 20 µl of HRP-Streptavidin concentrate into a tube with 14 ml 1X Assay Diluent B to prepare a final 700 fold diluted HRP-Streptavidin solution (don't store the diluted solution for next day use). Mix well.

Typical Data

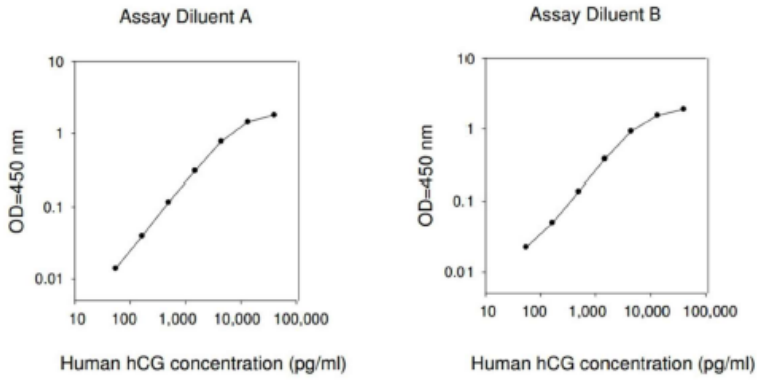

Sensitivity

The minimum detectable dose of Human hCG was determined to be 50 pg/ml. Minimum detectable dose is defined as the analyte concentration resulting in an absorbance that is 2 standard deviations higher than that of the blank (diluent buffer).

Recovery

Recovery was determined by spiking various levels of Human hCG into the sample types listed below. Mean recoveries are as follows:

Sample Type	Average % Recovery	Range (%)
Serum	113.7	103-124
Plasma	90.57	83-103
Cell culture media	130.0	120-135

10.2.4 Giudeline for Zeiss LSM 710 and ZEN Software usage

Live Cell Imaging Core Facility | Department BioMedical Research

Zeiss LSM710 and ZEN Software

This device belongs to the LCI Core Facility and users need to be trained by the LCI staff. Please contact Carlos Wotzkow (carlos.wotzkow@dbmr.unibe.ch) for a training.

Before using the LSM710 microscope, please book your time through the OpenIRIS (https://openiris.io/) reservation system

- **DBMR_MU50_Zeiss_LSM 710 with Airyscan**

In case of issues, please contact in priority order Carlos Wotzkow, Dr. Fabian Blank or Selina Steiner.

Objectives available

- Plan-Apochromat 10x/0.3 M27 /a=2.00mm
- Plan-Apochromat 20x/0.8 M27 /a=0.55mm
- EC Plan-Neofluar 40x/1.30 Oil DIC M27 /a=0.21mm
- Plan-Apochromat 60x/1.40 Oil DIC M27

Starting the System

Note: Microscope lasers should be used for more than a half hour before switch them OFF!

- Turn ON the 3 switches (Main, System/PC and Components) on top of the power remote switch (don't touch the safety lock key)
- Switch ON the HXP 120 C (Fluorescence) lamp. The power supply 232, located just at the right side should remain ON all the time.
- Switch ON the PC. Realtime controller located at the right side should be automatically ON all the time.
- At the power supply of the Ar-ML Laser, turn the key from "0" to "I" (the toggle switch between the electrical and laser cables should not be touched and remains ON all the time).
- At the LASOS Modulator, turn on switch (from idle to run) and wait a few minutes.
- Once the laser reached the set output power (green light), adjust the power level, by turning the control knob clockwise until the led turn red, then turn counterclockwise until green light reappears again.
- Place specimen on microscope stage. Coverslip must face objective lens. Do not forget immersion medium if the objective chosen requires it!!!!
- Select the appropriate eyepiece (usually the smallest amplification) to locate the target at your sample and then switch to the desired magnification for capturing your image.
- For focus purpose light paths can be quickly changed at convenience at the buttons on the left C-wheel of the microscope's stand. You can also change all ocular settings and transmitted light intensity via the "Ocular" tool.

Starting the ZEN software (black icon).

Note: ZEN's blue icon is for image processing only!

- Double click Zen icon at the desktop to start the Carl Zeiss LSM software.
- Once the Zen main application windows opens, click "Start System"
  - At this point, in rare cases, boot status may fail (generally around 14%) or complete properly. If it fails, make a restart of the realtime controller by pressing the large button (RTC-RESET) and wait for the program to resume.
  - If a restart was necessary, repeat step 2.
- To visualize your sample via the eyepieces, click "Locate" and "Online" in order to turn ON the lasers.
- To configure your chosen set of dyes use "Smart Setup"
- Select each track configuration by adding the name of your dye and assigning a color. You can use the dye list for your dye selection.
- Once finished with the input, choose one of the following considerations (Fastest, Best signal, Best compromise, Linear unmixing) depending on the expected emission signals and the cross-talk. Usually "Best Signal" is optimal (however, not the quickest way to acquire pictures). Then "Apply".
- At "Scan Mode" choose "Frame" and check for the "Optimal" values for X*Y (it will calculate the appropriate number of pixels depending on objective).
- At "Speed" choose between 9 (good) and 6 (better signal-to-noise ratio) with the help of the bar slide.
- On "Averaging" a Number = "8" is very good for 2D images, while 2-4 are ideal for Z-stacks.
- At "Bit Depth" settings higher than 8 bit may be chosen.
- Under "Light Path" adjust the pinhole size (airy unit) in each track by clicking the "AU" button (it will adjust it automatically to 1).
- To individually configure the channels do so by activating/deactivating (via the check boxes) each channel. Reduce the "Gain (Master)" until the red pixels just disappear; increase "Digital Offset" until blue pixels are just slightly positive. Repeat to every track removing the others. Adjustments are not possible if channels are not highlighted.
- Once your settings are done, "Snap" (do not "Set Exposure" or you will get an image with an optimization which is generally far from optimal).
- Remember, an unsaved 2D in active image tab will be overwritten by a new scan

Scanning a Z-stack

- Select Z-stack in the main tools area.
- Open Z-stack in the left tool area.
- Click on "Live" or "Continuous" button.
- Use the focus drive of the microscope to search for the upper position where scanning should start. Then click "Set First" button.
- Repeat for the lower position and click "Set Last".
- Click the "Optimal" button to set the number of slices (it will match the intervals of the given size, wavelength, objective and pinhole).
- Be sure all channels are active before scanning the Z-stack.
- Click "Start Experiment" to start recording.

- Please be reasonable concerning the settings of your experiment. If you apply for the best-to-all options, you may receive your retirement papers before your Z-stack is completed. The "Optimal" button may help with the frame size, as well as a "9" speed, and "2" of averaging.

Saving your data

- You can save your images and Z-stacks by clicking the floppy-like icon button of the file handling area, or in the main toolbar. ZEN will do it directly as .lsm 5, which is the native Carl Zeiss LSM image data format.
- You can also save your image in other formats by choosing the "Export" window from the File menu. There you may choose what is appropriate for your "Format", "Data" and "Channels". From there you can proceed to Windows "Save as" to the "D" partition of the hard disk.

Switching OFF the System (order is IMPORTANT)

- Click the "File" button, then "Exit".
- If any lasers are still running you should now shut them off in the pop-up window indicating the lasers in use.
- At this time you should retrieve your data from the hard disk with the help of a memory stick.
- Shut down the computer.
- At the Ar-ML laser modulator (fig 1) switch to idle and turn the knob counterclockwise.
- Turn the key (fig 2) from "I" to "0" (but NOT the toggle switch between the electrical and laser cables), then wait until the fan of the Argon laser has switched off.
- Switch OFF the HXP 120 C (Fluorescence) lamp (fig 3).
- On the power remote switch you can turn OFF "Components" and "System/PC".
- As soon as the fan of the Argon laser is OFF (you will notice a noise reduction), you can switch OFF the main power on the power remote switch (fig 4).

If you're in a middle of your working session and need help, please call Fabian Blank (27634), or Carlos Wotzkow or Selina Steiner (20954). We will be very glad to help you as soon as possible!

Figures

Fig 1

Fig 2

Fig 3

Fig 4

Contacts

Selina Steiner, Email: selina.steiner@dbmr.unibe.ch, Phone +41 31 632 09 54

Carlos Wotzkow, Email: carlos.wotzkow@dbmr.unibe.ch, Phone +41 31 632 09 54

Lab Managers at the LCI Core Facility, Laboratory G809, DBMR, Murtenstrasse 35, 3008 Bern

PD Dr. Fabian Blank, Email: fabian.blank@dbmr.unibe.ch, Phone: +41 31 632 76 34

Head of the LCI Core Facility, Office D304, DBMR, Murtenstrasse 50, 3008 Bern

Declaration of consent

on the basis of Article 30 of the RSL Phil.-nat. 18

Name/First Name: Roman Bächler

Registration Number: 13-277-306

Study program: Master of Science in Molecular Life Sciences

Bachelor ☐ Master ☑ Dissertation ☐

Title of the thesis: Establishment and comparison of static and fluidic microvessel systems as cell models for studying trophoblast physiology

Supervisor: Prof. Dr. Christiane Albrecht

I declare herewith that this thesis is my own work and that I have not used any sources other than those stated. I have indicated the adoption of quotations as well as thoughts taken from other authors as such in the thesis. I am aware that the Senate pursuant to Article 36 paragraph 1 litera r of the University Act of 5 September, 1996 is authorized to revoke the title awarded on the basis of this thesis.

For the purposes of evaluation and verification of compliance with the declaration of originality and the regulations governing plagiarism, I hereby grant the University of Bern the right to process my personal data and to perform the acts of use this requires, in particular, to reproduce the written thesis and to store it permanently in a database, and to use said database, or to make said database available, to enable comparison with future theses submitted by others.

Bern, 10 February 2021

Place/Date

Roman Bächler

Digital unterschrieben von Roman Bächler
Datum: 2021.02.10 11:47:50 +01'00'

Signature